■■■■■ **CHAPTER 17**

# Mixing in the Fine Chemicals and Pharmaceutical Industries

EDWARD L. PAUL, MICHAEL MIDLER, and YONGKUI SUN

*Merck & Co., Inc.*

## 17-1 INTRODUCTION

This chapter is directed toward the unique mixing issues that may be encountered in the fine chemicals and pharmaceutical industries. Relevant mixing issues are the subjects of other chapters in this book, and extensive references to these chapters will be made. Mixing in chemical reactions is very important in many fine chemical and pharmaceutical processes. Because of this critical aspect, the reader is referred to the detailed discussion and examples in Chapter 13. Other chapters relevant to the pharmaceutical industry are Chapters 15 and 18. The mixing concerns in the fine chemicals and pharmaceutical industries that are addressed in this book include those associated with the synthesis of intermediates and active ingredients but do not include pharmaceutical operations such as granulation.

One of the unique aspects of the pharmaceutical and agricultural-chemical industries is the degree of regulatory control over processing, both in limiting operations to narrow ranges and in restricting process changes directed at improvement. Mixing issues are often a part of these regulatory concerns because of the sensitivity of some operations, to changes in mixing conditions either on scale-up or on changes in vessels in manufacturing operations. The operations that are among the most sensitive to these concerns are mixing sensitive reactions and crystallization. In this chapter we address many of the sensitivities of these operations, with the intent of providing guidelines for development and scale-up that can be helpful in the design of mixing systems to minimize regulatory issues.

## 17-2    GENERAL CONSIDERATIONS

Although the subject of this chapter is general mixing in the fine chemical and pharmaceutical industries, much of the focus is on reactions and their associated operations, since they present a wide range of mixing challenges. In addition, multipurpose plants are designed with a series of vessels that are used for reactions as well as extraction, distillation, crystallization, and so on, and in some applications, these operations may all be performed in the same vessel. A major challenge for mixing in stirred vessels for the pharmaceutical and fine chemical industries is, therefore, the variety of functions that must be performed—often simultaneously, such as heat transfer, reaction, mixing and so on. To make matters worse for the development and design engineer, mixing that may be good for one aspect of an operation may be deleterious to another. A central question is: Can one set of operating conditions [e.g., impeller(s), rotational speed(s), power input, baffles, internals, control systems] cover all requirements?

Consider a reacting solid–liquid–gas system with mass transfer occurring among the phases. The operations involved may include chemical reaction and mass transfer for gas absorption. The solids are reagents that are dissolving as the reaction proceeds. The operations are solids suspension and solids dissolution. The products or by-products, whose physical and purity characteristics are important in downstream processing, are crystallizing out of solution. The operations are mass transfer and crystal growth. Overall, the system is highly complex. Furthermore, it should be apparent that no single set of design correlations can cover this range of simultaneous interactions, even though it might be possible to design adequate systems for each of the operations.

One simple solution to the problem would be to specify a mixing system with enough energy to exceed the requirements for the most difficult individual operation. Often, this is done. A pilot plant version of the process may even run satisfactorily using this design strategy. However, for scale-up to the manufacturing plant, this strategy may give detrimental results due to overmixing e.g., overmixing with regard to crystallization and possible production of excessive fines, emulsions, or intractable foam from vapor-phase incorporation. In some cases, it may not be possible to accomplish the most difficult individual operation on the scale required by the manufacturing facility. It may then be necessary to use a specialty design such as a continuous in-line device or other special mixing system.

This scale-up problem is posed to illustrate the interacting features of multiphase batch reactors and the importance of developing a comprehensive strategy for scale-up. It stresses the need for versatility that must be built into reactor systems, the effectiveness that this can achieve in plant operation, and the limitations in cases that exceed such capabilities. In the laboratory, there is no substitute for testing reaction sensitivity over a broad range of conditions to provide as much information on allowable ranges as possible. The reader is referred to Section 17-2.6 for a discussion of this important tool for this type of experimentation.

## 17-2.1    Batch and Semibatch Reactors

A large majority of reactions are run in the batch or semibatch mode, making the stirred vessel the mainstay of chemical reaction engineering in the pharmaceutical and specialty chemical industries. The reasons for this reactor choice include:

1. *Complete conversion.* Reactions are generally run to achieve complete conversion of the limiting reagent—controlled by time and not subject to differences in completeness of conversion because of residence time distribution in a continuous stirred tank reactor.
2. *Accuracy of charge.* Reagent quantities can be carefully controlled and procedures for overchecks of quantities actually utilized.
3. *Productivity.* Reactor volume is often consistent with the limited productivity requirements characteristic of this industry.
4. *Flexibility.* Batch reactors can process a large variety of homogeneous and heterogeneous reactions successfully with little modification of internals and can be used in dedicated or multipurpose facilities. The use of variable speed drives along with versatile impellers are key factors.

Another aspect of flexibility is with respect to process changes (e.g., reaction times can be changed in response to scale-up problems), often resulting from short lead times from lab to manufacture, ability to rework material, and so on. The *disadvantages* of batch reactors in processing should also be noted.

1. *Reaction environment.* There may exist nonuniformity of mixing intensity throughout the vessel that can lead to undesirable side reactions caused by variations in local concentration environments.
2. *Optimum conditions.* One aspect of a reaction system may require different conditions than another which may overlap in time (i.e., a reaction that results in precipitation of a product or by-product may require different mixing intensities for the reaction and precipitation).
3. *Heat transfer.* High rates of heat transfer are not achievable without external pumping through a heat exchanger or by utilization of unwieldy internal coils. In these systems, heat transfer is often achieved by operating at reflux and using an external condenser to remove the heat.
4. *Thermal hazards.* A large volume of a reacting system with highly exothermic reactions or decompositions can pose severe thermal hazards.

Given this conflicting set of advantages and disadvantages, the mixing system design challenge is to identify the requirements of each reaction and to recognize the need for alternative reaction systems when a fit is not practical or possible for scale-up. The latter aspect is discussed later in this section. For homogeneous reactions, blending in the required micro-time scale is required, as discussed at

length in Section 13-2.5. For heterogeneous reactions, all combinations of liquid–liquid, gas–liquid, and solid–liquid conditions may be encountered, requiring evaluation of power requirements, impeller design, and vessel internals. As in the case of special reactor considerations, the role of the process development engineer is to determine when the standard batch reactor must be augmented in some way to carry out a particular reaction or reaction sequence successfully.

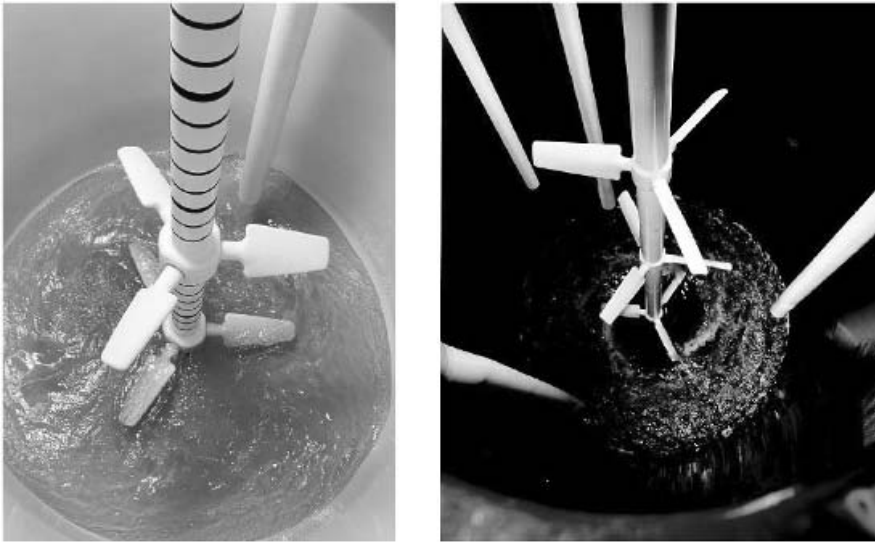## 17-2.2   Batch and Semibatch Vessel Design and Mixing

The versatility of the glass-lined vessel in a large variety of chemical environments has made it the workhorse of the industry. These reactors range in size from 80 to 20 000 L and larger. One limitation in the use of glass-lined vessels that is related to mixing and heat transfer is that the limit of temperature difference between jacket and batch is about 125°C. (The manufacturer should be consulted for specific limitations for the type of glass lining and base metal in use.)

The retreat-blade and anchor impellers that have been widely used for many years are now being replaced by glass-lined turbines and other shapes that have been developed by manufacturers using sophisticated methods of applying the glass to more sharply angled shapes. These turbines are available for vessels as small as 80 L, although shafts with removable interchangeable impellers are not available for tank sizes smaller than about 1200 L. These new impellers, especially in multitier configuration, have greatly improved the mixing capabilities of the glass-lined reactor by providing increased shear and circulation. A number of glassed impeller types are now available, including curved, pitched, vertical blade, and gas-handling turbines, several types of hydrofoils, helical ribbon, and traditional anchor. Some examples of these are shown in Figure 17-1. The lower turbine can be positioned within about 10 cm of the vessel bottom. For single turbines in larger vessels, however, the low turbine position may not provide the desired overall circulation.
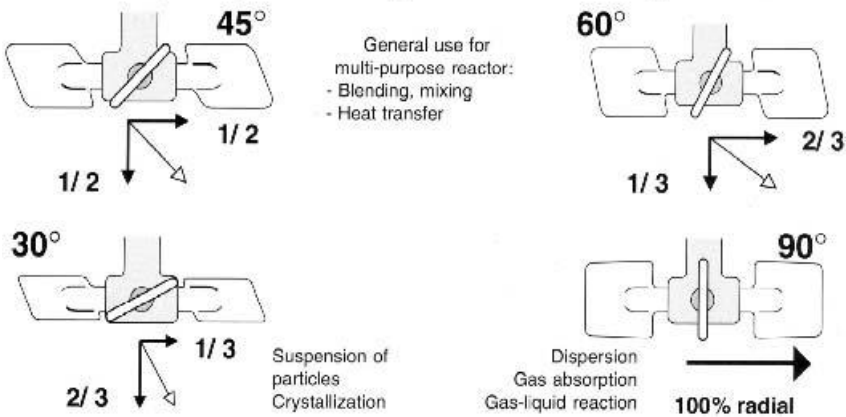
An additional consideration in the choice and testing of glassed mixing systems is that glassed turbines, because of at least minimal required rounding at the edges, do not provide exactly the same fluid dynamics (e.g., vortex shedding) as that of their metal counterparts, and this could affect some operations. The three manufacturers of glass-lined mixing systems use different methods of attachment of the blades of the impeller(s) to the shaft, Table (17-1).

Glassed baffle design changes have significantly improved mixing performance. However, most glass-lined vessel applications are limited to only a single baffle, to maximize the number of tank nozzles available for other purposes. Figure 17-2 shows baffling efficiency (power loading) of some traditional glassed baffle designs, relative to four wall baffles in a metal tank. For mixing applications that require more than one baffle, but for which additional nozzles cannot be spared, specialized multiple baffle configurations have been provided by several manufacturers.

The other commonly used batch reactor is the fully baffled turbine-agitated vessel, made from stainless steel and other alloys. This reactor can be used for

## A single agitator adapted for each requirement

**45°**
General use for
multi-purpose reactor:
- Blending, mixing
- Heat transfer
1/ 2
1/ 2

**60°**
2/ 3
1/ 3

**30°**
1/ 3
Suspension of
particles
Crystallization
2/ 3

**90°**
Dispersion
Gas absorption
Gas-liquid reaction
100% radial

(*a*)

**Figure 17-1** Typical glass-coated impellers showing recently developed technology by the manufacturers to coat sharp edges. (*a*) GlasLock® glass-lined still impellers. (Courtesy of DeDietrich Process Systems.)

some chemical environments that are not compatible with glass (i.e., strong bases, hydrofluoric acid). This reactor also has several advantages in construction and internal configuration, because of the advantages and versatility of stainless steel and other alloys in fabrication. An additional advantage is that, in general, a wider variety of impellers can be used, and as noted above, they do not have the (at least minimally) rounded surfaces required for glass. The most common metal
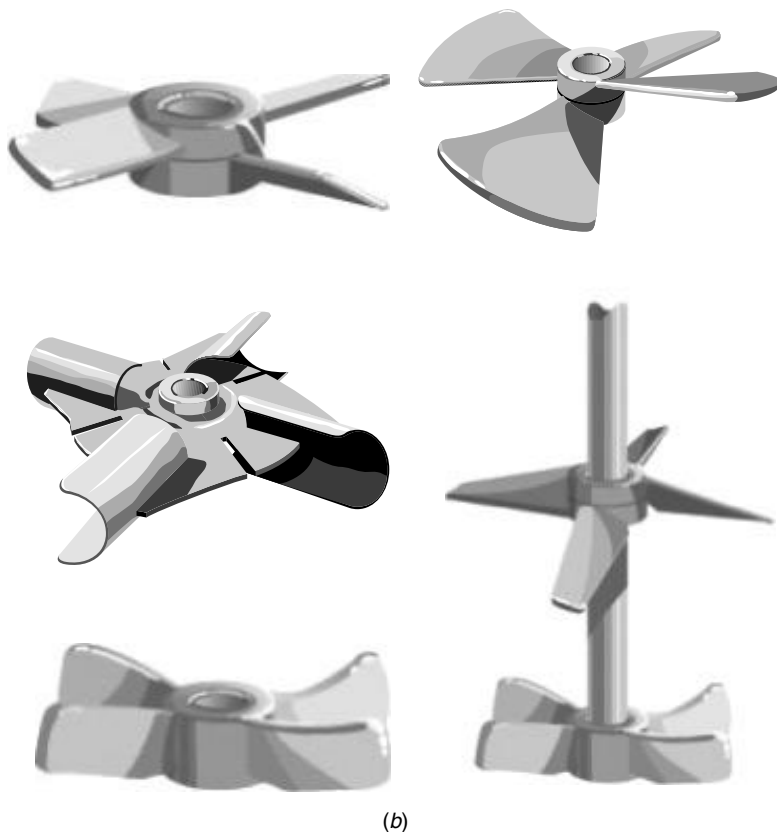
(b)

**Figure 17-1**   (b) Cryo-Lock® impeller. (Courtesy of Pfaudler, Inc.)

impellers are pitched blade turbines and hydrofoils for axial flow and flat-blade (Rushton) turbines for increased dispersion. See Chapter 6 for specifics on stirred vessel components, and Chapter 21 for the mechanical aspects of stirred vessels.

## 17-2.3   Multipurpose Design

Mixing requirements of batch and semibatch reactors vary over the full range of the mixing spectrum, from simple blending to high-shear specialty designs. A well-designed mixing system using the impellers described above, equipped with a variable speed drive, can cover the majority of cases. Variable speed capability permits mixing to be adjusted for specific functions such as dissolution of solids, crystallization during reaction, addition of gases, and so on. Scale-up is also greatly facilitated when the speeds of both the pilot and production scale vessels can be varied, thereby decreasing dependence on the reliability of mixing scale-up correlations to achieve specific results. Although variable speed drives add additional capital expense (∼5% of vessel cost) and may not be needed in many

<center>(*c*)</center>

**Figure 17-1** (*c*) ElcoLock® and fixed impellers. (Courtesy of Tycon Technoglass, a Robbins & Myers company.)

cases, the versatility of a reactor is greatly enhanced for future applications or in multipurpose applications (see Chapter 21 for specifics on variable speed drives).

Mixing in semibatch vessels is also complicated by the range in volume that may be encountered during the course of a particular series of steps being carried out in the same vessel. Correlations normally characterize mixing at

**Table 17-1**    Glass-Lined Impellers and Their Methods of Attachment

|  | Blade Attachment | Removable? | Variable Pitch? |
|---|---|---|---|
| DeDietrich | GlasLock: friction fit of blades into holes in the hub | Yes | Yes (up to power limit of motor, gearbox, shaft) |
| Pfaudler | Cryo-Lock: liquid $N_2$ cooling to shrink the shaft | Yes | No (different pitches available) |
| Tycon | ElcoLock | Yes | No (different pitches available) |
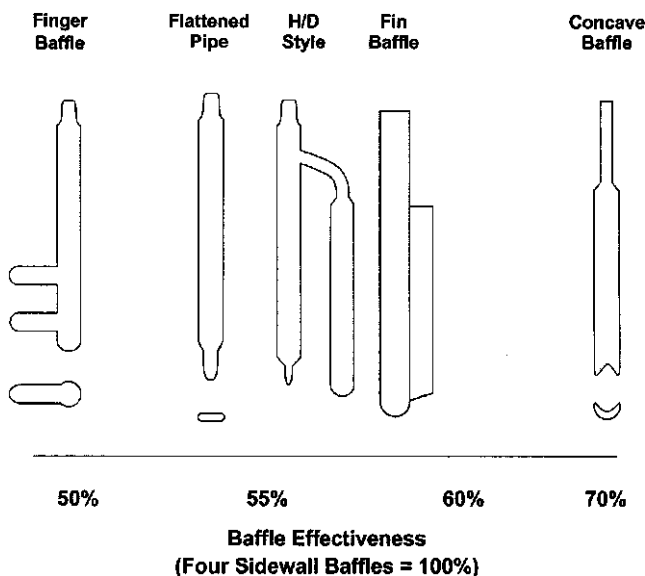


**Figure 17-2**    Power-loading efficiency of some typical glass-coated baffles. (Data courtesy of Pfaudler, Inc.).

height/diameter ratios from 2 to 1. However, low volume ratios ($<0.5$) are often encountered at the beginning or end of an operation when reagents are added or solvents removed. Under these conditions, vapor may be entrained, causing foaming (may be prevented by reduced speed), or solids may not be suspended properly (may require provision of a special low-volume blade in some cases). In glass-lined vessels, the batch may actually be below the bottom of the baffle(s), leading to instabilities, especially with solids present.

Different types of impellers are used for a variety of mixing requirements. Although it is not possible to cover all cases, applications of the various impellers can be classified by their relative input of shear and circulation (see Chapter 6 for power numbers and mixing characteristics of various impellers). Velocity

distributions and shear can be determined by laser Doppler anemometry and other methods (Chapter 4). More specific mixing requirements are discussed in the sections on homogeneous and heterogeneous reactions later in this chapter and in Chapter 13, as well as in Chapters 18 and 20. Chemical reaction engineering issues in the fine chemicals industry are discussed by Carpenter (1985, 2001).

### 17-2.4   Batch and Semibatch Scale-up Methods

Much of the literature on scale-up of reaction systems has focused on continuous systems. However, scale-up methods for batch and semibatch operations have been included in several books, including Oldshue (1983), Whitaker and Cassano (1986) Carberry and Varma (1987) Froment and Bischoff (1990), Tatterson (1991), Harnby et al. (1992), and Baldyga and Bourne (1999). Correlations for heat transfer, mass transfer, liquid–liquid dispersions, solids suspensions, and dissolution are available and are discussed in these references and in several chapters of this book. Mixing requirements for scale-up of homogeneous reactions are discussed in Chapter 13, including explanation of the limitations of the usual mixing scale-up parameter of equal power per unit volume. The reader is referred to the texts listed in the references, in which these correlations are well developed. These correlations are not reproduced in this chapter.

Characterization of the physical and chemical parameters of multiphase systems with complex reactants and interfacial phenomena is extremely difficult and may limit the usefulness of the correlations mentioned above. Achievement of a scalable microenvironment is also difficult but may be crucial to successful scale-up. These factors, combined with the multiplicity of uses for batch reactors, argues for maximizing the versatility of both pilot and production scale equipment to encompass a range of operating conditions for specific reactions, as well as to maximize the number of different reactions that can be run successfully. Methods of achieving this versatility are discussed in later sections and in Chapter 13. However, as wide as this range may be, there will be many reactions that cannot be scaled-up successfully without incorporation of reactor design alternatives. We discuss some of these in the next section.

### 17-2.5   Continuous Reactors

Continuous reactors in the pharmaceutical and specialty chemical industries may not only be needed for high productivity as in other segments of the chemical industry, but additionally to solve specific reactor design problems caused by limitations in batch operation. These limitations include heat transfer, mass transfer, and mixing. Continuous reactors are also used to minimize the reacting volume of thermally potent and/or noxious reactions and to decrease the potential and exposure for catastrophic failure of a vessel. Chemical industry reactor standards such as packed bed, fluid bed, and trickle bed reactors find limited utility since this type of phase contacting can usually be achieved in a slurry reactor, where residence time distribution variations, which can lead to changes in product distributions, are eliminated. Continuous stirred tank reactor operation is used only

rarely to increase productivity. Operation in this mode can be subject to product selectivity problems.

Tubular reactors with high mixing efficiency and good control of reaction temperature profiles and contact times are used for fast consecutive reactions. An interesting and effective variation on a tubular line mixer is the addition of a centrifugal extractor in series to achieve rapid separation of phases (Example 13-8a, Chapter 13). The local mixing intensity of a well-designed in-line mixer can exceed that of a well-mixed reactor even in the zone of an impeller. The line mixer has the added advantage of allowing the reaction to proceed under more constant conditions of concentration and mixing intensity than can be achieved in a batch or semibatch reactor (Examples 13-3, 13-6, and 13-8a).

The design of continuous reactors has received extensive coverage in the literature. Operating parameters such as residence time, residence time distribution (Nauman and Buffham, 1983), and mixing requirements must be rigorously established for successful scale-up. Since most of the applications are for fast reactions, however, large scale-up factors are often not encountered. The limitation to experimentation may well be the amount of intermediates available for testing at the piloting stage since throughput of the smallest prototype may be relatively large. The combination of high heats of reaction, high reactant concentration, extremely fast reaction rate, and simultaneous or consecutive reactions to undesired products presents an extreme challenge to development and design engineers. Heat transfer and micromixing requirements must be satisfied simultaneously. Stirred tank, wiped film evaporator, and tubular reactors with static mixing elements are compared in an industrial study by Schutz (1988). This system is described in Example 13-7.

## 17-2.6  Reaction Calorimetry

Reaction calorimetry is hardly a new technique. One often thinks of thermodynamics when one thinks of calorimetry since calorimetry has long been used to determine thermodynamic properties of materials and chemical processes. However, with the advent of automated reaction calorimeters such as Mettler's RC1, calorimetry began to be employed as a powerful laboratory tool for studying kinetics and mechanisms as well as scale-up and mixing properties of chemicals and processes in process development for pharmaceutical applications (Landau et al., 1994, 1995; Sun et al., 1996a).

Accurate measurement of kinetics is essential for investigation of reaction mechanisms, since kinetics are a "reflection" of the reaction mechanism, as well as for successful process development and optimization. It is important to evaluate the impact of process parameters such as agitation rate, mixing intensity, and mass transfer on overall rate and selectivity of the chemical process. According to the types of data obtained, methods for measurement of kinetics may be classified into two categories. The first category provides information on concentrations and conversion, or *integral properties*, since they measure integration of variables such as rate from the beginning of the reaction to the point of measurement.

To obtain rate, one has to differentiate these integral results with respect to time. Obviously, an accurate determination of rate from these integral properties requires high rates of sampling.

The most commonly used integral method for monitoring kinetics of synthetic organic reactions is direct sampling from the reactor followed by chemical analysis. Although this method is valuable in providing concentration, or conversion information, and in particular, chemical identities of components in the reactor, it has a threefold deficiency insofar as a determination of kinetics is concerned. First, only integral properties (e.g., concentration) are measured. Second, in reality, only a limited number of samples may be taken per reaction, a factor that makes it highly inaccurate to determine instantaneous rate by differentiating the concentration data with respect to time. Finally, it is not an in situ method. The sample has to be taken away from the reacting atmosphere for workup and analysis, during which period the sample may undergo chemical changes, thus distorting the true profile of components in the reactor.

Other integral methods include in situ spectroscopic techniques, such as time-resolved infrared spectroscopy, which measures concentration or conversion as well as provides information on chemical identities of components in the reactor. In contrast to the chemical sampling method, the infrared (IR) spectrum of the reacting system may be collected at a much faster pace than that normally possible for the chemical sampling method. Consequently, rate data may be derived with good accuracy by differentiating the IR intensity data with respect to time.

The second category of methods is characterized by direct measurement of *differential properties* such as the instantaneous rate of the reaction. Reaction calorimetry, representing this category of methods, is a more powerful method for monitoring kinetics. Modern reaction calorimetry measures the *rate* of heat flow into or out of a reactor, typically 1 L in volume, during reaction while maintaining precise control of the temperature of the contents in the reactor. A schematic of a reaction calorimeter is shown in Figure 17-3. The characteristics of the reactor and the reaction mixture, i.e., UA, and $mC_p$, are determined through a simple and automatic sequence, thus allowing accurate determination of the heat flow, $q_r$, as a function of time during reaction. The heat flow measured under isothermal conditions is directly proportional to reaction rate, or to be more precise, a summation of the rate of each reaction step as weighed by heat of reaction $\Delta H_i$ of the corresponding step:

$$q_r = V_r \sum_i \Delta H_i \frac{dC_i}{dt}$$

where $V_r$ is the volume of the contents in the reactor and $\Delta H_i$ is the heat of reaction for the ith step. In addition, the reaction calorimeter conducts the measurements in an in situ, noninvasive, and continuous fashion, which is difficult, if not impossible, to achieve using the chemical sampling method. Although the chemical sampling method is most valuable in providing information on the
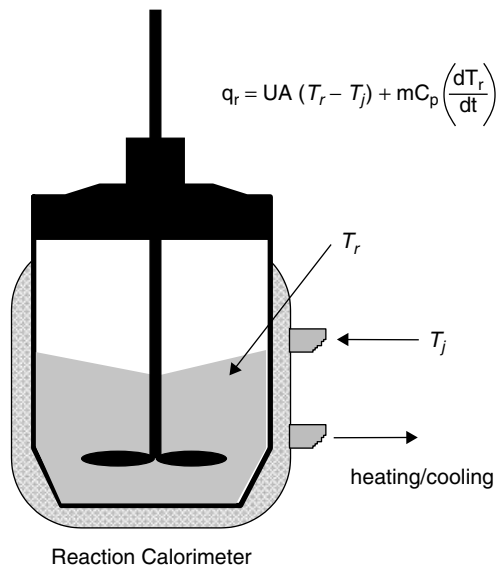
$$q_r = UA\,(T_r - T_j) + mC_p\left(\frac{dT_r}{dt}\right)$$

$T_r$

$T_j$

heating/cooling

Reaction Calorimeter

**Figure 17-3**   Schematic of a reaction calorimeter.

chemical identities of components in the reactor, it is not an accurate kinetic tool. The salient advantages of the reaction calorimetry may make up for its obvious shortcoming in such a way that accurate measurements of kinetics may be achieved. Furthermore, when combined with other in situ compositional analysis tools, such as infrared spectroscopy as well as direct sampling, reaction calorimetry would enable one to obtain a complete picture of kinetics and reaction pathways associated with a chemical reaction. This integrated approach has been used successfully to elucidate the reaction pathways of a number of catalytic selective hydrogenation reactions (LeBlond et al., 1998), to evaluate the effects of mixing intensity and gas–liquid mass transfer on enantioselectivity of asymmetric hydrogenation (Sun et al., 1996b,c) and to determine whether a process is operating under mass diffusion limitations (Landau et al., 1995). Reaction calorimetry allows measurement of the intrinsic kinetics of a chemical process as well as a determination of the influence of process parameters, including mixing intensity, on the outcome of a chemical process, such as rate and selectivity, thus allowing one to predict process scale-up properties.

## 17-3   HOMOGENEOUS REACTIONS

The reader is referred to Chapter 13 for detailed discussion of this topic. A comprehensive treatise is that of Baldyga and Bourne (1999).

Reactions that are truly homogeneous throughout their entire course may or may not be affected by mixing or other scaling variables, depending on their reaction rates. Slow, homogeneous reactions can be scaled up directly by appropriate

increase in volume, when blend time for reagents is rapid compared with reaction rates and when heat transfer rates are adequate to maintain any fixed temperature or temperature profile. The reaction(s) must be sufficiently slow that significant conversion occurs only after the reagents are homogeneously blended on a molecular scale (i.e., the meso- and micromixing conditions have been satisfied).

### 17-3.1  Mixing-Sensitive Reactions

Many examples of mixing-sensitive reactions have been identified in reactions that are homogeneous but whose reaction rates are sufficiently rapid to result in significant conversion during mixing of reagents prior to the achievement of complete homogeneity on a molecular scale. Many of these examples are from reaction types that are run in the fine chemicals and pharmaceutical industries, and their identification can be essential to successful development and scale-up. Homogeneity of the reaction systems makes them more accessible to analysis than the more frequently encountered heterogeneous reactions. However, the generalizations that are developed can be applied qualitatively, and in some cases quantitatively, to heterogeneous systems.

One of the most difficult aspects of the scale-up of both homogeneous and heterogeneous reactions is the prediction and control of by-product distribution. Mixing sensitivity is not only an issue through loss of yield of the major product by consecutive and/or parallel reactions but also by an increase in the amount of by-products formed. These by-products may be negligible on a laboratory or even a pilot plant scale, but may increase on scale-up to production. An increase of as little as 0.1 to 1.0% in the amount of a particular by-product may not be acceptable when it cannot be adequately removed by downstream processing. These impurities may affect physical form, particle size, downstream liquid–liquid separation, or foaming tendency. If the impurity level rises above about 0.1%, product registration may be affected.

This problem is difficult because the threshold reaction rates and rate constant ratios that are significant may be far lower than anticipated by laboratory experiments. In addition, the mixing scale-up issue with regard to a decrease in local mixing intensity and an increase in circulation time may result in an unexpected increase in by-products. The reader is referred to Chapter 13 for additional discussion and several examples.

*17-3.1.1  Laboratory Prediction of Mixing Sensitivity*. The challenge in development is to predict mixing-sensitive behavior so that the mixing and/or reaction system can be modified to circumvent the issue. The use of estimates of the Damkoehler number (Da), the ratio of the reaction rate to the mixing rate, is recommended as outlined in, Sections 13-2 and 13-4. As a first approximation, the following types of laboratory experiments can be recommended to attempt to establish whether or not a potential problem exists:

1. For consecutive reactions, the mixing sensitivity can be assessed by running the reaction in the reverse addition mode such that there is a large

excess of the reagent that can cause overreaction. One reason for no over-reaction is that there is no pathway in the reaction system for a consecutive reaction. That information can be very helpful on scale-up by eliminating one possible pathway for failure.

2. For consecutive or parallel reactions, runs comparing very poor mixing and very good mixing can be helpful as a first indication of sensitivity. Any differences, however small, should be cause for further study. In some cases, laboratory mixing, even when very poor, can be sufficient to prevent differences in product distribution. In these cases, pilot scale experiments may be required.

3. A step-by-step recommended procedure for determining mixing sensitivity based on evaluation of the Damkoehler number may be found in Section 13-4.

4. A laboratory reaction calorimeter can be very helpful in this type of experimentation. Use of this device is described in Section 17-2.6.

5. Although there is no general rule or agreement on minimum size since there are critical dependency requirements of the specific operation, 4 L is considered a minimum, recognizing the probable limited amounts of materials available or practical to obtain. Larger vessels can obviously provide better scale-up data. Smaller vessels (1 L) can also be adequate provided that they follow a standardized configuration.

6. The reaction vessel should be cylindrical with a standard turbine, alloy or glass, agitation system, with baffles.

7. A laboratory favorite, the round-bottomed flask, must be avoided since the results cannot be deemed reliable for mixing information and even for accurate assessment of selectivity for fast reactions.

Additional methods of assessing sensitivity are available for heterogeneous systems and are discussed in Section 17-4 and in Chapter 13.

### 17-3.1.2 *Previous Work on Mixing and Homogeneous Reactions*. The earliest work on the effect of mixing on homogeneous reactions as initially carried out by Danckwerts (1957, 1958) was focused on the effect of mixing on conversion rate resulting from incomplete blending in continuous reactors. Several papers appeared on this subject, including those of Toor (1962), Keeler, et al. (1965), Vassillatos and Toor (1965), Kattan and Adler (1967), and Harris and Srivastava (1968). Experimental and theoretical work in this area has continued with a primary focus on the study of micromixing. Acid–base neutralizations are essentially instantaneous and therefore mixing controlled. These and other reactions have been used in studies by Rice et al. (1964), Mao and Toor (1971), Klein et al. (1980), Li and Toor (1985), Shenoy and Toor (1989, 1990), to measure micromixing using indicators and other means to measure instantaneous reactions.

Kinetic problems with reaction systems in the pharmaceutical industry are more concerned with selectivity in complex systems than with conversion rate.

However, the fundamental mixing characteristics that affect mixing-controlled conversion are the same as those that can affect selectivity and yield in complex systems. The effect of mixing on selectivity was predicted qualitatively by Levenspiel (1962) in his classic text on chemical reaction engineering. Several studies on specific reactions have since appeared in the literature, including Paul and Treybal (1971), Truong and Methot (1976), Bourne and Kozicki (1977), Bourne et al. (1977a,b, 1981b), and Nabholz and Rys (1977).

In addition, excellent papers on the chemical and physical aspects of mixing-sensitive reactions, including modeling of the mixing effects, have been published, including Ott and Rys (1975), Canon et al. (1977), Belevi et al. (1981), Bourne et al. (1981a), Angst et al. (1982a,b), Bolzern and Bourne (1983), Baldyga and Bourne (1984a, 1988, 1989), Bourne (1984), Mann and Hamouz (1991), Wang and Mann (1990), Angst et al. (1982a), and Laufhutte and Mersmann (1987). A recent publication by Heeb and Brodkey (1990) presents a molecular-based statistical simulation model that was developed to study the covariance terms for mass transfer during mixing of reactants undergoing complex reactions. Finally, some publications on the effect of scale-up have appeared, including Bourne and Dell'ava (1987), Bourne and Hilber (1990), Paul (1990), Rice and Baud (1990), and Wang and Mann (1992). The subject is covered comprehensively in the treatise of Baldyga and Bourne (1999).

### 17-3.1.3 *Mixing-Kinetic Problem*.

The reaction scheme that has received the most attention in both theoretical and experimental investigations of the effects of mixing on selectivity is the competitive-consecutive reaction. In addition, the parallel reaction system is receiving attention for its importance in reactions and pH adjustments. These systems are discussed in Chapter 13 and highlighted here because of their fundamental importance in the fine chemicals and pharmaceutical industries. The reaction scheme is as follows:

$$A + B \xrightarrow{k_1} R$$

$$R + B \xrightarrow{k_2} S$$
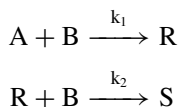
with B added to A in the semibatch case or A and B mixed continuously in the tubular reactor case. R is considered as the desired product. The objective is to determine how mixing conditions can affect the yield of R. We are concerned with the time period during which the reactants are first contacted and when they are completely mixed to a molecular scale. During this time, zones of local B concentration can vary from an upper limit equal to the feed concentration to a lower limit of essentially zero. The course of any reaction that is influenced by concentration has the potential to be influenced by mixing. The effect can be on the reaction rate, the product distribution, or both (see Examples 13-3, 13-4, and 13-6).

Parallel reactions can also be subject to mixing effects, as shown by Baldyga and Bourne (1990), Paul et al. (1992), and Wang and Mann (1992), (see Example 13-8b). A critically important type of parallel reaction is the potential for decomposition of substrates during pH adjustments. Such reactions are very

common in the fine chemical and pharmaceutical industries and in fermentation (see Chapter 18). Scale-up to large vessels can result in serious losses in selectivity.

Mixing effects are of far greater importance on product distribution in multiple reactions because the impact on design and economics is more profound. In such reactions the product desired is one of two or more possible products. The selectivity of a reacting system is defined as the ratio of the amount of desired product to the total amount of limiting reagent actually reacted. The yield, Y, is the ratio of the amount of limiting reagent reacting to produce the desired product to the total amount of limiting reagent charged.

### 17-3.1.4   *Selectivity in Homogeneous Reactions*.   In semibatch operations, provided that reactant B is mixed instantaneously to a molecular level with the vessel contents, the maximum selectivity in a competing-consecutive reaction system is a function of the rate constants $k_1$ and $k_2$, the overall molar charge ratio of A to B, and the degree of conversion of A. The degree of conversion of A can depend on the charge ratio and residence time. This discussion is limited to the case of sufficient residence time such that all of the B charge will react, provided that B is not charged in excess for complete reaction to S. The maximum selectivity of R, in the absence of mixing effects, then becomes a function only of $k_1/k_2$ and the molar charge ratio. For purposes of the present discussion, it is convenient to establish a fixed molar charge ratio. The ratio chosen is not necessarily intended to give the maximum selectivity since consumption of starting material may be a prime consideration. For a particular reaction system, (fixed $k_1/k_2$), a fixed molar charge ratio, and conditions of perfect mixing, the selectivity is also fixed, as is the yield and the degree of conversion of A.

At this point it is convenient to discuss the yield of R rather than the selectivity. The term *expected yield* is used to denote the yield that would be obtained under conditions of perfect mixing, as derived by van de Vusse (1966) and Levenspiel (1962).

$$Y_{exp} = \frac{R}{A_0} = \frac{1}{(1 - k_2/k_1)} \left[ \left( \frac{A}{A_0} \right)^{k2/k1} - \frac{A}{A_0} \right] \qquad (17\text{-}1)$$

where capital letters denote molar concentrations. This equation applies to both batch and semibatch operations, provided that both reaction rates depend on B in the same way and provided that B is added to A in the semibatch case.

Less than perfect mixing may reduce, but not increase, the yield in homogeneous systems. The primary concern is the magnitude of the yield reduction attributable to deviation from instantaneous, perfect mixing to a molecular level. The reader is referred to Chapter 13 for additional discussion of these key issues.

## 17-3.2   Scale-up of Homogeneous Reactions

Scale-up of reacting systems in the pharmaceutical industry is often considered to be a simple matter of an appropriate increase in size of the reaction vessel. This

simplification is indeed applicable to homogeneous reactions in which the product distribution is a function of the kinetics only and thermal effects can be controlled by conventional methods. The majority of homogeneous reactions fall into this category or at least appear to. In the pharmaceutical industry this scale-up issue requires particular attention during process development. Even very small deviations in product distribution can result in significant separation problems that must be addressed to meet the stringent requirements for consistency of product purity between laboratory-, pilot-, and production scale operations. Reaction scale-up problems are thus better resolved by reactor design modification than by downstream purification modifications. The objective is to achieve constant product distribution on scale-up: changes in product distribution profiles as small as 0.1% in an impurity level may make the product unacceptable.

The primary function of the development chemist or engineer, therefore, is to determine for each reaction whether or not special design considerations are required. In some cases, laboratory work at different mixing levels will indicate mixing selectivity. In other cases, however, even pilot plant operation will not reveal subtle deviations from expected product distribution. In general, the absolute value of the primary reaction rate is the most reliable predictor of mixing sensitivity. If the reaction half-life is within one or two orders of magnitude of the blend time for the plant scale reactor, a mixing dependence might be expected, as can be determined by estimation of the Damkoehler number.

It is important to note that the reaction rate as represented by $k_1$ may apply either to the principal reaction or to addition of a substance that could react with any of the substrates in a parallel reaction. For example, if an acid or base is added to adjust pH, the local concentrations at the point of addition could cause reactions that would not be expected over the intended pH limits. Such unexpected reactions could lead to substrate decomposition. The reader is referred to Chapter 13 and Example 13-8b for more information on this effect.

Scale-up studies on mixing-sensitive homogeneous reactions were run using diazotization of 1-naphthol as the model system as reported by Bourne and Dell'ava (1987), Paul (1988), Bourne and Gablinger (1989), and Rice and Baud (1990). These studies showed that both micromixing and macromixing must be considered in larger vessels because the circulation time increases even when local micromixing at the point of addition can be maintained relatively constant. Increased circulation may therefore be required to maintain the mole ratio balance between reagents A and B in the mixing zone where the actual reaction is occurring. A local insufficiency in A will result in an overreaction to S regardless of local micromixing intensity. B may also be less available because of "engulfment" (mesomixing effect), discussed in Chapter 13.

## 17-3.3   Reactor Design for Mixing-Sensitive Homogeneous Reactions

***17-3.3.1   Semibatch Reactors***.   When other considerations preclude the use of in-line mixers and large vessels must be used, two methods of minimizing or eliminating mixing deficiencies can be used. Both multiple turbines and multiple

addition points have been shown to be effective in reducing overreaction. These methods are compatible and can both be used in the same reactor. The effectiveness of multiple turbines was shown by Paul (1988) and for multiple addition points by Bourne and Hilber (1990). A preferred configuration for multiple turbines with a single optimal addition point is shown in Figure 13-9. The addition of a multiple-point feed distributor would be expected to further enhance this effectiveness. Care must be taken, however, in the design of this type of addition line with regard to placement and nozzle discharge velocity. Furthermore, the time of addition must be sufficient to prevent macromixing and mesomixing from becoming factors.

**17-3.3.2   *In-line Mixers*.** The preferred reactor design for extremely fast or sensitive reactions is an in-line mixer of appropriate design. Various possibilities have been investigated, including centrifugal pumps (Bolzern and Bourne, 1985), rotor–stator mixers (Bourne and Garcia-Rosas, 1986), impinging thin liquid sheets (Demyanovich and Bourne, 1988, 1989), reaction injection molding (Lee et al., 1980), and vortex mixing (Bowe, 1990). The impinging jet design inherent in the technology of reaction injection molding and the vortex design seem to present high degrees of micromixing such that the blending of reagents should be completed to the molecular level in the minimum time. The advantage of in-line mixing devices is to eliminate the need for scale-up of macromixing and mesomixing parameters since the correct mole ratio can be maintained by the feed system and the mixer is required to provide adequate micromixing only. An example of a homogeneous consecutive reaction is presented in Example 13-3.

## 17-4   HETEROGENEOUS REACTIONS

Heterogeneous reaction systems are very common in the pharmaceutical and specialty chemical industries because of the limited and unusual solubility of many reagents and reaction products. Contributing factors to these characteristics are high-molecular-weight (300 to 1000) and multifunctional molecular structures. In addition, because heterogeneous systems can in some cases be manipulated to achieve improved yields compared to a homogeneous system with the same reactions, there can be an advantage in running under heterogeneous conditions or in some cases to deliberately create a heterogeneous system for the purpose of improving selectivity.

The discussion of selectivity considerations in homogeneous reactions in Section 17-3 is intended to provide an introduction to the far more complex issues involving heterogeneous reactions. The continuity of theoretical and practical considerations between these different types of reacting systems is provided by the obvious fact that the course of reactions is determined by events at the molecular scale whether or not the reactive molecules are in the liquid, solid, or gas phase when they enter the reaction zone. As in the case of homogeneous reactions, the course of a complex reaction will be determined by local molar

ratios and kinetics. The degree of deviation from expected kinetic behavior is determined by the reaction rate relative to the rates of mass transfer and mixing. Differences in selectivity between the same reaction run under homogeneous conditions and heterogeneous conditions are illustrated in Example 13-4.

This example indicates that the homogeneous reaction environment with regard to minimizing a consecutive reaction is more selective than the film around a dissolving reagent. The result can be represented as an increase in the apparent rate constant ratio, $k_2/k_1$, for the heterogeneous condition as indicated in Figure 13-11, where the loss in selectivity [increase in X, where $X = 2S/(2S + R)$] is plotted against $k_1$. Deviations in the case of homogeneous reactions are more amenable to quantitative analysis and can therefore be developed more completely. The same local considerations apply in heterogeneous reactions where expected overall molar ratios between reactions cannot be maintained because of mass transfer limitations at phase boundaries. For simple reactions, overall reaction rates may be affected and usually decrease, but yield is unaffected, given equal degrees of conversion. For complex reactions, the selectivity may be decreased, but unlike homogeneous systems, can also be increased under certain circumstances.

The other key difference between homogeneous and heterogeneous reactions regarding selectivity is that significant effects can occur in heterogeneous systems at far lower absolute reaction rates because the mass transfer limitations can be very severe. In addition, these effects can be subject to considerable magnification on scale-up to plant operations.

### 17-4.1 Laboratory Scale Development

Laboratory experimentation is the primary approach to characterization of reaction systems. This work must be designed carefully to prevent diffusion and mixing limitations from appearing unimportant at this scale when they may be significant at the manufacturing scale. Extremes of mixing and/or reaction conditions must be explored to fully characterize the interacting responses of these complex physical and chemical factors (see Section 13-4 for a recommended laboratory program). One final consideration in the selection of equipment is the subsequent purification and isolation process. It may prove advantageous or even essential to integrate key elements, such as simultaneous extraction or crystallization with the reaction step. This consideration is developed further in Examples 13-8a and 17-2.

### 17-4.2 Gas–Liquid and Gas–Liquid–Solid Reactions

***17-4.2.1 Gas as Reagent***. With the exception of fermentation, which is the subject of Chapter 18, the most common gas–liquid reaction in the pharmaceutical industry is hydrogenation. The intrinsic reaction rates of hydrogenation reactions vary over several orders of magnitude and can fall into any of the reaction categories discussed in Table 13-8. Design of a hydrogenation system is generally focused on supplying a sufficient quantity of hydrogen so that hydrogen concentrations in the bulk or adsorbed on the catalyst will not be limiting. In

many cases, this can be accomplished by suitable design of a subsurface sparger to accomplish absorption during transit from sparger discharge to vapor space. In some cases, however, the absorptivity or reaction rate is slow enough so that reabsorption from the pressurized vapor space is required. This can be accomplished with special gas–liquid mixing designs, such as the Praxair advanced gas reactor (Litz, 1985). Both cases are often seen in batch operations with high rates and in mass transfer control initially, changing to slow rates with kinetic control at the end. Liquid levels may vary, making reabsorption difficult to predict.

Many gas–liquid reactions other than hydrogenations are run in the pharmaceutical industry. Reaction system design depends primarily on the solubility of the gas in the reaction mixture and on its rate of reaction. Soluble gases can often be added without sparging via a vortex created by impeller design. Pitched blade turbines with partial baffles are effective in this regard. For complex reactions, the product distribution can be affected by mixing in direct analogy to the homogeneous case discussed earlier. Some of the first experiments in this area were conducted on chlorination of *n*-decane by van de Vusse (1966) in which mixing was shown to affect the distribution of chlorinated products. The chlorination of acetone (Example 13-6) also shows an effect of mixing on this reaction.

### 17-4.2.2  *Gas as By-product*.

Removal of a volatile reaction product by fractionation to drive equilibrium reactions to completion (e.g., esterification) is well known and presents no mixing issues beyond heat transfer rate and suspension. When a volatile product reacts in competing or consecutive reactions to form an undesired side product, special design measures must be considered. The goal is to accomplish removal of the volatile product rapidly enough to maintain its concentration in the reaction mixture at a suitably low level. In most cases, the volatile product can be removed by simultaneous distillation provided that the distillation rate and volatility are sufficient to maintain the desired critical solution concentration. Poor mixing could cause reduced selectivity by causing a reduction in heat transfer rate, thereby reducing the effective primary reaction rate and extending the time available for the production of by-products. Foaming may often be a problem, especially due to impurities, fine solids, or second liquid phase.

In some cases, other methods for removing the volatile product are required. The distillation may be too slow, relative to the reaction rate, or low relative volatilities may preclude removal of the volatile product to a concentration low enough to prevent overreaction. This problem can be solved by the addition of adsorbents, such as ion-exchange resins or molecular sieves, for the in situ removal of the volatile product (e.g., water or HCl). Mass transfer considerations will govern the effectiveness of such solid adsorbents; surface area and particle size are the critical factors. In cases where the mass transfer limitation is still significant under all practical surface areas and particle sizes, it is sometimes possible to add a chemical scavenger that removes the by-product by homogeneous chemical reaction. These mixing and mass transfer issues are illustrated in Example 17-1.

***Example 17-1: Removal of By-product Gas by Adsorption*** (Weinstock 1986).
This example is of a reaction system in which a by-product (HCl) that is gener-
ated by the primary reaction would decompose both the desired product and the
starting material to give essentially no product yield unless its concentration is
controlled. The actual selectivity as well as the conversion rate is a function of
the method and extent of this control. The chemistry is shown in Figures 17-4
and 17-5, and the reaction system is summarized in Figure 17-6. The method of
controlling the concentration of HCl below a value that causes excessive decom-
position while maintaining its concentration high enough for its participation in
the required reactions is critical to the success of the overall scheme. The product,
R, is made in relatively large volume. A feasible, commercially viable synthesis
of this compound was essential for operation in a manufacturing environment.

There are two distinct reaction types taking place: (1) reactions to form imides
and (2) HCl-promoted imide cleavages producing amides and an acid chloride.
Consecutive decomposition by reaction with HCl always proceeds depending on
the concentration of HCl. If no method of mediating the HCl concentration was
applied, the concentration of HCl would increase to 0.1 $M$ and result in complete
decomposition of R. It was determined that an optimum concentration of 0.004
$M$ is required for imide cleavage.

Molecular sieves (3A or 4A) were found to be very effective for this mediation
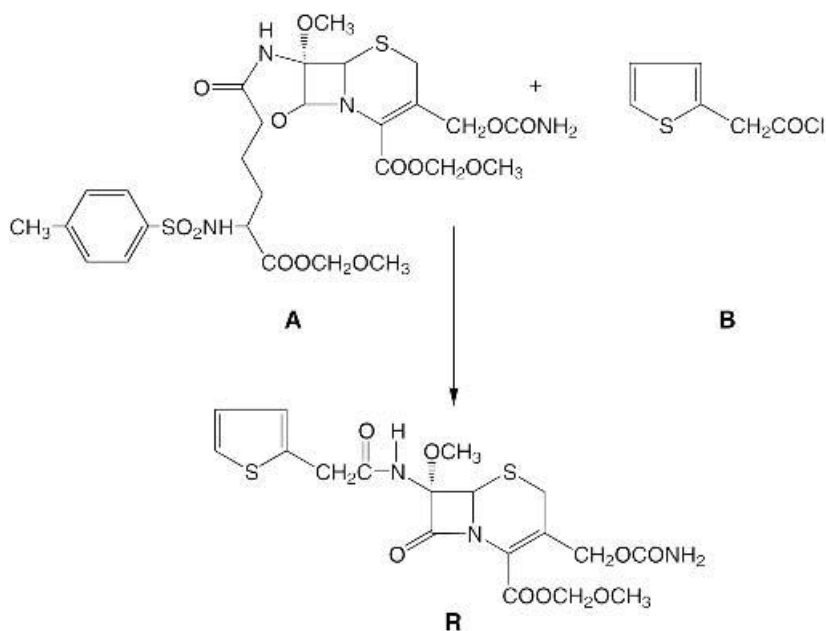under very well defined conditions. The HCl concentration in solution is affected



**Figure 17-4**   Overall chemistry of the transacylation reaction in an antibiotic synthesis
in which rapid removal of by-product HCl is essential for practical operation.
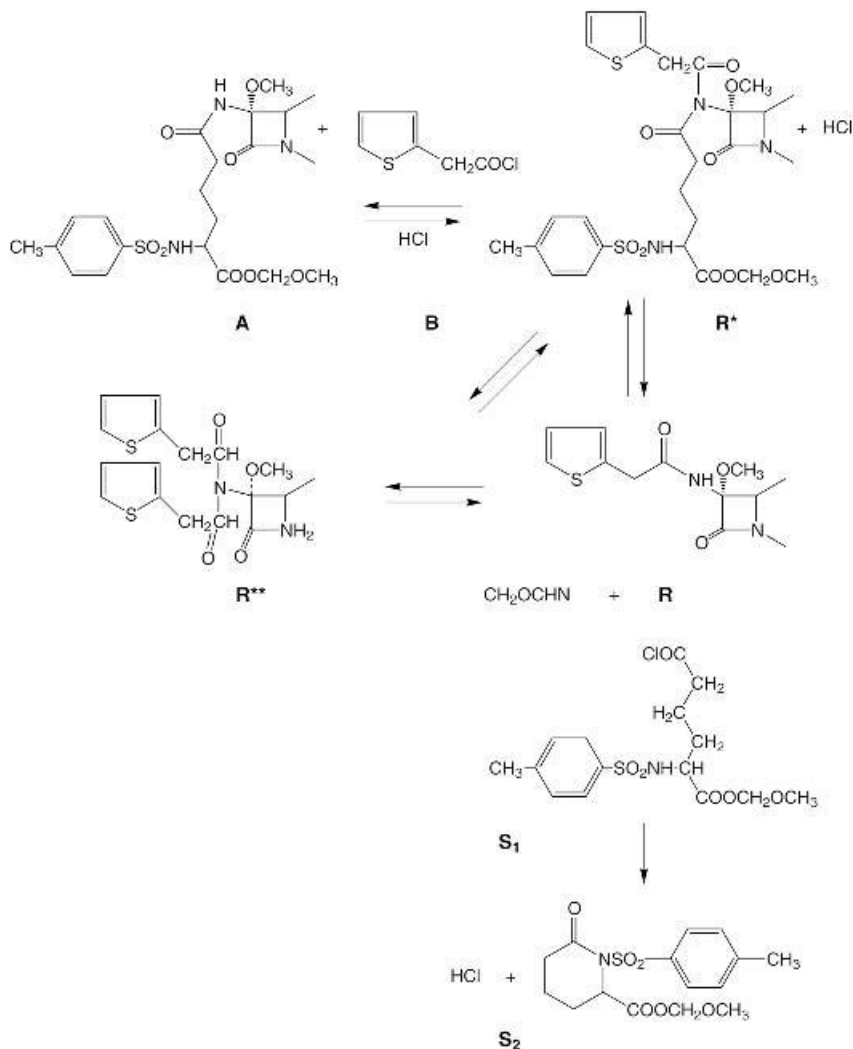
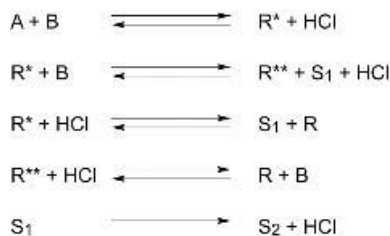**Figure 17-5**   Chemical intermediates in the transacylation reaction pathway.



**Figure 17-6**   Kinetic representation of the transacylation pathway.

**Table 17-2** Comparison of Reaction Selectivity for Different Methods of By-product Removal

| Method | Relative Selectivity |
|---|---|
| None | Essentially zero |
| Distillation | Essentially zero |
| Molecular sieves | $+$ |
| Homogeneous scavenger | $++$ |

by both the amount of sieves used as well as their external surface area. Sieve pellets ($-400$ μm) were not satisfactory because of rate-controlling diffusion in the pores, whereas powdered sieves (1 to 4 μm) were. The concentration and removal rate of HCl were critical. Improvements in selectivity were subsequently achieved through the development of a homogeneous HCl scavenger, trimethyl silyl methyl carbamate. Elimination of the mass transfer resistance at the sieve surface by the presence in solution of a reagent that reacts directly with HCl resulted in a significant yield increase. Comparison of selectivity of R by four different methods of HCl mediation is shown in Table 17-2. All of the reaction studies were carried out in the laboratory. Scale-up of sieve and homogeneous scavenger mediated reactions was relatively straightforward once the concentrations and reaction were defined in the laboratory. Successful plant scale operation required rapid heat-up and cool-down, however, to minimize time at other than optimum temperature.

Typical production scale reaction kinetic profiles, as determined by high-performance liquid chromatography, are shown in Figure 17-7. If the run had been allowed to continue, a significant yield loss would have been experienced, as indicated by the dashed lines.

**17-4.2.3 *Scale-up*.** A great deal of work has been done to characterize gas–liquid mixing for prediction of power requirements to achieve equivalent mass transfer on scale-up. Much of this work concerns gas–liquid–solid where the solids are catalysts. The reader is referred to Chapter 11 and many excellent texts and literature articles, including Nagata (1975), Oldshue (1983), and Smith (1985). Oldshue (1985) pointed out the relation between the gas flow energy and mixer energy. For a radial flow impeller, the mixer energy must be about three times greater than the energy in the expanding gas stream or the mixer will not control the flow pattern. For axial systems, this ratio is about 10. Below this mixer energy level, the axial flow pattern is destroyed completely by the gas flow. In both cases, however, satisfactory performance may be possible if other aspects of mixing are not critical. Oldshue (1983) points out that although axial flow impellers are often specified for solid–liquid suspensions, the effect of gas sparging can disrupt the flow pattern to the extent that radial flow impellers could be a better choice. Scale-up requires consideration of the balance of these characteristics as well as consideration of the power per volume.
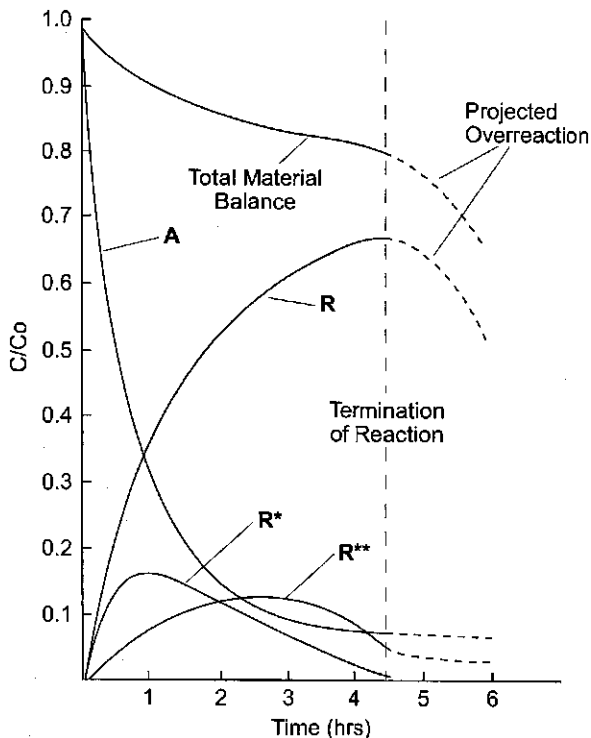
**Figure 17-7**   Profile of a manufacturing scale reaction as determined by high-performance liquid chromatography.

## 17-4.3   Liquid–Liquid Dispersed Phase Reactions

***17-4.3.1   Reactivity***. Reactions in liquid–liquid dispersed phase systems are common, and the reaction rates span all the regimes of reactivity. For slow reactions of reactants with low solubility in their respective phases, the actual conversion rate for even very well-mixed systems may be negligible. In these cases, a third solvent may be added to improve mutual phase solubility, or a phase transfer catalyst may be added to transfer one reagent, usually ionic, from aqueous to solvent phase. Both additions add downstream separation operations, however, so their use is avoided if possible. Strategies to promote reactivity include (1) generation of large interfacial area by intense mixing, and (2) removal of one of the phases by distillation of the more volatile solvent, thereby combining the reactants in the remaining phase. The last method may be complicated by the formation of a solid phase (reagent or product becoming insoluble) but may still be preferable to an additive.

***17-4.3.2   Selectivity in Liquid–Liquid Dispersed Phase Reactions***. Enhancement of selectivity because of the presence of an immiscible phase is

an important aspect of liquid–liquid systems. The improvement in selectivity is achieved by protection of the reactant(s) or product in a separate phase from an active reagent to reduce consecutive or competitive reaction to undesired by-products. Sharma (1988) discusses this subject and presents examples of very large increases in selectivity. Wang et al. (1984) present an example in which isocyanates were prepared from amides or N-bromoamides by Hofmann rearrangement under phase catalysis conditions. Without a second phase the isocyanate overreacted under alkaline conditions in the aqueous phase. Addition of a carefully selected solvent achieves reaction and rapid extraction of the isocyanate, which can then be obtained in high yield. This route to isocyanates obviates the use of phosgene.

Another example of reactive extraction is provided in Example 13-8a (King et al., 1985). In this case an acid hydrolysis could be replaced by a highly advantageous change to alkaline hydrolysis to achieve improved selectivity, productivity, quality, and waste minimization. However, the decomposition rates of reagent and reaction product under aqueous alkaline conditions are prohibitive. By running under reactive-extractive conditions, the objectives were achieved. Conventional mixing in a vessel was not feasible because of the rapid decomposition. Line mixing followed by rapid phase separation proved to be an extremely effective method to carry out this complex reaction.

### 17-4.3.3 *Scale-up*. 
Despite the frequent need to run reactions in immiscible liquid systems, the reliability and applicability of correlations to predict drop size distribution and surface area of the dispersed phase, especially in the presence of reactions, is limited. This is due, in part, to effects that small changes in geometry such as small agitator blade width can have on dispersed phase drop size as well as in surfactant effects resulting from reacting substrates. It is sometimes even difficult to predict which phase will be continuous and which dispersed. Although the continuous phase is normally a property of the system, the phases can sometimes be inverted by the manner in which they are contacted (e.g., by mixing during addition as opposed to starting with both phases present).

Care must be taken during laboratory and pilot plant studies to examine a wide range of interfacial areas (drop sizes). This allows the engineer to determine the extent to which interfacial area affects the conversion and selectivity. Changes in dispersion characteristics are very likely to occur on scale-up. In many cases these changes may not be significant because other aspects of the reacting system are controlling. However, phase dispersion can be critical to selectivity in some cases because of complex interfacial interactions. Selection of impellers and speeds to achieve the desired drop size distribution—which has a direct effect on settling rate—can also be critical to reaction processes that require subsequent phase separation. If when adding a reagent to the dispersed phase it is difficult to ensure good mixing of the drops, it can be concluded that concentration variations in dispersed phase can lead to problems.

Despite these qualifications, much can be gained from applying scale-up correlations to specific problems to establish guidelines and limits for performance.

As in the case of gas–liquid systems, the reader is referred to Chapter 12 and the text by Nagata (1975) for additional discussion. Scale-up from laboratory data on the same system can be predicted to some extent. Constant power per unit volume is a good guide, but care must be taken with large tanks and density differences, as mentioned above.

### 17-4.4   Solid–Liquid Systems

Solids in reacting systems can be either heterogeneous catalysts, dissolving reagents, precipitating products, or other reaction components, such as adsorption agents and ion-exchange resins. Reaction rates can fall in all regimes of the kinetic spectrum. The reader is referred to Chapter 10 for a discussion of solid–liquid mixing. As with all other types of heterogeneous reactions, very slow reactions in the liquid phase are unaffected by mass transfer in the film surrounding dissolving reagents or adsorption agents, and mixing is required only to maintain solids suspension. However, in the case of precipitating or crystallizing products, mixing can affect the particle size of the product just as it would in a precipitation without chemical reaction. Therefore, an effect of mixing must always be considered. Reactions in which reaction rates compete with mass transfer rates are all sensitive to local conditions and the films around solids and are therefore subject to mixing affects.

***17-4.4.1  Solids as Dissolving Reagents***. Both organic and inorganic reagents are often incompletely soluble in reaction solvents for a variety of reaction types. The particle size of these reagents can be a major factor in rate and/or selectivity. One objective of a laboratory development program is to determine the effect of particle size and to separate dissolution kinetics from chemical kinetics. An effective method of studying these reactions is to run the reaction under homogeneous conditions to measure true kinetics. This can be accomplished by preparing a saturated solution of the reagent, even if the maximum concentration is very low, and determining the reaction rate. Once having established true chemical kinetics, the overall reaction rate can be evaluated for dissolution limitations.

A second, effective but less quantitative method is to run the reaction with different particle size distributions of the insoluble reactant to determine the effect on overall reaction rate. If no effect is measured, it could be concluded that regime 1 applies and kinetics—not dissolution—controls. This method must be used with care, however, since other factors, such as surface coatings and incompletely characterized particle size distribution, can mask kinetic effects and lead to erroneous conclusions. An example of a reaction with dissolving solids was discussed previously (Example 13-4) in which a direct comparison can be made with the same reaction run in the same pilot scale vessel under homogeneous conditions. The effect on selectivity is significantly different between the heterogeneous and homogeneous conditions.

**17-4.4.2  *Solids as Precipitating Products*.** Studies have appeared on the effect of mixing on the precipitation of inorganic salts. Mixing intensity was shown by Pohorecki and Baldyga (1988) to affect particle size for the instantaneous reaction to form $BaSO_4$. Particle size was found to increase with increasing impeller speed in a segregated feed CSTR. Barthole et al. (1982) and Meyer et al. (1988) used a modification of the precipitation of $BaSO_4$ (modified to indicate the degree of micromixing) by characterizing product distribution of a $BaSO_4$ ethylenediaminetetracetic acid complex in alkaline medium under the influence of an acid.

Garside and Tavare (1985) modeled the effect of micromixing limits on elementary chemical reaction and subsequent crystallization. Two limiting cases are analyzed, and although the conversions of the chemical reactions are the same, the crystal size distributions can be very different. These differences are caused by the nonuniformity of supersaturation profiles that can be experienced by different fluid elements within a tank, owing to micromixing as well as macromixing effects. This modeling work also explores the sensitivity of two mixing models to reaction rate constant and nucleation kinetic parameters.

Literature references to experimental work on the crystallization or precipitation of products of organic reaction is rare even though this is a common reaction type. The difference between crystallization and precipitation is not well defined and is interpreted differently by different investigators. The interpretation that is implied here is that crystallization generates a crystalline product, whereas precipitates form rapidly and can be crystalline or amorphous. The differences are often blurred, however, because many organics actually appear first as amorphous noncrystalline solids which later turn truly crystalline. In these cases, nucleation is difficult to separate from precipitation of an amorphous solid. A further complication is that organics often separate first as oils or gums. This problem is very common when a reaction product is formed that is insoluble in the reaction system. Mersmann and Kind (1988) present an excellent discussion on precipitation as it is affected by micromixing.

An experimental study by Marcant and David (1991) of the crystallization of calcium oxalate concluded that the resulting particle size distribution was affected significantly by impeller speed and other mixing variables. The particle size distribution increased, passed through a maximum, and then decreased as the impeller speed was increased. This result is interpreted as changes in the key factors controlling nucleation and growth as well as reaction. Other mixing variables were also significant and affected particle size distribution in different ways.

The initial appearance of a solid that results from generation of supersaturation by a chemical reaction is a very complex series of events. As mentioned in the introduction to this section, the conditions affecting crystallization can be critical to the overall process result for several possible reasons. Selectivity of a complex reaction can be a function of the rate of crystallization and degree of supersaturation since these factors determine the concentration of that reaction product in solution at any given time. When in solution, all of the factors affecting selectivity can be significant, as discussed in Section 17-3. Delayed

nucleation because of improper seeding or excessive impurity levels can result in significantly reduced selectivity.

The purity of the crystallization product can be affected by the parameters that control any crystallization as well as the presence of the other chemical species, including the starting materials, that can be occluded from the reaction mixture. The particle size distribution can be affected by supersaturation, reaction rate, mixing, and other factors that affect crystallization in general. The degree to which control of the crystallization must be of concern obviously depends on the downstream processing. In some cases, physical attributes may not be significant, and the reaction can be optimized on a kinetic basis only. In other cases, however, the requirements for maximum selectivity may be different from those for physical attributes requiring a trade-off in actual system design.

An example of reaction-induced crystallization where the particle size and purity must be controlled is discussed in Example 17-2. In this case, mixing played a key role by balancing circulation with shear to achieve sufficient micromixing and mesomixing for the reaction but avoiding overmixing to achieve growth without shedding and/or crystal fracture.

***Example 17-2: Reaction and Simultaneous Crystallization*** (Larson et al., 1995)

- *Goal:* scale-up of a reactive crystallization with crystal growth and impurity rejection
- *Issue:* determination of conditions to limit nucleation and promote growth

One of the steps in the preparation of a side chain in the synthesis of an antibiotic involves a reaction between two soluble reactants to form a product that crystallizes from the reaction solvent, toluene. The reaction itself is relatively straightforward, requiring no special consideration for scale-up once the reaction conditions are established in the laboratory. The problem on scale-up to the pilot plant proved to be the crystal size distribution of the product. The crystals were bimodal with fines mixed with very large crystals. The filtration rate proved to be impracticably slow, and severe occlusion of starting material was experienced.

Development of this reaction system was then focused on the crystallization. A laboratory experimental program established the following:

1. The crystallization was inhibited by a component of the reaction mixture (determined by crystallizing the product from the same solvent but without chemical reaction, in which case large, well-shaped crystals were obtained).
2. When crystallization occurred as the result of reaction, the system developed a high degree of supersaturation before self-nucleation, leading to the generation of small crystals with little growth.

These observations led to the conclusion that the reaction system had to be modified to achieve controlled nucleation and crystal growth while minimizing the concentration of nucleation-inhibiting compound (identity unknown but

known to a component of the reaction mixture). The reaction was run under conditions in which one reagent was added last to the otherwise complete reaction mixture. The addition was sufficiently rapid to generate a high level of supersaturation, and crystallization did not initiate when the saturation concentration was reached by reaction.

The traditional approaches to inducing crystal growth were then explored, including seeding, control of supersaturation, and optimization of mixing to prevent crystal fracture. Control of supersaturation was achieved by control of reagent addition rate. The reagents were added simultaneously to a seeded mixture over a several-hour period to minimize concentrations of reactants and supersaturation of product. Crystallization was improved. However, crystal fracture of the improved crystals was then observed, which continued to cause slow filtration rates. Crystal fracture was reduced dramatically by a change in impeller to the Ekato Intermig (Chapter 6). This impeller was capable of providing sufficient blending for the reaction while providing the necessary low-shear environment for crystal growth. The resulting crystals from the slow addition (6 h) are shown in Figure 17-8*a* for comparison to those for more rapid addition (Figure 17-8*b*) (2 h), in which the bimodal distribution causing slow filtration is apparent. The key factor is control of low supersaturation and sufficient mixing for the fast reaction while avoiding shear damage to the crystals.



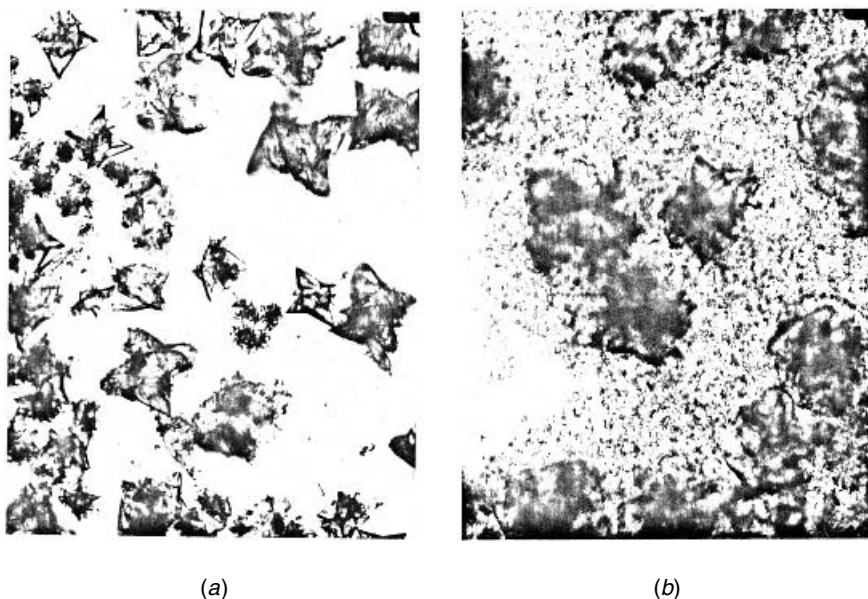(*a*)                                                   (*b*)

**Figure 17-8**   Photomicrographs of crystals from manufacturing scale reactive crystallizations using two addition rates, showing (*a*) minimization of fines by essentially all-growth at low rates, and (*b*) fines formation and bimodal distribution at high rates caused by nucleation.
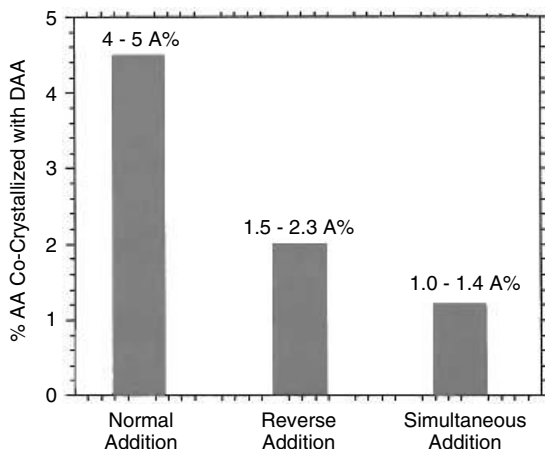
**Figure 17-9**   Inclusion of impurities from three addition modes in pilot scale operation.

This method of controlling supersaturation was also effective in rejecting impurities from the growing crystals, as shown in Figure 17-9, where impurity occlusion for a faster addition is shown to be increased substantially.

*Resolution:* Crystal growth in this reactive crystallization can be controlled by limiting supersaturation by slow reagent addition, high level seeding, and low-shear, high-circulation mixing.

This example illustrates the complex role that mixing is often required to play in providing the necessary shear for reagent blending while simultaneously suspending a crystal slurry in a growth environment without causing overnucleation (small crystals) or crystal breakage. In cases involving these conflicting requirements, it is necessary to select the most critical criteria and to design the mixing system on that basis. In some cases, this will result in a compromise of the optimum for some of the criteria. In this example, all of the requirements could be met.

### 17-4.4.3  *Scale-up*.
Scale-up of liquid–solid suspensions has been well characterized by many studies. The reader is referred to Chapter 10 for a comprehensive discussion. For reacting systems, power and speed should be above the minimum for homogeneous suspension since energy consumption is generally a smaller contributor to cost than other aspects of scale-up uncertainty (conversion and selectivity). Even this recommendation must be qualified by the potentially negative aspects of overmixing, as discussed in the introduction to Section 17-2. Reacting solids can also agglomerate and thereby require large increases in energy to maintain adequate dispersion.

These system-dependent properties are extremely difficult to characterize quantitatively and require specific scaling studies at extremes of possible operating ranges to determine sensitivity. Such systems are primary contributors to the case for built-in versatility. The more important consideration in reacting systems than

solid suspension may be mass transfer, since considerably more power and speed may be required to achieve expected reaction rate for reacting solids than that required for homogeneous suspension. As developed in Section 17-4.3.2, selectivity can also be affected in complex reactions because of the potential overreaction in the diffusive film around the dissolving or precipitating particles. An excellent discussion of mass transfer and reaction is presented by Fogler (1986).

Another critical aspect in the effectiveness of mass transfer correlations to predict coefficients in reacting systems is the very troublesome but all-too-common tendency for the surface of a reacting solid, catalyst, or precipitating product to become covered by another solid or second-phase liquid, or by a gas in a three-phase mixture. Such a heterogeneous film would obviously have a profound effect on the expected mass transfer coefficient and in many cases can cause a reaction to stop before the expected conversion. These films are obviously unique to each reacting system, thereby preventing any generalizations as to whether they are susceptible to chemical or physical manipulation. Chemical manipulation could be achieved by addition of a surfactant that would be able to modify surface properties to prevent or modify formation of the film.

Physical manipulation of such films may be possible through variation in mixing intensity primarily by local shear. Such interactions would be very scale dependent and could readily be masked in smaller scale operations. The extent to which reactions can be affected by coating of particles is well illustrated in an excellent example by Wiederkehr (1988). Other aspects of reaction system design are included in this case study, such as the choice of continuous smaller-volume reactors over batch reactors to reduce the size (and potential energy) of the reacting mass as well as the criticality of residence time distribution in complex reactions.

Another example of the impact of dissolving solids on reaction performance on the industrial scale is provided by Yamazaki et al. (1989). This example highlights the difficulty of scale-up of systems in which the mass transfer rate influences the product distribution and selectivity of complex reactions and may control the overall reaction rate. In this example the rate-determining step is the dissolution of $K_2CO_3$ particles in dipolar solvents.

## 17-5   MIXING AND CRYSTALLIZATION

Interactions between mixing and crystallization are often ignored. They should not be. In many cases, these interactions can affect every aspect of a crystallization operation, including nucleation, growth, and maintenance of a crystal slurry. To complicate the problem further, mixing optimization for one aspect of an operation may require different parameters than for another aspect, even though both requirements must be satisfied simultaneously. In addition, these operations are often scale dependent. For these and other reasons discussed below, many would contend that crystallization is the most difficult operation to scale-up—successfully.

*Successful scale-up implies that both physical and chemical properties have been duplicated between pilot plant and plant operations. These rigid criteria*

*are not always required but are for example, for final bulk active pharmaceutical products by biobatch regulations (duplication of physical attributes and chemical purity from pilot plant to plant scale operation). In all cases, however, it is prudent to apply these criteria in development, planning, and experimentation in order to reduce the risk of a dramatic failure (i.e., increased impurity levels or small crystal size causing drastically reduced filtration rates, poor washing, and slow-drying product). An even more drastic failure would be the inability to reproduce the required biobatch physical and chemical attributes.*

Successful operations depend on identifying the mixing parameters for the most critical aspects of the process and then evaluating whether those parameters will be satisfactory for the other aspects. Although this approach may be satisfactory in most cases, there will be crystallization procedures that require operation at conditions that are not optimum for mixing for some aspects of the operation, as discussed below. This discussion is limited to crystallization in stirred vessels by batch and semibatch operation. The crystallizers normally employed in the fine chemical and pharmaceutical industries are multipurpose vessels with various impeller and baffle configurations, as shown in Figures 17-1 and 17-2 and Chapter 6. The workhorse impeller is the pitched blade turbine because of its ability to create good circulation at relatively low shear. These attributes help reduce secondary nucleation and crystal breakage while achieving good suspension and circulation. The flat-blade turbine is less applicable because of high shear and less overall circulation. The Intermig (Ekato, Chapter 6) has proven to have superior performance in some crystallization operations because of its combination of excellent circulation with low shear. Baffles are required in all cases to prevent poor mixing due to swirling as well as entrainment of vapor that can provide nucleation sites. This discussion does not include more specific types of equipment, such as vessels with draft tubes or fines dissolution loops (see Mersmann, 2001; Mullin, 2001; Myerson, 2002).

Two important alternative types of crystallizers are fluidized beds and impinging jets. The fluidized bed is a very effective crystallizer for minimizing nucleation and promoting growth by providing very low shear, low energy, and minimum velocity impact between crystals. Both continuous and semicontinuous operation can be utilized. This principle has been applied successfully in the resolution of optical isomers in which nucleation must be minimized, preferably eliminated, to achieve isomer separation as described by Midler (1970, 1975, 1976). Impinging jet crystallization achieves an opposite extreme of mixing, high shear, and energy input, to promote nucleation by intense mixing. This principle has been utilized successfully in an industrial application to achieve a small average particle size (3 to 5 μm) and a narrow particle size distribution. Impinging jet crystallization is described by Midler et al. (1994) for an industrial application and by Mahajan and Kirwan (1996), Benet et al. (1999), and Condon (2001) in laboratory studies. This technology has been employed to produce nanoparticles stabilized by block copolymers (Johnson, 2003; Johnson and Prud'homme, 2003). Impinging jet crystallization with sonication (Lindrud et al. 2001) is another variant.

### 17-5.1  Aspects of Crystallization that Are Subject to Mixing Effects

The aspects of crystallization that may be affected by mixing are discussed below.

***17-5.1.1  Nucleation***. Primary nucleation may be induced by mixing. The effects of mixing on true primary nucleation are exceedingly complex. The overall result is a reduction in the width of the metastable region when the width for a static solution is compared to that for an agitated solution. Therefore, an unagitated solution can be cooled further before nucleation than can an agitated solution. Since an industrial system will always be agitated (except for operations such as melt crystallization), this has theoretical interest only. Since secondary nucleation becomes important as soon as nuclei appear, the nucleation mechanisms become virtually impossible to characterize. In addition, any seeded crystallization is by definition secondary even though some nuclei may form simultaneously by a primary mechanism. Therefore, the major part of this discussion will be on secondary nucleation.

Secondary nucleation is mixing dependent as follows:

- *Crystal–crystal impact:* a function of both the local micromixing environment and the overall macromixing circulation
- *Crystal–impeller and crystal–wall impact:* functions of the impeller speed, shape of blade, and material of construction
- *Adsorbed layer:* thickness decreased by increased mixing

These factors affect the rate of nucleation, which in turn determines the number of nuclei formed and their size. These events can then dominate the entire crystallization operation with respect to both physical and chemical purity attributes. Ultimate crystal size is a function of the number of nuclei generated, as shown in Table 17-3. Nominal dimensions of the resulting crystals for cubic particles (3D growth), flat plate (2D growth), and needle-shaped crystals (1D growth) are shown versus the quantity of nuclei (each "nucleus" assumed to be a 5 μm cube). It can be seen that the number of nuclei generated by the various causes of nucleation, including agitation, has an exponential effect, as expected from this purely geometrical relationship, on the ultimate size that can be achieved by growth subsequent to nucleation. Since the nucleation rate can often increase on scale-up because of local power dissipation differences, the average particle size on scale-up could be reduced. Other mixing factors that affect growth could increase the size distribution as well, as discussed below.

The effect of agitation on secondary nucleation has been reported in the literature and several references are discussed by Mullin (2001). This discussion highlights the complex nature and unpredictability of these interactions. Moreover, the critical nature of these interactions is the key factor in causing difficulty in scale-up of nucleation-dominated crystallization processes, even with small quantities of seed. The critical mixing factors are impeller speed and type and their influence on local turbulence and overall circulation. Since neither the localized turbulence distribution nor the overall circulation time can realistically be

**Table 17-3**   Effect of Extent of Nucleation on Final Crystal Particle Size

| % Nucleation | Product Particle Dimensions ($\mu$m) | | |
| | Length | Width | Thickness |
| --- | --- | --- | --- |
| *a. Cubic Particles (3D Growth)* | | | |
| 0.5 | 29 | 29 | 29 |
| 1 | 23 | 23 | 23 |
| 5 | 14 | 14 | 14 |
| 10 | 11 | 11 | 11 |
| *b. Flat Plates (2D Growth)[a]* | | | |
| 0.5 | 71 | 71 | 5 |
| 1 | 50 | 50 | 5 |
| 5 | 22 | 22 | 5 |
| 10 | 16 | 16 | 5 |
| *c. Needles (1D Growth)[a]* | | | |
| 0.5 | 1000 | 5 | 5 |
| 1 | 500 | 5 | 5 |
| 5 | 100 | 5 | 5 |
| 10 | 50 | 5 | 5 |

[a] Very thin particles unlikely to survive attrition in tank.

maintained constant on scale-up, the extent to which changes in the crystallizing environment will affect nucleation are extremely difficult to predict. To the mixing issue must be added the uncertainties caused by soluble and insoluble impurities that may be present in sufficiently different concentrations from batch to batch to cause variation in nucleation rate.

It is important to remember that low-level impurities can also have significant impact on crystal growth, usually by blocking growth sites on the growth surface, reemphasizing the importance of controlling reaction conditions with suitable local mixing. However, impurities can more easily disturb a molecular cluster trying to arrange itself into a critical sized nucleate than they can an already formed growing surface, so the effect is clearly more pronounced in nucleation In general, the greater the dependence on nucleation, the greater the difficulty in developing a stable process for scale-up and/or ongoing production.

If no process alternative is possible to avoid dependence on nucleation, mixing scale-up can be based on equal power per unit volume assuming that the same impeller type is used and geometric similarity is maintained. In most cases, however, this approach will result in changes in particle size distribution (PSD) on scale-up, which may or may not be acceptable. In general, the PSD will be broader and the average particle size smaller if the P/V scale-up criterion is used. This generalization is suggested by Nývlt (1971). As often experienced in crystallization scale-up, however, the opposite of this expectation can be realized, depending on the specific nucleation characteristics of the system. A further generalization may be proposed: that fast nucleating systems tend toward smaller

size distribution on scale-up, whereas slow nucleation can give the opposite result. An alternative to equal power per unit volume was suggested by Nienow (1976) and is discussed further below. For excellent insight into this complex phenomenon of nucleation, the reader is referred to Mersmann (2001), Mullin (2001), and Myerson (2002).

*17-5.1.2* *Growth*. Mixing can affect crystal growth in several ways, as summarized below:

- Mass transfer rate in the diffusion film around growing crystals
- Bulk turnover rate and its affect on minimizing differences in the supersaturation ratio throughout the vessel
- Heat transfer rate and wall film thickness
- The effect of shear on crystal breakage
- Dispersion of an antisolvent or reagent
- Growth rate dispersion
- Minimizing impurity concentration at the crystal surface

The need to maintain high mass transfer rates to minimize supersaturation gradients in the film around a growing crystal is one of the primary functions of mixing in a crystallization operation. As in other types of mass transfer operations, the coefficient increases with increased mixing, although at high Reynolds numbers, this increase becomes less significant. Additional factors that improve with increased mixing are (1) heat transfer, (2) bulk turnover, (3) dispersion of an additive such as an antisolvent or reagent, (4) uniformity of crystal suspension, (5) avoidance of settling and minimization of wall scale, and (6) minimization of impurity concentration at the crystallizing surface. However, these needs must be balanced against the possibly negative results of overmixing, which can cause crystal breakage and/or shedding of nuclei as well as increased secondary nucleation. Increased growth dispersion is also possible, since increased mixing can increase the growth rate of large crystals (assuming that the growth rate is dependent on mass transfer), but has little effect on small crystals ($<10\ \mu$m) since these crystals are smaller than the turbulent eddies and have little relative movement. The latter effect may be a contributing factor in the increase in size distribution that is common on scale-up.

These concerns lead to the conclusion referred to above that it is often necessary to choose a mixing condition (impeller speed, type, etc.) that may not be optimum for every aspect of the crystallization and may actually not be optimum for any of them. In many cases, however, one end result [i.e., PSD, bulk density, uniformity of suspension, approach to equilibrium solubility (yield)] may dictate the choice of mixing conditions. In this case it becomes essential to determine if the negatively affected aspects can be tolerated.

All of these factors are properties of a given crystallization system, thereby requiring choices for each specific operation. Experimentation is required to determine the key responses to mixing for each system and could include determination of the following:

- *Effect of impeller speed and type on PSD at a minimum of two seed levels and two supersaturation ratios.* These results should indicate the sensitivity of the system to mixing. A small response could indicate that other system properties were controlling (i.e., inherent crystal growth rate or nucleation rate). A large response would indicate sensitivity to secondary nucleation and/or crystal cleavage and require additional experimentation and evaluation of scale-up requirements. The laboratory results should be evaluated relative to each other since scale-up can be expected to make additional changes in PSD, especially when a large response is experienced in these simple experiments.
- *Effect of impeller speed on crystallization rate and approach to equilibrium solubility (yield).* Failure to achieve equilibrium solubility may indicate accumulation of impurities at the crystallizing surfaces. An increase in impeller speed resulting in further reduction in solution concentration could indicate resumption in growth or additional nucleation (see Example 17-3).
- *Suspension requirements as indicated by the settling rate to achieve off-bottom suspension.* The impeller speed that is found necessary to achieve off-bottom suspension should be the minimum speed on which to base scale-up, as calculated for the appropriate scale of operation. Higher speeds may be required to satisfy other requirements, as indicated below.

For nucleation-dependent operations, it is recommended that additional information be obtained as follows:

- Effect of impeller speed on width of metastable region
- Effect of impeller speed and type on rate of nucleation

This experimentation is focused primarily on evaluation of mixing sensitivity.

### 17-5.2   Mixing Scale-up in Crystallization Operations

The compromises in mixing optimization that may be required on scale-up often result in use of the common mixing criterion of equal power per unit volume or in some cases equal tip speed. Both of these require utilization of the same impeller type as well as geometric similarity in order to have a reasonable chance of success. Preliminary laboratory evaluation of the mixing requirements for a crystallization operation should be carried out in a minimum 1 L vessel, with further evaluation at 100 to 1000 L—as much as is practical. The smaller scale operations will generally produce more uniform PSD and larger mean crystal size than the manufacturing scale (typically, 10 000 L) when using equal power

per unit volume. These changes typically are caused by the local differences in impeller shear (an unavoidable result of the equal power per unit volume criterion) that cause increased nucleation, leading to a larger number of particles, an increased spread in PSD, and a smaller particle average diameter.

For transfer of a crystallized mixture to another operation, there may be a requirement to have a homogeneous dispersion. One example would be feeding a centrifuge or other solid–liquid separation device. A guideline that can be helpful in avoiding local overmixing, other than equal power per unit volume, was suggested by Nienow (1976). Using this guideline, the agitator speed at the manufacturing scale would be selected to be sufficient to just maintain off-bottom suspension, thereby resulting in reduced nucleation, fewer particles, and more growth. In general, this speed would be considerably less than equal power per unit volume. Limitations on this guideline would be cases of high-density crystals, which could require higher speeds to prevent excessive settling. In addition, antisolvent and reactive crystallization applications may require higher speeds to prevent local supersaturation at the point of addition. In the latter case, scale-up based on equal local energy dissipation at the point of addition may be necessary. This subject is discussed in many literature references, including Sohnel and Garside (1992) and Mersmann (2001). The requirements for particle off-bottom suspension are also discussed in Chapter 10. A further caution on reduced speed is a possible increase in encrustation caused by crystal contact with the bottom surface and potential for sticking.

The effect of mixing on PSD has been determined experimentally by Marcant and David (1991) for the reactive crystallization of calcium oxalate. This work is an excellent example of the multiple dependencies on mixing that can be experienced in a crystallization operation. The factors noted above that are mixing dependent are shown to have positive or negative influences on the resulting physical characteristics, thereby illustrating the necessity of selecting the most important result to be achieved. The effect of increasing agitator speed is shown initially to cause an increase in particle size, followed by passing through a maximum and then decreasing particle size. This result is attributed to changes in controlling factors resulting from the changes in mixing.

***Example 17-3: Slow Approach to Equilibrium***.  Scale-up of the crystallization of an intermediate (MW ∼850) in a multistep synthesis resulted in a slow approach to equilibrium solubility at the end of a combined cooling/antisolvent crystallization. Agitation rate was held at a minimum value for off-bottom suspension because of concern for shear damage of the crystals. Accumulated soluble impurities were known to be present, and it was suspected that their accumulation at the crystallizing surfaces could be a factor in stopping growth. An increase in agitation rate by about 20% late in the cooling cycle was successful in causing a further reduction in dissolved product solubility. The increased agitation was successful in resuming growth because of reduction in diffusion film thickness. (Another possibility is a resumption in nucleation resulting from the increased energy of the impeller.)

Incorporation of impurities in the crystals was a major concern that indicated higher impeller speeds but generated excessive fines, and the resulting poor filtration rates were a counterbalancing influence on the determination of impeller speed. The two-level agitation rate scheme was a balance between these conflicting factors, which gave passable purity, yield, and filtration rate. As in many high-impurity systems, however, the average particle size was small because of the need to operate at relatively high supersaturation to achieve practical growth rates, thereby incurring more nucleation than desired. The qualitative aspects of this difficult crystallization provide examples of the trade-offs that are often encountered in development and scale-up.

# REFERENCES

Angst, W., J. R. Bourne, and R. N. Sharma (1982a). Mixing and fast chemical reaction: V. Influence of diffusion within the reaction zone on selectivity, *Chem. Eng. Sci.*, **37**, 1259–1264.

Angst, W., J. R. Bourne, and R. N. Sharma (1982b). Mixing and fast chemical reaction: IV. The dimensions of the reaction zone, *Chem. Eng. Sci.*, **37**, 585–590.

Baldyga, J., and J. R. Bourne (1984a). Mixing and fast chemical reactions: VIII. Initial deformation of material elements in isotropic, homogeneous turbulence, *Chem. Eng. Sci.*, **39**, 329–334.

Baldyga, J., and J. R. Bourne (1988). Calculation of micromixing in inhomogeneous stirred tank reactors, *Chem. Eng. Res. Des.*, **66**, 33–38.

Baldyga, J., and J. R. Bourne (1989). Simplification of chemical engineering calculations, *Chem. Eng. J.*, **42**, 83–101.

Baldyga, J., and J. R. Bourne (1990). The effect of micromixing on parallel reactions, *Chem. Eng. Sci.*, **45**(4), 907–916.

Baldyga, J., and J. R. Bourne (1999). *Turbulent Mixing and Chemical Reactions*, Wiley, Chichester, West Sussex, England.

Barthole, J. P., R. David, and J. Villermaux (1982). A new chemical method for the study of local micromixing combinations in industrial stirred tanks, *ACS Symp. Ser.* **196U**, 545–554.

Belevi, H., J. R. Bourne, and P. Rys (1981). Mixing and fast chemical reaction: II. Diffusion reaction model for the CSTR, *Chem. Eng. Sci.*, **36**, 1649–1654.

Benet, N., L. Falk, H. Muhr, and E. Plasari (1999). Experimental study of a two-impinging-jet mixing device for application in precipitation processes, *Proc. 14th International Symposium on the Industrial Crystals (Computer Optical Disc)* pp. 1007–1016.

Bolzern, O., and J. R. Bourne (1983). Mixing and fast chemical reactions: VI. Extension of the reaction zone, *Chem. Eng. Sci.*, **38**, 999–1003.

Bolzern, O., and J. R. Bourne (1985). Rapid chemical reactions in a centrifugal pump, *Chem. Eng. Res. Des.*, **63**, 275–282.

Bourne, J. R. (1984). Micromixing revisited, *Proc. 8th International Symposium on Chemical Reaction Engineering, Symp. Ser. Ind. Chem. Eng. (London)*, **87**, 797–814.

Bourne, J. R., and P. Dell'ava (1987). Micro- and macromixing in stirred tank reactors of different sizes, *Chem. Eng. Res. Des.*, **65**(3), 180–186.

Bourne, J. R., and H. Gablinger (1989). Local pH gradients and the selectivity of fast reactions, *Chem. Eng. Sci.*, **44**(6), 1347–1352.

Bourne, J. R., and J. Garcia-Rosas (1986). Rotor–stator mixers for rapid micromixing, *Chem. Eng. Res. Des.*, **64**, 11–17.

Bourne, J. R., and C. P. Hilber (1990). The productivity of micromixing-controlled reactions: effect of feed distribution in stirred tanks, *Chem. Eng. Res. Des.*, **68**, 51–56.

Bourne, J. R., and F. Kozicki (1977). Mixing effects during the bromination of 1,3,5-trimethoxybenzene, *Chem. Eng. Sci.*, **36**, 1538–1539.

Bourne, J. R., E. Crivelli, and P. Rys (1977a). Chemical selectivities disguised by mass diffusion, *Helv. Chim. Acta*, **60**(8), 2944–2957.

Bourne, J. R., P. Rys, and R. Suter (1977b). Mixing effects in the bromination of resorcin, *Chem. Eng. Sci.*, **32**, 711–716.

Bourne, J. R., et al. (1981a). Mixing and fast chemical reaction: III. Model–experiment comparisons, *Chem. Eng. Sci.*, **36**, 1655–1663.

Bourne, J. R., F. Kozicki, and P. Rys (1981b). Mixing and fast chemical reaction: I. Test reactions to determine segregation, *Chem. Eng. Sci.*, **36**, 1643–1648.

Bowe, M. (1990). Fluidics puts mixing in a spin, *Processing*, Feb., pp. 43–44.

Canon, R. M., et al. (1977). Turbulence level significance of the coalescence-dispersion rate parameter, *Chem. Eng. Sci.*, **32**, 1349–1352.

Carberry, J. J., and A. Varma, eds., (1987). *Chemical Reaction and Reaction Engineering*, Marcel Dekker, New York.

Carpenter, K. J. (1985). A fine chemicals view of the mixing world, *Proc. 5th European Conference on Mixing*, BHRA, pp. 233–241.

Carpenter, K. J. (2001). Chemical reaction engineering aspects of fine chemicals manufacture, *Chem. Eng. Progr.*, **56**, 305–322.

Condon, J. M. (2001). Investigation of impinging jet crystallization for a calcium oxalate model system, Ph.D. dissertation, Rutgers University, New Brunswick, NJ.

Danckwerts, P. V. (1957). Measurement of molecular homogeneity in a mixture, *Chem. Eng. Sci.*, **7**(1), 116–117.

Danckwerts, P. V. (1958). The effect of incomplete mixing on homogeneous reactions, *Chem. Eng. Sci.*, **8**(1), 93–102.

Demyanovich, R. J., and J. R. Bourne (1988). A new method using thin liquid sheets, *Proc. 6th European Conference on Mixing*, BHRA, pp. 177–182.

Demyanovich, R. J., and J. R. Bourne (1989). Rapid micromixing by the impingement of thin liquid sheets, *Ind. Eng. Chem. Res.*, **28**(6), 825–839.

Fogler, H. S. (1986). *Elements of Chemical Reaction Engineering*, Prentice Hall, Englewood Cliffs, NJ.

Froment, G. F., and R. B. Bischoff (1990). *Chemical Reactor Analysis and Design*, Wiley, New York.

Garside, J., and N. S. Tavare (1985). Mixing, reaction, and precipitation: limits of micromixing in an MSMPR crystallizer, *Chem. Eng. Sci.*, **40**(8), 1485–1493.

Harris, I. J., and R. D. Srivastava (1968). The simulation of single phase tubular reactors with incomplete reactant mixing, *Can. J. Chem. Eng.*, **46**, 66–69.

Heeb, T. G., and R. S. Brodkey (1990). Turbulent mixing with multiple second-order chemical reactions, *AIChE J.*, **36**(10), 1457–1470.

Johnson, B. K. (2003). Flash nanoprecipitation of organic actives via confined micromixing and block copolymer stabilization, PhD Thesis, Princeton Univ.

Johnson, B. K., and R. J. Prud'homme (2003). Chemical processing and micromixing in confined impinging jets, *AIChE J.*, in press.

Kattan, A., and R. J. Adler (1967). A stochastic mixing model for homogeneous, turbulent, tubular reactors, *AIChE J.*, **13**(3), 580–585.

Keeler, R. N., E. E. Petersen, and J. M. Prausnitz (1965). Mixing and chemical reaction in turbulent flow reactors, *AIChE J.*, **11**(2), 221–227.

King, M. L., A. L. Forman, C. Orella, and S. H. Pines (1985). Extractive hydrolysis for pharmaceuticals, *Chem. Eng. Prog.*, **81**(5), 36–39.

Klein, J. P., R. David, and J. Villermaux (1980). Interpretation of experimental liquid phase micromixing phenomena in a continuous stirred reactor with short residence times, *Ind. Eng. Chem. Fundam.*, **19**, 373–379.

Landau, R. N., D. Blackmond, and H. H. Tung (1994). Calorimetric investigation of an exothermic reaction: kinetic and heat flow modelling, *Ind. Eng. Chem. Res.*, **33**, 814.

Landau, R. N., U. K. Singh, F. G. Gortsema, Y.-K. Sun, S. C. Gomolka, T. Lam, M. Futran, and D. G. Blackmond (1995). A reaction calorimetric investigation of the hydrogenation of a substituted pyrazine, *J. Catal.*, **157**, 201.

Larson, K. A., M. Midler, and E. L. Paul (1995). Reactive crystallization: control of particle size and scale-up, presented at the Association for Crystallization Technology 1995 Meeting, Charlottesville, VA.

Laufhutte, H. D., and A. Mersmann (1987). Local energy dissipation in agitated turbulent fluids and its significance for the design of stirring equipment, *Chem. Eng. Technol.*, **10**, 56–63.

LeBlond, C., J. Wang, R. Larsen, C. Orella, and Y. -K. Sun (1998). A combined approach to characterization of catalytic reactions using in situ kinetic probes, *Topics Catal.*, **5**, 149.

Lee, L. J., J. M. Ottino, W. E. Ranz, and C. W. Macosko (1980). Impingement mixing in reaction injection molding, *Polym. Eng. Sci.*, **20**, 868–874.

Levenspiel, O. (1972). *Chemical Reaction Engineering*, Wiley, New York.

Li, K. T., and H. L. Toor (1985). Chemical indicators as mixing probes: a possible way to measure micromixing time, *Ind. Eng. Chem. Fundam.*, **25**, 719–723.

Lindrud, M. D., S. Kim, and C. Wei (2001). Sonic impinging jet crystallization apparatus and process, U.S. Patent 6,302,958.

Litz, L. M. (1985). A novel gas–liquid stirred tank reactor, *Chem. Eng. Prog.*, **81**(11), 36–39.

Mahajan, A. J., and D. J. Kirwan (1996). Micromixing effects in a two-impinging-jets precipitator, *AIChE J.*, **42**(7), 1801–1814.

Mann, R., and A. E-Hamouz (1991). Effect of macromixing on a competitive consecutive reaction in a semi-batch stirred reactor: Paul's iodination experiments interpreted by networks of zones, presented at the 7th European Conference on Mixing, Brugge, Belgium, Sept. 18–20.

Mao, K. W., and H. L. Toor (1971). Second-order chemical reactions with turbulent mixing, *Ind. Eng. Chem. Fundam.*, **10**(2), 192–197.

Marcant, B. N., and R. David (1991). Experimental evidence for and prediction of micromixing effects in precipitation, *AIChE J.*, **37**(11), 1698–1710.

Mersmann, A. (2001). *Crystallization Technology Handbook*, 2nd ed., Marcel Dekker, New York.

Mersmann, A., and M. King (1988). Chemical engineering aspects of precipitation from solution, *Chem. Eng. Technol.*, **11**, 264–276.

Meyer, T., R. David, A. Renken, and J. Villermaux (1988). Micromixing in a stator mixer and an empty tube by a chemical method, *Chem. Eng. Sci.*, **43**, 1955–1960.

Midler, M. (1970). Production of crystals in a fluidized bed with ultrasonic vibrations, U.S. patent 3,510,266.

Midler, M. (1975). Process for production of crystals in fluidized bed crystallizers, U.S. patent 3,892,539.

Midler, M. (1976). Crystallization system and method using crystal fracturing external to a crystallizer column, U.S. patent 3,996,018.

Midler, M., E. Paul, E. Whittington, M. Futran, P. Liu, J. Hsu, and S. Pan (1994). Crystallization method to improve crystal structure and size", U.S. patent 5,314,506.

Mullin, J. W. (2001). *Crystallization*, 4th ed., Butterworth-Heinemann, Oxford.

Myerson, A. S., (ed.) (2002). *Handbook of Industrial Crystallization*, 2nd ed., Butterworth-Heinemann, Newton, MA.

Nabholz, F., and P. Rys (1977). Chemical selectivities disguised by mass diffusion, *Helv. Chim. Acta*, **60**(8), 2937–2943.

Nagata, S. (1975). *Mixing: Principles and Applications*, Wiley, New York.

Nauman, E. B., and B. A. Buffham (1983). *Mixing in Continuous Flow Systems*, Wiley, New York.

Nienow, A. W. (1976). The effect of agitation and scale-up on crystal growth rates and on secondary nucleation, *Trans. Inst. Chem. Eng.*, **54**, 205.

Nývlt, J. (1971). *Industrial Crystallization from Solutions*, Butterworth & Co. Ltd, London.

Oldshue, J. Y. (1983). *Fluid Mixing Technology*, McGraw-Hill, New York.

Oldshue, J. Y. (1985). Scale-up of unique industrial fluid mixing processes, *Proc. 5th European Conference on Mixing*, BHRA, pp. 35–42.

Ott, R. J., and P. Rys (1975). Chemical selectivities disguised by mass diffusion, *Helv. Chim. Acta*, **58**(7), 2074–2091.

Paul, E. L. (1988). Design of reaction systems for specialty organic chemicals, *Chem. Eng. Sci.*, **43**(8), 1773–1782.

Paul, E. L. (1990). Reaction systems for bulk pharmaceutical production, *Chem. Ind.*, **21**, May, pp. 320–325.

Paul, E. L., and R. E. Treybal (1971). Mixing and product distribution for a liquid-phase, second-order, competitive-consecutive reaction, *AIChE J.*, **17**(5), 718–724.

Paul, E. L., H. Mahadevan, J. Foster, M. Kennedy, and M. Midler (1992). The effect of mixing on scaleup of a parallel reaction system, *Chem. Eng. Sci.*, **47**, 2837–2840.

Pohorecki, R., and J. Baldyga (1988). The effects of micromixing and the manner of reactant feeding on precipitation in stirred tank reactors, *Chem. Eng. Sci.*, **43**, 1949–1954.

Rice, R. W., and R. E. Baud (1990). The role of micromixing in the scaleup of geometrically similar batch reactors, *AIChE J.*, **36**(2), 293–298.

Rice, A. W., H. L. Toor, and F. S. Manning (1964). Scale of mixing in stirred vessels, *AIChE J.*, **10**(1), 125–129.

Schutz, J. (1988). Agitated thin-film reactors and tubular reactors with stator mixers for a rapid exothermic multiple reaction, *Chem. Eng. Sci.*, **43**, 1975–1980.

Sharma, M. M. (1986). Intensification of heterogeneous reactions: theory and practice, *Proc. Indian Natl. Sci. Acad.*, **52A**, 449–475.

Sharma, M. M. (1988). Multiphase reactions in the manufacture of fine chemicals, *Chem. Eng. Sci.*, **43**(8), 1749–1758.

Shenoy, U. V., and H. L. Toor (1989). Turbulent micromixing parameters from reactive mixing measurements, *AIChE J.*, **35**(10), 1692–1700.

Shenoy, U. V., and H. L. Toor (1990). Unifying indicator and instantaneous reaction methods for measuring micromixing, *AIChE J.*, **36**(2), 227–232.

Smith, J. M., and M. M. G. G. Warmoeskerken (1985). The dispersion of gases in liquids with turbines, Proc. 5th European Conference on Mixing, BHRA, pp. 115–126.

Sohnel, O., and J. Garside, (1992). *Precipitation*, Butterworth-Heinemann, Oxford.

Sun, Y. -K., C. LeBlond, J. Wang, R. Larsen, C. J. Orella, A. Forman, R. N. Landau, J. Laquidara, J. R. Sowa, Jr., and D. G. Blackmond (1996a). Reaction calorimetry as an in situ kinetic tool for characterizing complex reactions, *Thermochim. Acta*, **289**, 189.

Sun, Y.-K., R. N. Landau, J. Wang, C. LeBlond, and D. G. Blackmond (1996b). A re-examination of pressure effects on enantioselectivity in asymmetric catalytic hydrogenation, *J. Am. Chem. Soc.*, **118**, 1348.

Sun, Y. -K., J. Wang, C. LeBlond, and D. G. Blackmond (1996c). Asymmetric hydrogenation of ethyl pyruvate: diffusion effects on enantioselectivity, *J. Catal.*, **161**, 759.

Tatterson, G. B. (1991). *Fluid Mixing and Gas Dispersion in Agitated Tanks*, McGraw-Hill, New York.

Toor, H. L. (1962). Mass transfer in dilute turbulent and non-turbulent systems with rapid irreversible reactions and equal diffusivities, *AIChE J.*, **8**(1), 71–78.

Truong, K. T., and J. C. Methot (1976). Segregation effects on consecutive competing reaction in a CSTR, *Can. J. Chem. Eng.*, **54**, 572–577.

van de Vusse, J. G. (1966). Consecutive reactions in heterogeneous systems, *Chem. Eng. Sci.*, **21**, 631–643, 1239–1252.

Vassillatos, G., and H. L. Toor (1965). Second-order chemical reactions in a nonhomogeneous turbulent fluid, *AIChE J.*, **11**(4), 666–673.

Wang, S., et al. (1984). Study on the Hofmann rearrangement in a two phase system, *Jilin Daxue Ziran Kexue Xuebao*, **2**, 89–93 (Chinese).

Wang, Y. D., and R. Mann (1990). Mixing in a stirred semi-batch reactor: partial segregation for a pair of competing reactions analyzed via networks-of-zones, *Inst. Chem. Eng. Symp. Ser.*, **121**(Fluid Mixing 4), 241–258.

Wang, Y. D., and R. Mann (1992). Partial segregation in stirred batch reactors: effect of scale-up on the yield of a pair of competing reactions, *Chem. Eng. Res. Des.*, **70**(A3), 282–290.

Weinstock, L. M. (1986). Evolution of the cefoxitin process, *Chem. Ind. (London)*, **86**(3), 86–90.

Whitaker, S., and A. E. Cassano, eds. (1986). *Concepts and Design of Chemical Reactors*. Gordon & Breach, New York.

Wiederkehr, H. (1988). Examples of process improvements in the fine chemicals industry, *Chem. Eng. Sci.*, **43**, 1783–1791.

Yamazaki, H., H. Yazawa, and K. Minima (1989). Effect of mixing on esterification of cepharosporic acid in a solid–liquid system, *Chem. Eng. Sci.*, **41**, 109–116.

# Mixing in the Fermentation and Cell Culture Industries

ASHRAF AMANULLAH and BARRY C. BUCKLAND

*Merck & Co., Inc.*

ALVIN W. NIENOW

*University of Birmingham*

## 18-1 INTRODUCTION

Given the importance of mixing and mass transfer in fermentation and cell culture processes and the potentially huge literature available on the subject, it is not possible to cover all aspects of this topic within the scope of this chapter. What are considered the most important subject matters are addressed here. In Section 18-2 we focus on the aspects of scaling up and scaling down fermentation processes. Although only microbial and fungal systems are considered, similar principles can be applied for cell culture processes. Scale-up of industrial fermentation processes occurs either when a new process is scaled up or when an existing process is subjected to modifications (e.g., media or strain improvements). Since scale-up is still largely performed using empirical knowledge and although scale-up can sometimes be successful, it is difficult to use it for optimization purposes. A more rapid, process-specific approach that is capable of predicting the performance with greater confidence on scale-up is desired. The limitations of traditional scale-up methods have been highlighted, and alternative methods using a scale-down approach are described in detail. Only stirred tank bioreactors have been considered in this discussion since the use of such systems is overwhelmingly dominant in the fermentation and cell culture industries. A significant part of this chapter is devoted to a description of studies that have measured spatial variations in dissolved oxygen, substrate, and pH at large scales of operation and

those that have investigated the effects of repeated exposure of microorganisms to the nonhomogeneous distribution of microenvironmental conditions. Such studies form the basis for the rational design of scale-down models used to simulate the microenvironment experienced by cells at the large scale. Particular emphasis is given to the practical design of scale-down models.

One of the most challenging tasks in the fermentation industry today is the design of bioreactors for highly shear thinning, viscous fermentation broths, including those for commercially important antibiotic and polysaccharide fermentations. In such fermentations, the maximum productivity, product concentration, and quality achievable depends primarily on bulk mixing and oxygen mass transfer, which in turn are governed by process operation, impeller type, and fluid properties. These generic problems inherent in viscous polysaccharide fermentations have been investigated and reported in Section 18-3 using xanthan gum as a model fermentation system. In addition, the effects of bulk mixing oxygen transfer on the quality of xanthan and other polysaccharide gums are also discussed.

Fungal strains for secondary metabolite, organic acid, and heterologous protein production are widely used industrially. In fungal fermentation, engineering variables such as agitation conditions require attention due its effect on the morphology, which in some cases can affect productivity. In many fungal fermentations, the high apparent viscosities and the non-Newtonian behavior of the broths necessitate the use of high agitation speeds to provide adequate mixing and oxygen transfer. However, mycelial damage at high stirrer speeds (or power input) can limit the acceptable range of speeds, and consequently, the oxygen transfer capability and volumetric productivity of the fermenter. The effects of hydrodynamic stress on fungal physiology are not always readily understood. An understanding of how agitation affects mycelial morphology and productivity ought to be valuable in optimizing the design and operation of large scale fungal fermentations for the production of secondary metabolites and recombinant proteins. The effects of agitation intensity on hyphal morphology and product formation in two commercially important fungal fermentations (*Penicillium chrysogenum* and *Aspergillus oryzae* for penicillin and recombinant protein production, respectively) are considered in Section 18-4.

Protein production by recombinant technology has been the subject of much industrial interest. However, production has been limited to a few well-known overexpression systems such as *Escherichia coli*, although knowledge of the process engineering variables on performance is still limited. The cultivation of *E. coli* in fed-batch mode using high-substrate feed concentrations to produce high cell densities is the preferred industrial method for increasing the volumetric productivity of bacterial derived products. Mixing is critical in such situations to ensure that addition of the concentrated feed is mixed as quickly as possible. However, information on the impact of intense mixing on bacterial physiology is very scarce. This subject is dealt with briefly in Section 18-5.

The commercial use of animal and insect cell culture at scales up to 20 m$^3$ (20 000 L) for the production of posttranslationally modified proteins using recombinant DNA techniques has made cell culture a cornerstone of modern

biotechnology. Given that both suspension and microcarrier cell cultures are potentially more sensitive then microbial cells, to agitation and aeration in stirred tank bioreactors, proper design and operation of bioreactors in relation to agitation and aeration, including the use of surfactants to minimize cell damage, are critical for process optimization. These issues are described in Section 18-6. In addition, limitations on the use of Kolmogorov's theory of isotropic turbulence for the prediction of shear damage are discussed.

Issues related to mixing in plant cell cultures with reference to hydrodynamic shear are discussed in Section 18-7. Generally, plant cell damage mechanisms due to agitation have been difficult to identify given the diversity of cell lines, aggregate morphologies, culture age, and history. Greater understanding of these interactions is still required to for widespread commercialization of plant cell cultures.

## 18-2   SCALE-UP/SCALE-DOWN OF FERMENTATION PROCESSES

Successful scale-up often depends on the extent to which system characteristics resemble each other on the production and laboratory scales. One problem frequently encountered in the scale-up of bioprocesses is the nonideal or even unknown fluid flow behavior at large scale. Whereas the time constants of a biological reaction remain independent of vessel size, this is not true of many of the physical parameters involved. Mixing is sufficiently intense and uniform in laboratory scale fermenters that the microenvironment experienced by cells is effectively homogeneous throughout. With increasing fermenter dimensions, circulation times increase and the microenvironment experienced by the cells becomes a function of bulk flow, mixing, and turbulence. The behavior of such a system with its numerous interrelated processes is complex and difficult to predict, particularly when significant spatial variations exist within the bioreactor. It is in most cases the nonhomogeneous distributions of dissolved oxygen, substrate, pH, temperature, and dissolved carbon dioxide that are responsible for differences in performance at large scales of operation.

Although the effects of environmental extremes may be predictable in general terms, the overall effects of continually fluctuating conditions are not well understood. Whether the biological performance of the microorganisms is influenced by the changing environment in dissolved oxygen, substrate concentration, pH, and dissolved carbon dioxide depends on the magnitude of the characteristic times of the cell reactions. In this context, scale-down models can be used effectively to understand the effects of a nonhomogeneous microenvironment on cell metabolism and for process optimization.

### 18-2.1   Interaction between Liquid Hydrodynamics and Biological Performance

In aerobic fermentations, the most important consideration is often the adequate supply of oxygen to the cells. Oxygen is used continuously by growing cells and

due to its low solubility in the liquid phase, a continuous supply is necessary from the gas phase. Oxygen gradients can occur as a result of the interaction between oxygen transfer, long circulation times, and microbial kinetics. Since oxygen consumption occurs in segregated fluid elements circulating in the fermenter, the time constant for oxygen consumption is often the same order of magnitude as the liquid circulation. Depletion of the oxygen may occur at long circulation times, whereas the oxygen concentration remains relatively high at short circulation times. The time scales for circulation in large scale bioreactors may be comparable to the time scales for certain metabolic processes and adjustments (Roels, 1982). Bailey and Ollis (1986) assumed that the circulation time in a stirred vessel is lognormally distributed and that oxygen consumption rate follows a zero-order reaction. They showed that the exposure of cells to starvation conditions increases as the mean circulation time and the standard deviation of circulation times increases. This may also indicate that the kinetic models developed under the very different mixing conditions in a small reactor may not apply when greater mixing times and environmental fluctuations are encountered at the large scale.

Several authors have indicated the presence of dissolved oxygen concentration gradients, resulting from insufficient mixing and mass transfer. Their existence has been inferred from regime analysis (see Section 18-2.6) (Oosterhuis, 1984; Sweere et al., 1986) and in some cases by physical measurement (Carilli et al., 1961; Steel and Maxon, 1966; Manfredini et al., 1983; Oosterhuis and Kossen, 1983, 1984). Oosterhuis and Kossen (1984) reported the existence of dissolved oxygen concentration gradients in a 25 m$^3$ production scale fermenter equipped with two Rushton impellers, using a low viscosity broth (refer to Figure 18-1). The values of dissolved oxygen were corrected for hydrostatic pressure. Relatively high concentrations were measured in the impeller region (8 to 15% of air saturation at ambient pressure) and low values (0 to 6% of saturation) away from the vicinity of the impeller region in the macromixed zones. A strong radial gradient was also observed at the level of the agitator. Therefore, cells circulate in agitated vessels from the well-mixed impeller region (active zone) to the relatively poorly mixed regions (quiescent zones) and will experience fluctuations in dissolved oxygen concentration.

In some fermentations, performance may be governed by the efficiency with which nutrients such as glucose are mixed. Gradients in glucose concentration and their effects on microbial metabolism are discussed further in Section 18-2.7.1. Inhomogeneities also occur when the addition or removal of a component in a system is made in a nonuniform manner. Thus, the addition of concentrated acid or base for pH control will raise the local pH to a high value that will persist for longer if the mixing rate is slow. Solution pH is a fundamental parameter in the regulation of cellular metabolism, and the effects of spatial variations in pH can be important for successful scale-up. The effect of pH on cell metabolism is discussed in Section 18-2.11.

The viscosity of the broth will influence the bulk mixing, air dispersion, and power draw by the agitator. The rheological behavior of fermentation broths have been reviewed (Metz, 1976; Charles, 1978; Riley et al., 2000) and will generally
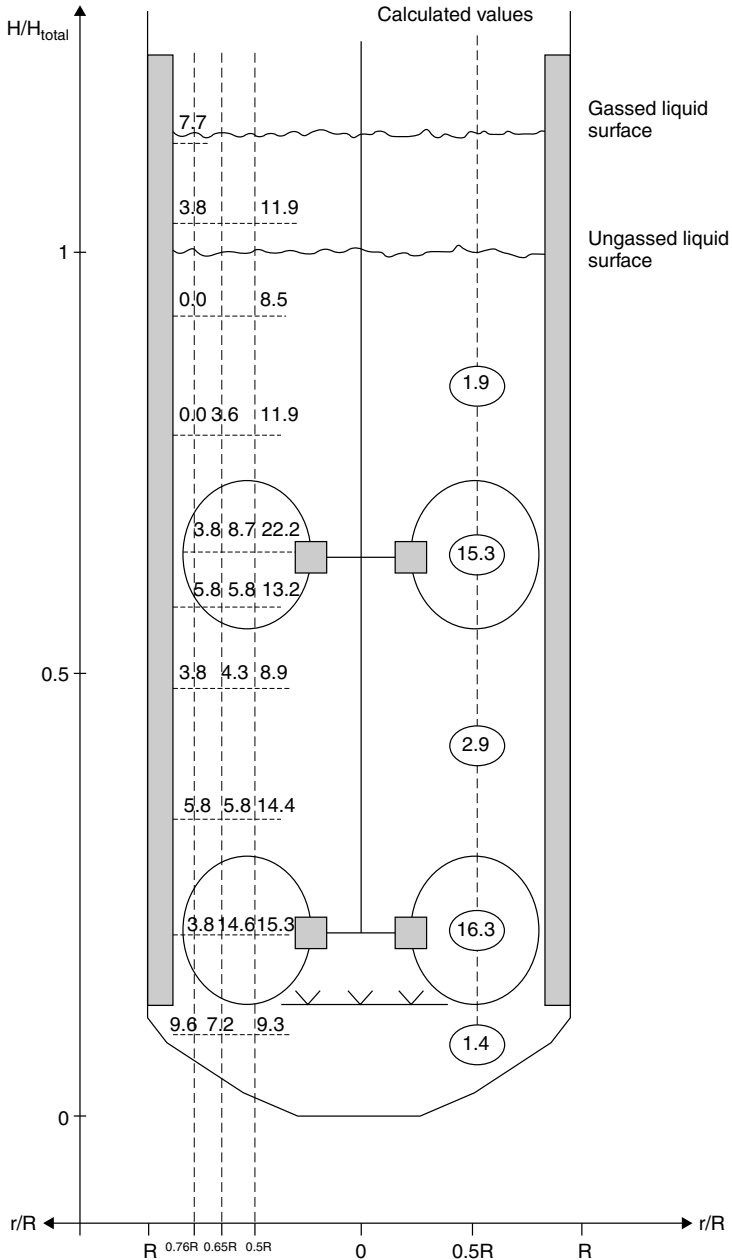
**Figure 18-1**  Dissolved oxygen concentration profiles in a 25 m$^3$ (19 m$^3$ working volume) fermenter. Relatively high concentrations of DOT were measured in the well-mixed impeller regions, while low values were measured in the radial and axial planes away from the impellers. The calculated values of DOT (using a two-compartment model for oxygen transfer as shown in the right of the figure in circles) were in broad agreement with the measured values. (From Oosterhuis and Kossen, 1984.)

be influenced by the morphology of the microorganism and in some cases by the formation of extracellular products such as xanthan gum (Amanullah et al., 1998b) and gellan gum (Dreveton et al., 1996). In suspensions of filamentous microorganisms, such as *Streptomycetes, Penicillium*, or *Aspergillus* species, the mycelial hyphae readily become entangled. Together with a high biomass concentration, this can lead to very viscous non-Newtonian suspensions, many exhibiting a yield stress or shear thinning behavior. These properties will have serious implications for bulk mixing. The presence or absence of a yield stress (or very low shear rates) will dictate whether there is flow in regions of low shear stress in the vessel. The stagnant regions outside the cavern persist even in aerated suspensions, and hence adequate oxygen transfer may take place effectively only in the vicinity of the impeller. Low dissolved oxygen levels as a result of poor oxygen transfer and mixing may cause changes in microbial metabolism, productivity, and product quality. For instance, the level of dissolved oxygen can have a marked effect on the recombinant protein production in fungal cultures (Amanullah et al., 2002) as well as on the quality of microbial polysaccharides as determined by the molecular weight (Trujillo-Roldan et al., 2001). In some instances microorganisms such as *Streptomycetes* can aggregate to form pellets, mats, or flocs. This can give rise to diffusional limitations. Steel and Maxon (1966) suggested that the limiting factor in the *Streptomyces* fermentation, where the microorganism was in the form of clumps, was the transfer of oxygen within the clump and not, as in unicellular fermentations, the transfer of oxygen into the liquid phase.

Important interactions between the turbulence intensity at different scales and the morphology (and hence the metabolic state) of certain organisms can be expected. The interaction is most important for organisms that grow to a size scale comparable to the turbulent Kolmogorov eddy scales expected. These scales range from the largest eddies, on the scale of the height of a turbine blade of an agitator ($\approx$0.1 m), to the smallest eddies, which are produced by the cascade of turbulent eddies. In agitated bioreactor systems, the smallest eddy size is on the order of 10 to 100 $\mu$m (Bailey and Ollis, 1986). Flocs of microorganisms, mycelial aggregates, and animal cells are intermediate in the size spectrum of turbulence and therefore may potentially be influenced by mixing intensity and the distribution of turbulence fields encountered in the reactor. On the other hand, unicellular bacteria and yeast are generally considered "shear" insensitive since their size is considerably smaller than the Kolmogorov eddy scale. The effects of hydrodynamic stress in fungal, bacterial, and animal cells are discussed in Sections 18-4.1, 18-5.1, and 18-6.1, respectively.

## 18-2.2   Fluid Dynamic Effects of Different Scale-up Rules

The scale-up of biotechnological processes developed in the laboratory often presents problems that owing to the complexity of multiple parameters do not permit a generalized solution. This section focuses on the empirical approach to scale-up and highlights the difficulties in maintaining kinematic similarity at different scales. In addition, it highlights the need to account for the biological

response of cells to the effects of changing scale. Later, a more process-specific approach is described in which the biological response of microorganisms can be predicted on scale-up using a scale-down approach. The effects of using different scale-up criteria on mixing of aerated stirred vessels has been discussed in this chapter with the aim of understanding the physical phenomena that may affect the biological response of microorganisms. Traditionally, many methods of scale-up of aerated, stirred fermenters have been considered and reviewed (Hempel and Dziallas, 1999). These include the following criteria:

1. Equal specific energy dissipation rates
2. Maintaining geometric similarity
3. Equal impeller tip speeds
4. Constant mixing times
5. Equal volumetric mass transfer coefficients
6. Equal oxygen transfer rates
7. Extrapolation or interpolation of test data generally secured for two scales
8. Combination of more than one of the criteria above

In the following section, the effects of the most commonly used scale-up methods on the mixing process are discussed using mixing theory, with the aid of theoretical and empirical correlations. Particular emphasis has been given to the use of equal specific energy dissipation rates. Correlations to predict the energy dissipation rate are essential, and the problems with their use are also mentioned.

### 18-2.2.1 *Scale-up at Equal Specific Energy Dissipation Rate*. Equal specific energy dissipation, $P/V$, is commonly used to scale-up fermentation and cell culture processes. In the following analysis of the use of equal $P/V$, only geometrically similar systems have been considered. Geometric similarity implies that all vessel dimensions have a common ratio ($H/T$, $D/T$, $C/T$, etc.). Furthermore, the power dissipated due to aeration is not considered, which may be significant compared to power input, due to agitation in cell culture processes (Langheinrich et al., 1998).

The ungassed power, $Po$, required by an impeller is given by

$$P = Po\rho ND^3 \qquad (18\text{-}1)$$

where $P$ is the power input, $\rho$ the fluid density, $N$ the impeller speed, and $D$ the impeller diameter.

Correlations for the gassed power number are discussed in Section 18-2.2.3, but it is reasonable to assume that the gassed power input is proportional to the ungassed power input in the turbulent flow regime. Thus,

$$P \propto P_g \propto N^3 D^5 \quad \text{and} \quad V \propto D^3 \qquad (18\text{-}2)$$

where $P_g$ is the gassed power input and $V$ is the liquid volume.

Using $(P/V)_{large} = (P/V)_{small}$, where $(P/V)_{large}$ and $(P/V)_{small}$ represent P/V at the large and small scales, respectively, results in $P \propto D^3$, and substituting for P gives $N^3D^2 = $ constant, resulting in

$$N \propto D^{-2/3} \qquad (18\text{-}3)$$

Therefore, the impeller speed will decrease on scale-up for geometrically similar vessels at constant P/V.

Revill (1982) recommends an impeller flow number, Fl, defined as $Q/ND^3$, of 0.75 for Rushton turbines in a fully turbulent system. Thus the impeller pumping capacity, Q, will increase with scale:

$$Q \propto D^{-2/3}D^3 \propto D^{7/3} \qquad (18\text{-}4)$$

However, the specific pumping capacity, Q/V, will decrease:

$$\frac{Q}{V} \propto D^{7/3}D^{-3} \propto D^{-2/3} \qquad (18\text{-}5)$$

The impeller tip speed,

$$U_T \propto ND \propto D^{-2/3}D \propto D^{1/3} \qquad (18\text{-}6)$$

Therefore, higher tip speeds are found on scale-up for geometrically similar vessels at constant P/V.

$$\text{Reynolds number, } Re \propto ND^2 \propto D^{-2/3}D^2 \propto D^{4/3} \qquad (18\text{-}7)$$

$$\text{Froude number, } Fr \propto N^2D \propto D^{-4/3}D \propto D^{-1/3} \qquad (18\text{-}8)$$

Thus, higher Reynolds number and smaller Froude numbers are found on scale-up. The Froude number is usually important only in situations where gross vortexing exists and can be neglected if the $Re < 300$ (Harnby et al., 1997). For higher Reynolds numbers, the effects of the Froude number can be eliminated by the use of baffles.

$$\text{circulation time, } t_c = \frac{V}{Q} \quad \text{or} \quad t_c \propto N^{-1} \propto D^{2/3} \qquad (18\text{-}9)$$

Since mixing time, $t_m \propto t_c$, therefore

$$t_m \propto D^{2/3} \qquad (18\text{-}10)$$

This inherent increase in mixing time is one of the major problems in scale-up (see also eq. 9.9). Fermentation processes are often scaled up using constant

$P_g/V$ and volumetric flow of gas per liquid volume per minute (vvm) or constant $P_g/V$ and $v_s$ (superficial gas velocity) and the effects of their use on the mass transfer coefficient and gas holdup also can be illustrated. The vvm is defined as

$$vvm = \frac{60Q_G}{(\pi/4)T^2H} \tag{18-11}$$

where $Q_G$ is the gas flow rate, T, the tank diameter, and H the liquid height. The superficial gas velocity is given by

$$v_s = \frac{Q_G}{(\pi/4)T^2} \tag{18-12}$$

Substituting for $Q_G$ from eq. (18-11) into (18-12) results in

$$v_s = vvm\frac{H}{60} \tag{18-13}$$

and for $H = T$,

$$v_s \propto vvm(T) \tag{18-14}$$

This implies that higher superficial gas velocities will result from scaling up at constant vvm using geometrically similar systems.

To calculate $k_La$ for noncoalescing salt solutions (typical of fermentation media), van't Riet (1979) suggests a correlation of the form

$$k_La \propto \left(\frac{P_g}{V}\right)^{0.7} v_s^{0.2} \tag{18-15}$$

Therefore, scaling up at constant $P_g/V$ and $v_s$ results in $k_La = $ constant (if the exponents on $P_g/V$ and $v_s$ are constant).

Scaling up at constant $P_g/V$ and vvm and substituting $v_s$ in eq. (18-15) using (18-14) gives

$$k_La \propto (vvm \cdot T)^{0.2} \propto T^{0.2} \tag{18-16}$$

At constant $P_g/V$ and vvm, $k_La$ will increase with scale for geometrically similar systems.

The effect on gas hold-up, $\varepsilon$, can be analyzed by using the correlation proposed by Smith et al. (1978):

$$\varepsilon \propto \left(\frac{P_g}{V}\right)^{0.48} v_s^{0.4} \tag{18-17}$$

By means of an analysis similar to that for $k_La$, it can be shown that scaling up at constant $P_g/V$ and $v_s$ results in $\varepsilon = $ constant, and scaling up at constant $P_g/V$ and vvm and assuming that $H = T$ results in

$$\varepsilon \propto T^{0.4} \tag{18-18}$$

### 18-2.2.2  Effect of Viscosity on Scale-up Equal Specific Energy Rates.

High viscosity broths arise as a result of product formation in polysaccharide fermentations (refer to Section 18-3) such as the production of xanthan or pullulan gum or due to the growth of filamentous species such as *Penicillium* or *Aspergillus* (refer to section 18-4). For non-Newtonian fluids obeying the power law, the average shear rate concept of Metzner and Otto (1957) can be used to estimate Reynolds number. Aeration of these fluids in stirred tanks results in the formation of stable equi-sized cavities behind each impeller blade. Increases in the aeration rate do not change the cavity size significantly and hence the power draw (Nienow et al., 1983). In viscous shear thinning fermentation broths (whether a yield stress exists or not is debatable; see Amanullah et al., 1998a), cavern formation can occur. These are regions around the impeller where there is intense gas–liquid mixing and motion. Outside these regions, the fluid is stagnant, and in this situation, the shear stress at the cavern boundary equals the fluid yield stress. More recently, an alternative mathematical model based on a fluid velocity approach has been proposed to estimate cavern sizes and can be applied to radial as well as axial impellers (Amanullah et al., 1998a) (see Section 18-3.3). Elson et al. (1986) proposed a correlation to predict the size of the cavern relative to the impeller diameter for Rushton turbines (using fluids with a yield stress) and also demonstrated the implications for scale-up:

$$\left(\frac{D_c}{D}\right)^3 = \frac{1.36 Po}{\pi^2} \rho N^2 D^2 \tau_y \tag{18-19}$$

where $D_c$ and $D$ are the cavern and impeller diameters, respectively, and $\tau_y$ is the fluid yield stress.

Expanding eq. (18-19) for constant fluid properties gives $D_c^3 \propto Po N^2 D^5$. At constant power input (assuming that Po is constant) $N \propto D^{-5/3}$, and with Re > 30 gives

$$D_c \propto D^{5/9} \tag{18-20}$$

Therefore, for a given power input, the cavern size will increase with larger impellers. Also,

$$\frac{D_c}{D} \propto N^2 D^2 \tag{18-21}$$

Therefore, the size of the cavern relative to the size of the vessel increases on scale-up at constant P/V. Also, a constant impeller tip speed is required to maintain the same value of $D_c/D$ on scale-up (see also Section 9-3.6).

### 18-2.2.3  Correlations for Impeller Power Consumption under Gassed Conditions.

The gassed power consumption is one of the most important parameters in the successful design and scale-up of stirred tank bioreactors since it influences numerous mixing parameters whose interactions are complex. However, a major weakness of scale-up at constant $P_g/V$ is in the estimation of the

gassed power consumption. Typically, the power consumption of Rushton turbines under aerated conditions is approximately 50% (or less) than the ungassed power, provided that the flow is turbulent. The nature of the gas cavities and bubble dynamics in the vessel affects the flow patterns and the power draw. Most of the correlations in the literature do not account for the flow regime. Establishing the flow regime is important since significant changes in power consumption can occur as a result of changing the flow regime. Studies by Nienow et al. (1985) and Warmoeskerken and Smith (1985) incorporating this concept have proposed different correlations for each type of gas cavity, which is determined essentially by the gas flow number and is discussed later. A selection of correlations from the literature to estimate gassed power is included below.

Calderbank (1958) proposed two correlations for $P_g/P$:

$$\frac{P_g}{P} = 1 - 12.6 \left( \frac{Q_G}{ND^3} \right) \qquad \text{for } Fl_G < 0.035 \qquad (18\text{-}22)$$

where $Fl_G$, is the gassed flow number, defined as $Q_G/ND^3$, and

$$\frac{P_g}{P} = 0.62 - 1.85 \frac{Q_G}{ND^3} \qquad \text{for } Fl_G > 0.035 \qquad (18\text{-}23)$$

Nagata (1975) proposed

$$\log \frac{P_g}{P} = -192 \left( \frac{D}{T} \right)^{4.38} \left( \frac{\rho D^2 N}{\mu} \right)^{0.115} Fr^{1.96(D/T)} Fl \qquad (18\text{-}24)$$

Luong and Volesky (1979) correlated $P_g/P$ by

$$\frac{P_g}{P} = 0.497 \left( \frac{Q_G}{ND^3} \right)^{-0.38} \left( \frac{\rho D^3 N^2}{\sigma} \right)^{-0.18} \qquad (18\text{-}25)$$

where $\sigma$ is the fluid surface tension.

Reuss et al. (1980) used dimensional analysis to obtain the following correlation:

$$\frac{P_g}{P} = 0.0312 Fr^{-0.16} Re^{0.064} Fl^{-0.38} \left( \frac{T}{D} \right)^{0.8} \qquad (18\text{-}26)$$

Hughmark (1980) reviewed the various correlations for the gassed power ratio and suggested

$$\frac{P_g}{P} = 0.1 \left( \frac{Q_G}{NV} \right)^{-0.25} \left( \frac{N^2 D^4}{g w V^{0.67}} \right)^{-0.2} \qquad (18\text{-}27)$$

where w is the blade width and g is the gravitational constant.

Greaves and Kobaccy (1981) proposed the following correlation to calculate the gassed power input in watts:

$$P_g = 1007 \left[ \frac{N^{3.33}D^{6.33}}{(\eta Q_G)^{0.404}} \right] \tag{18-28}$$

The efficiency index, $\eta$, was correlated depending on whether or not there was recirculation. For $N_F < N < N_R$, $\eta = 1$, where $N_R$ and $N_F$ represent the minimum impeller speed to prevent flooding and the speed at which the onset of recirculation occurs, respectively. To determine $N_F$ and $N_R$, they used

$$N_F = 1.52 \left( \frac{T^{0.2}Q_G^{0.29}}{D^{1.74}} \right) \tag{18-29}$$

$$N_R = 0.57 \left( \frac{T^{0.97}Q_G^{0.13}}{D^{2.34}} \right) \tag{18-30}$$

Warmoeskerken (1986) showed that plots of the power ratio $P_g/P$ versus the dimensionless flow number for different impeller speeds yield separate curves. This is due to increased gas recirculation at higher speeds. Most correlations for predicting the aerated power input do not take gas recirculation into account. Nienow et al. (1979) quantified the recirculation rate for a single Rushton turbine and found that it could be as high as three times the sparged rate. Van't Riet (1975) noted the presence of vortices behind the blades of Rushton impellers in a single-phase system. When the stirrer was operated in a gas–liquid system, gas was drawn to these regions (vortices) of low pressure and this led to the formation of gas-filled cavities. Van't Riet distinguished and defined three cavity forms, dependent on stirrer speed and gas flow rate; vortex, clinging, and large cavities. Warmoeskerken (1986) has identified flow regimes to relate the formation of these cavities to the power consumption of Rushton impellers and has proposed correlations, which take gas recirculation into account, to calculate the gassed power input for each type of cavity structure. Warmoeskerken (1986) combined the concepts of cavity formation and gas recirculation with empiricism to give:

- For vortex and clinging cavities, $0 < Fl_G < (Fl_G)_{3-3}$, where

$$(Fl_G)_{3-3} = 0.0038 \left( \frac{Re^2}{Fr} \right)^{0.07} \left( \frac{T}{D} \right)^{0.5} \tag{18-31}$$

$$\frac{P_g}{P} = 1 - 16.7(Fl_G)(Fr)^{0.35} \tag{18-32}$$

- For small 3–3 cavities, $(Fl_G)_{3-3} < Fl_G < 0.1$,

$$\frac{P_g}{P} = B - \left[ \frac{0.1(A - B)}{(Fl_G)_{3-3} - 0.1} \right] + \frac{(A - B)(Fl_G)}{(Fl_G)_{3-3} - 0.1} \tag{18-33}$$

where

$$A = 1 - 17(Fl_G)_{3-3}(Fr)^{0.35} \quad \text{and} \quad B = 0.27 + 0.022Fr^{-1} \qquad (18\text{-}34)$$

- For large 3–3 cavities, $0.1 < (Fl_G) < (Fl_G)_F$,

$$\frac{P_g}{P} = 0.27 + 0.022Fr^{-1} \qquad (18\text{-}35)$$

The correlations for predicting gassed power consumption of Rushton turbines mentioned earlier have been used to demonstrate the differences obtained in estimation of the gassed to ungassed power ratio, $P_g/P$, as a function of the flow number. For a fixed impeller size, the flow number can be varied by altering either the gassing rate or impeller speed. Thus, a low flow number can result from low gassing rates or a high impeller speed, and similarly, a high flow number can mean high gassing rates or low impeller speed. In the following example to demonstrate the effects of the use of different correlations to estimate $P_g/P$, the impeller speed has been held constant while the gassing rate has been varied from 0 to 3.5 vvm (Figure 18-2). The scale of the tank has been chosen such that it is within the range covered by the correlations. Considering a flat-bottomed tank equipped with a single Rushton impeller (unaerated power number $= 5.5$), with $T = 0.3$ m, $H/T = 1$, $D/T = 0.33$, $D = 0.1$ m, $w = 0.02$ m, containing water ($V = 0.0213$ m$^3$, $\rho = 1000$ kg/m$^3$, $\sigma = 72 \times 10^{-3}$ J/m$^2$) and operated at a
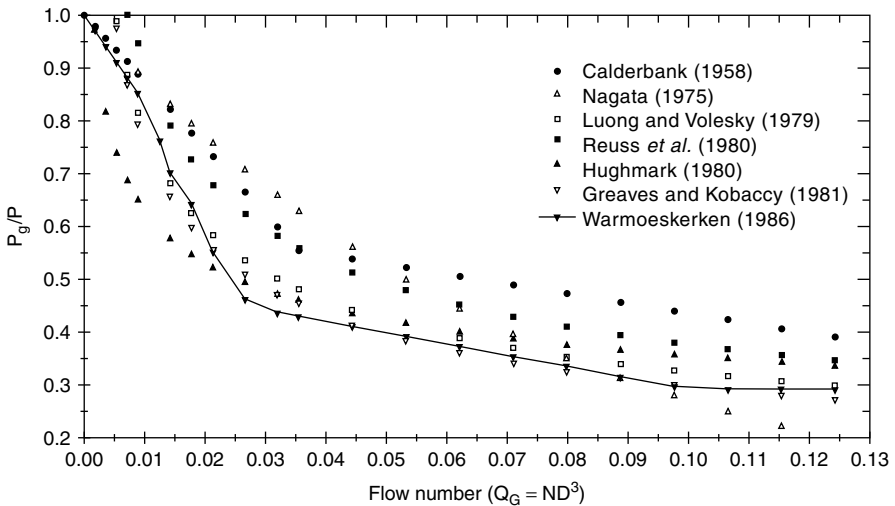


**Figure 18-2** Prediction of gassed power consumption using different correlations using a single Rushton turbine (unaerated power number $= 5.5$), with $T = 0.3$ m, $H/T = 1$, $D/T = 0.33$, $D = 0.1$ m, $W = 0.02$ m, containing water ($V = 0.0213$ m$^3$, $\rho = 1000$ kg/m$^3$, $\sigma = 72 \times 10^{-3}$ J/m$^2$) and operated at a constant impeller speed of 600 rpm. Under these conditions, the ungassed power consumption is 2.6 kW/m$^3$.

constant impeller speed of 600 rpm. Under these conditions, the ungassed power consumption is given by

$$P = (5.5)(1000)(10)^3(0.1)^5 = 55 \text{ W or } 2.6 \text{ kW/m}^3$$

At constant impeller speed, the gassed/ungassed power ratio has been calculated as a function of the gassing rate (in $m^3/s$, unless otherwise stated) for the various correlations. The $P_g/P$ ratio as evaluated by the use of these correlations, as a function of the flow number, is shown in Figure 18-2. It is not surprising that differences in the prediction of $P_g/P$ for the same flow number arise since some of the correlations have been obtained using different scales of operation and geometry. Also, most of these correlations have been derived from experiments in small scale vessels, and the power measurements may not be accurate (especially in the earlier studies). Thus, the differences in the predicted gassed power may be expected to increase with scale. Despite a lot of research in agitated gas–liquid systems, no satisfactory method exists for accurately predicting the gassed power consumption. This is due primarily to the complexity of the hydrodynamics of stirred gas–liquid systems. It is therefore difficult to predict the power consumption by simple correlations based on either empirical data or dimensionless analysis. The inaccuracy of this prediction is likely to increase in the case of multiple-impeller systems, which are commonly used in industrial fermentations. Further complications can arise when considering the power input in rheologically complex fermentations, where the availability of power input correlations are limited and further compounded by time-varying rheological characteristics of the fermentation broth.

### 18-2.2.4  *Scale-up by Maintaining Geometric Similarity*. Johnston and Thring (1957) have reviewed the principles of similarity for scale-up of processes and in particular for agitation applications. Although a useful purpose is served by the principle of similarity approach, it is seldom possible to apply it directly. Very few companies have geometrically similar bioreactors throughout their laboratory, pilot, and production scale facilities (Einsele, 1978). Geometric similarity may be maintained in going from bench to pilot scale tests. However, at the commercial scale, dimensions such as the H/T ratio may be changed from 1 to 2 or more to improve the efficiency of air utilization to reduce operating costs, and it may necessitate the use of multiple impellers to ensure adequate mixing. Most small scale fermenters are operated with Rushton turbines using a D/T ratio of 0.33. However, this ratio may be increased on scale-up since higher D/T ratios show advantages. Rushton impellers with large D/T ratios are more energy efficient for bulk blending in both low viscosity broths (Nienow, 1984) and for high viscosity shear thinning broths (Nienow and Ulbrecht, 1985).

The effect of the D/T ratio on gas dispersion can be demonstrated. Nienow et al. (1985) proposed the following equations for the flooding–loading transition

(denoted by the subscript F):

$$(Fl_G)_F = 30 \left(\frac{D}{T}\right) Fr_F \qquad (18\text{-}36)$$

and the complete dispersion (denoted by the subscript CD) phenomena:

$$(Fl_G)_{CD} = 0.2 \left(\frac{D}{T}\right)^{0.5} Fr_{CD}^{0.5} \qquad (18\text{-}37)$$

Considering the flooding correlation, at constant vvm using geometrically similar systems, we have

$$\frac{1}{N_F} \propto N_F^2 D \quad \text{since} \quad \frac{Q_G}{D^3} = \text{constant} \quad \text{and therefore} \quad \left(\frac{P_g}{V}\right)_F \propto D \qquad (18\text{-}38)$$

Similarly, using the complete dispersion correlation, it can be shown that

$$N_{CD} \propto D^{-0.25} \quad \text{and} \quad \left(\frac{P_g}{V}\right)_{CD} \propto D^{1.25} \qquad (18\text{-}39)$$

The analysis above shows that higher specific power input is necessary both to prevent impeller flooding and to achieve complete dispersion at the large scale. Also, from the flooding correlation, for constant aeration rate and a fixed vessel size,

$$\frac{1}{N_F D^3} \propto D^{4.5} N_F^2 \quad \text{and therefore} \quad N_F \propto D^{-5/2} \qquad (18\text{-}40)$$

Since constant pumping capacity implies that $N \propto D^{-3}$, eq. (18-40) may be taken to imply that at a fixed scale of operation, a constant pumping rate is required to disperse a given flow of gas. Also, the use of large D/T ratios is more economical since

$$P_F \propto N_F^3 D^5 \text{ and replacing } N_F \text{ using eq. (18-40) results in} \quad P_F \propto D^{-5/2} \qquad (18\text{-}41)$$

Therefore, lesser power is required to prevent flooding using large D/T ratios, or for the same power input, the gas-handling capacity of the impeller is increased. This would also imply that the drop in aerated power draw would be less when larger D/T ratios are used.

Similar analysis using the complete dispersion correlation results in

$$P_{CD} \propto D^{-1} \qquad (18\text{-}42)$$

The same conclusions as for flooding can be made, although the power dependence on the D/T ratio is reduced ($P_{CD} \propto D^{-1}$ compared to $P_F \propto D^{-2.5}$).

**18-2.2.5   *Scale-up at Equal Impeller Tip Speeds***. The impeller tip speed, $U_T$, has been used as a scale-up criterion for mycelial fermentations since it is often cited that the growth of the filamentous organisms is sensitive to the shear produced by the impeller. Typical values of $U_T$ employed are 5 m/s (Wang et al., 1979). The use of this scale-up criterion results in a higher power input ($P \propto D^2$), lower power per unit volume ($P/V \propto D^{-1}$), higher pumping capacity ($Q \propto D^2$), and longer circulation times ($t_c \propto D$). The effects of different scale-up rules, including tip speed and specific energy dissipation, on fragmentation of mycelial hyphae are considered in Section 18-4.1 and the use of $U_T$ as a scale-up criterion to correlate hyphal fragmentation in mycelial fermentations is shown to be unsatisfactory.

**18-2.2.6   *Scale-up at Constant Mixing Times***. Scaling up at constant mixing time or circulation time using geometrically similar systems is generally not acceptable since their use results in $P \propto D^5$ and $P/V \propto D^2$. It is rare to use a strategy that results in a higher P/V value at the large scale. If such a strategy is implemented, further benefits would have to be demonstrated to justify its use.

**18-2.2.7   *Scale-up at Equal Volumetric Mass Transfer Coefficients***. Scale-up at equal volumetric mass transfer coefficients ($k_La$) has to rely on the use of correlations to enable the calculation of overall values of $k_La$, which are of the form

$$k_La = A \left(\frac{P_g}{V}\right)^a v_s^b \tag{18-43}$$

where A, a, and b are approximately constant for a given fermenter system (geometry and system), independent of agitator type. Van't Riet (1979) has proposed correlations to predict $k_La$ within 20 to 40% accuracy for coalescing and noncoalescing salt solutions in stirred vessels. For water under coalescing conditions:

$$k_La = 2.6 \times 10^{-2} \left(\frac{P_g}{V}\right)^{0.4} v_s^{0.5} \tag{18-44}$$

where $0.002 \leq V \leq 2.6$ m$^3$ and $500 \leq (P_g/V) \leq 10\,000$ W/m$^3$. For salt solutions (noncoalescing):

$$k_La = 2.0 \times 10^{-3} \left(\frac{P_g}{V}\right)^{0.7} v_s^{0.2} \tag{18-45}$$

where $0.002 \leq V \leq 4.4$ m$^3$ and $500 \leq (P_g/V) \leq 10\,000$ W/m$^3$.

The effect of scaling up at equal $k_La$ and vvm using geometrically similar systems can be demonstrated as follows: Using eq. (18-45) for noncoalescing solutions (typical of fermentation broths) and assuming that $H = T$ and replacing $v_s$ using eq. (18-14) gives

$$k_La \propto \left(\frac{P_g}{V}\right)^{0.7} (vvm \cdot T)^{0.2} \tag{18-46}$$

Several authors (Humphrey, 1977; Moo-Young and Blanch, 1981; Oldshue, 1983; Charles 1985; Bailey and Ollis, 1986) recommend the use of equal $k_L a$ and vvm as a scale-up criterion together with the use of a correlation of the form of eq. (18-44) to calculate $k_L a$. The value of A in eq. (18-42) is sensitive to and is significantly reduced by antifoam (Martin et al., 1994). Humphrey (1977) reports that the exponents a and b vary with scale, and this is also in agreement with the observations of Bartholomew (1960). The apparently unspecific dependency of the exponents a and b in the correlation on a given fermenter system can lead to problems in using this approach for scale-up. For viscous fluids, a viscosity term, $\mu_a$, is introduced in eq. (18-44). Hickman and Nienow (1986) have shown that $k_L a \propto \mu_a^{-0.5}$.

### 18-2.2.8  *Scale-up at Equal Oxygen Transfer Rates*.

Often, the supply of oxygen is the factor limiting the productivity of large scale fermenters, especially in high-cell-density cultivations. The low solubility of oxygen in aqueous solutions necessitates the continual supply of oxygen from the gas phase. The lack of oxygen may result in the death of cells or may be responsible for diverting the metabolic pathways of some species. The oxygen transfer rate (OTR) can be calculated from

$$OTR = k_L a(C_L^* - C_L) \tag{18-47}$$

$C_L^*$ and $C_L$ represent the dissolved oxygen concentration at air saturation and in the liquid phase.

The maximum oxygen uptake rate ($OUR_{max}$) is related to biomass concentration (x) by

$$OUR_{max} = (Q_{O_2 \, max})x \tag{18-48}$$

where $Q_{O_2 \, max}$ is the maximum specific oxygen uptake rate.

Online oxygen uptake rate (and carbon dioxide production rate) have been possible to measure and calculate routinely for some time now using mass spectrometry (Buckland et al., 1985). Coupled with online dissolved oxygen measurements, this technique can also be used to measure online $k_L a$. Mass spectrometers offer fast, reliable, and accurate measurements of these parameters and have proved to be invaluable for process monitoring, control, and scale-up. In fact, the data generated using online exhaust gas analysis forms the basis of this widely used scale-up rule using the maximum oxygen transfer capability of fermenters (which, in turn, dictates its biomass production capability) as a scale-up criterion.

Successful scale-up (from 0.005 to 57 $m^3$), using constant OTR, of penicillin and streptomycin and baker's yeast (from 0.019 to 114 $m^3$) fermentations have been reported (Hempel and Dzialas, 1999). However, examples have also been reported (Bartholomew, 1960) where in vitamin $B_{12}$ fermentations, the use of equal OTR as a scaling parameter led to an oversizing of the large scale fermenter. This may occur partly due to the fact that the measurement of $C_L$ by point-positioned dissolved oxygen probes may be unrepresentative of the global $C_L$ distribution at the large scale in which dissolved oxygen gradients may be severe.

This can be due to several reasons. First, the rate of transfer to the liquid phase, and hence $C_L$, increases with increasing hydrostatic head. This is exacerbated by the depletion of oxygen from the gas phase by bubbles rising through the liquid. Second, both oxygen transfer and oxygen uptake are position dependent, due to the combined effects of regions of different mixing intensities, resulting in inhomogeneities and the presence of a circulation time distribution.

### 18-2.2.9 Effects of Different Scale-up Criteria Using a Linear Scale-up Factor of 10.
The extrapolation or interpolation of test data generally secured for two scales is used extensively in chemical engineering for scale-up. However, there is a limited range in which the results can be used and caution has to be exercised if extrapolation is extensive. The effects of the various scale-up criteria discussed in previous sections on the mixing process have been evaluated and their consequence for large scale operation is shown in Table 18-1. This is based on an extension from an earlier analysis conducted by Oldshue (1966) for geometrically similar systems under unaerated conditions and a linear scale-up factor of 10, or a 1000 fold increase in volume. The present analysis has been conducted for aerated conditions where the gassed power input has been assumed to be proportional to the ungassed power input. It has also been extended to include the effects of scale-up at equal $k_L a$ and vvm and equal $k_L a$ and $v_s$ as well as the consequence for scale-up on the impeller pumping capacity, Froude number, and the circulation time. Correlations proposed by van't Riet (1979) for noncoalescing salt solutions have been used to calculate $k_L a$.

From Table 18-1 it can be seen that scale-up at equal power per unit volume for geometrically similar systems results in a lower impeller speed, higher tip speed, pumping capacity, $k_L a$ (at constant vvm), and circulation time. Scale-up at equal impeller speed or mixing time is unrealistic since the power input per

**Table 18-1**   Effect of Different Scale-up Criteria Using a Linear Scale-up Factor of 10 and Maintaining Geometrical Similarity ($Re > 10^4$)

| Large Scale/ Small Scale Value | Equal P/V | Equal N | Equal $U_T$ | Equal Re | Equal $k_L a$ and vvm | Equal $k_L a$ and $v_s$ |
|---|---|---|---|---|---|---|
| $P \propto N^3 D^5$ | 1000 | $10^5$ | 100 | 0.1 | 829 | 1000 |
| $P/V \propto N^3 D^2$ | 1 | 100 | 0.1 | $10^{-4}$ | 0.8 | 1 |
| N or $T_m^{-1}$ | 0.22 | 1 | 0.1 | 0.01 | 0.3 | 0.22 |
| $U_T \propto ND$ | 2.2 | 10 | 1 | 0.1 | 2.7 | 2.2 |
| $Re \propto ND^2$ | 22 | 100 | 10 | 1 | 27.2 | 22 |
| $Q \propto ND^3$ | 220 | 1000 | 100 | 10 | 272 | 220 |
| $Fr \propto N^2 D$ | 0.48 | 10 | 0.1 | $10^{-3}$ | 0.5 | 0.48 |
| $T_c \propto N^{-1}$ | 4.55 | 1 | 10 | 100 | 9.4 | 4.55 |
| $k_L a$ at equal vvm | 1.59 | 39.8 | 0.32 | $2.5 \times 10^{-5}$ | 1 | — |
| $k_L a$ at equal $v_s$ | 1 | 25.1 | 0.20 | $1.6 \times 10^{-3}$ | — | 1 |

unit volume has to be increased substantially. Scale-up at constant Reynolds number is also not feasible since in this case the $P_g/V$ value is reduced by a factor of $10^4$ at the large scale. Equal impeller tip speed can be used, although the reduction in the $P_g/V$ value by a factor of 10 also results in lower $k_La$ values. Also, in this case there is a 10 fold increase in the circulation time. Equal $k_La$ and vvm and equal $k_La$ and $v_s$ are also commonly used for scale-up. One of the consequences of using the former scale-up criterion rather than the latter is that the power consumption is lower due to the higher superficial gas velocity, and this results in higher circulation times.

It is important to note that regardless of the choice of scale-up criterion (except scale-up at equal impeller speed or mixing time, both of which are economically unrealistic), there is an increase in the circulation time at the large scale. This increase, coupled with high oxygen demands, can cause severe oxygen gradients, and coupled with the addition of concentrated reagents for pH control and nutrient availability, can have a significant impact on fermentation yield. It is clear from Table 18-1 that different scale-up criteria result in entirely different process conditions at the larger scale. It is impossible to maintain similarity of all aspects of the microenvironment at different scales. The scale-up criteria are system specific and it is therefore necessary to select a scale-up basis depending on the transport property most critical to the performance of the bioprocess. Thus, if oxygen transfer is the limiting factor in a fermentation, scale-up at equal $P_g/V$ may be invoked, or if shear rates are significant, the energy dissipation/circulation function (see Section 18-4.1) may be employed. However, keeping one parameter constant also results in a change in other important variables. Therefore, the choice of scale-up rule is not easy given the potentially sensitive and diverse responses of cells to each of the transport phenomena influenced by impeller design, system geometry, scale, fluid properties, and operating parameters.

Kossen and Oosterhuis (1985) proposed two ways to solve the problem of scale-up of bioreactors: first, by acquiring more knowledge about the hydrodynamics and interaction of the hydrodynamics with other mechanisms in production scale fermenters, and second, by developing scale-up procedures that give an adequate estimation of the performance of production scale fermenters based on small scale investigations. This approach is discussed in detail in later sections.

## 18-2.3   Influence of Agitator Design

For many years, Rushton turbines of approximately one-third the fermenter diameter were considered as the optimum design for mixing of fermentation processes. These radial flow impellers induce high turbulence around the impeller region and thus promote good gas dispersion and bubble breakup. Bulk blending is considered to be poor, using such turbines due to their tendency to compartmentalize (Nienow and Ulbrecht, 1985) and can lead to broth inhomogeneities of either pH or oxygen. This may be expected to be amplified in viscous, non-Newtonian broths (Buckland et al., 1988a; Nienow et al., 1995; Amanullah et al., 1998b).

Bryant (1977) and Bajpai and Reuss (1982) have suggested that the critical factor that determines the overall effectiveness of oxygen uptake by microorganisms is the frequency at which cells are circulated through the highly oxygenated impeller region. However, the circulation capacity of standard Rushton impellers with D/T ratios of 0.33 may be insufficient to induce the necessary bulk flow to satisfy the oxygen requirements of cells. To improve the liquid pumping capacity, the use of large D/T ratios has been suggested (Nienow, 1984). Prochem hydrofoil impellers, which produce axial flow, have been tested for use in high viscosity mycelial fermentations. Buckland et al. (1988a) demonstrated, in viscous mycelial fermentations at the pilot scale, that the replacement of standard radial flow Rushton impellers with larger diameter axial flow Prochem impellers, significantly improved the oxygen transfer efficiency. This improvement was attributed to the increase in size of the well-mixed, low viscosity cavern in the impeller region. The reader is also referred to the publications by Nienow (1990, 1998) and Nienow et al. (1995) for detailed discussions regarding the role of agitator design in fermentations. The effects of impeller geometry and type (including Scaba impellers) in high viscosity xanthan fermentations and fungal fermentations are discussed in Sections 18-3 and 18-4, respectively.

## 18-2.4   Mixing and Circulation Time Studies

It is generally recognized that the performance of bioreactors depends on the intensity of mixing of the gas and liquid phases. Therefore, extensive efforts have been devoted to understanding the mixing characteristics in bioreactors. Mixing in agitated vessels is dependent on both the levels of turbulence in the region of the agitator and in the remainder of the vessel, as well as the bulk turnover of the vessel contents. Einsele (1978) reported mixing times on the order of 160 s in aqueous, unaerated bioreactors of up to 100 m$^3$ in volume. He correlated the mixing times measured at different scales using the equation

$$t_m \propto V^{0.3} \tag{18-49}$$

Longer mixing times may result in aerated Newtonian and non-Newtonian systems. Einsele and Finn (1980) reported mixing times in aerated stirred tanks (0.02 and 0.35 m$^3$) using different aqueous solutions. From the pH response to a pulse input, it was shown that these mixing times increased with increasing gas holdup, and this was found to be more pronounced in higher viscosity solutions. They concluded that the mixing efficiency of a stirrer is adversely affected by the interaction between gas bubbles and the eddies that are generated by the stirrer under turbulent conditions. Using a flow follower technique, Bryant and Sadeghzadeh (1979) and Middleton (1979) observed an increase in the mean circulation time and the standard deviation under gassed conditions. Middleton (1979) indicated that this was expected in view of the decrease in the pumping capacity of the impellers caused by gas-filled cavities behind the impeller blades. This phenomenon was also reported by van Barneveld et al. (1987), who

used a similar technique in a production scale 25 m$^3$ fermenter. In contrast, Paca et al. (1976) observed shorter mixing times in aerated completely dispersed non-Newtonian systems than in unaerated ones. Under conditions of flooding, they reported higher mixing times than in unaerated systems. Correlations to estimate mixing times are given in Chapter 9. Although knowledge of the mixing and circulation times is potentially useful, these times do not on their own provide sufficient criteria with which the effects of inhomogeneities on microorganisms can be quantitatively explained. It is, in fact, the microenvironment experienced by the cells that determines the biological performance, not the partial view of the same system, provided by overall mixing times or oxygen transfer coefficients. In this regard, the concept of a circulation time distribution is very useful to describe the environment experienced by microorganisms.

***18-2.4.1 Circulation Time Distribution Models***. Circulation time is an important concept in the study of fluctuating environmental conditions because it provides an indication of the characteristic time interval during which a cell circulates through different regions of the reactor and hence possibly encounters different reaction conditions along the way. Clearly, consideration of a single circulation time in an agitated tank is a conceptual approximation. Upon leaving the impeller region, different elements of fluid will follow different paths in the vessel, giving rise to correspondingly different circulation times. An alternative method for characterizing the circulation in a stirred vessel is by the circulation time distribution (CTD). This is defined as the probability for each possible time interval that a fluid element takes to return to a fixed point, which is usually taken as the impeller region or in the case of substrate and pH addition as the feed (or addition) zone (Noorman et al., 1993; Larsson et al., 1996). A CTD is characterized by a mean circulation time and a standard deviation. Bryant and Sadeghzadeh (1979) described the measurement of circulation time distributions by means of a neutrally buoyant radio transmitter and a monitoring antenna around the impeller. Middleton (1979) used this technique to measure the CTD in 0.18, 0.60, and 1.80 m$^3$ vessels with Rushton turbines using water under aerated and unaerated conditions. He showed that circulation times were lognormally distributed, with no relationship found between successive circulation times. Thus, in a fermenter, individual microorganisms will be subjected to oxygen depletion in a more-or-less random way. Under unaerated conditions, Middleton (1979) proposed the following equation to quantify the circulation time:

$$t_c = 0.5 V^{0.5} \frac{1}{N} \left( \frac{T}{D} \right)^3 \tag{18-50}$$

For aerated systems, the mean circulation time and the standard deviation increased. However, correlations under these conditions were not reported. A lognormal CTD was also reported by Oosterhuis (1984) and van Barneveldt et al. (1987), who measured circulation times using a similar technique in a 25 m$^3$ bioreactor using water. In mechanically agitated vessels, a very high degree of

turbulence exists in the vicinity of the impeller. Cutter (1966) reports that up to 70% of the energy dissipation takes place in the impeller region. In this region, micromixing is complete (Bajpai and Reuss, 1982) and through it, the entire fluid in the vessel passes at a frequency dictated by the CTD. Away from the impeller, where the turbulence intensity is less, the mixing of fluid elements may range from complete micromixing to segregation. Using this concept, Bajpai and Reuss (1982) proposed, after Manning et al. (1965), a two-environment model which they named the *micro–macromixer model*. The volume of the micromixed region is very small compared to the macromixed region. The recirculating stream from the macromixed region is completely mixed with the incoming component, if any, and returned to the macromixed zone. In this manner the micromixed zone produces elements of age zero for the macromixed zone. This two-zone model was coupled with microbial kinetics to evaluate the performance of bioreactors. The CTD was described using the following equations:

$$f(t_c) = \frac{1}{\sqrt{2\pi}\sigma_l t_c} \exp\left[\frac{(\ln t_c - \mu_l)^2}{2\sigma_l^2}\right] \tag{18-51}$$

$$\bar{t}_c = \exp\left(\mu_l + \frac{\sigma_l^2}{2}\right) \tag{18-52}$$

$$\sigma_\theta^2 = \frac{\sigma^2}{\bar{t}_c^2} = \exp(\sigma_l^2) - 1 \tag{18-53}$$

where $f(t_c)$ is the CTD, $t_c$ the range of circulation times, $\bar{t}_c$ the mean circulation time, $\sigma$ the standard deviation of the measured mean circulation time, $\sigma_\theta$ the normalized standard deviation with respect to the mean circulation time, and $\mu_l$ and $\sigma_l$ the mean and standard deviation of a lognormal distribution, respectively.

As an example, eqs. (18-51)–(18-53) have been used to calculate the CTD and the cumulative CTD for mean circulation times of 20, 40, and 120 s using a standard deviation of 8.9 s [as reported by Bajpai and Reuss (1982) for a 100 m³ fermenter] and are shown in Figure 18-3a. For $\bar{t}_c = 20$, 40, and 120 s, the circulation times are distributed in the ranges 0 to 90 s, 0 to 180 s, and 0 to 360 s, respectively. The cumulative CTD can be used with an estimate of the oxygen consumption time ($t_{oc}$) to determine the percentage of cells that may be subjected to conditions of oxygen starvation. The maximum oxygen consumption rate for a *Bacillus subtilis* culture was determined to be $4.73 \times 10^{-6}$ mol/g cell per second (Amanullah et al., 1993a,b). At a biomass concentration of 3 g/L and assuming zero-order kinetics, it would take $\approx 10$ s to reduce the DOT from 50% of air saturation to zero. As an example, this time ($t_{oc}$) is depicted by a dotted line in Figure 18-3a. Thus, the percentages of cells exposed to oxygen-depleted conditions for $\bar{t}_c = 20$, 40, and 120 s have been estimated as 66%, 88%, and 98%, respectively, from the intersection of this line with the respective cumulative CTD curves. Similar calculations to show the influence of increasing mean circulation times on the percentage of
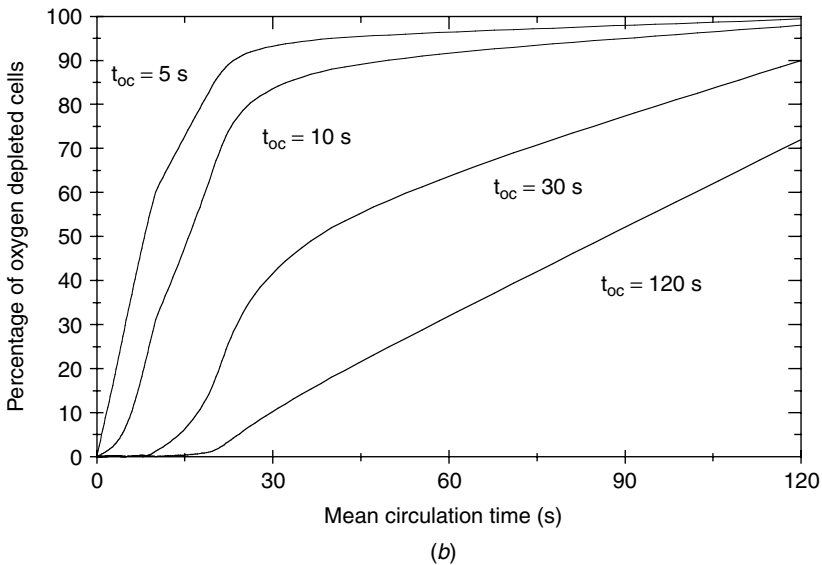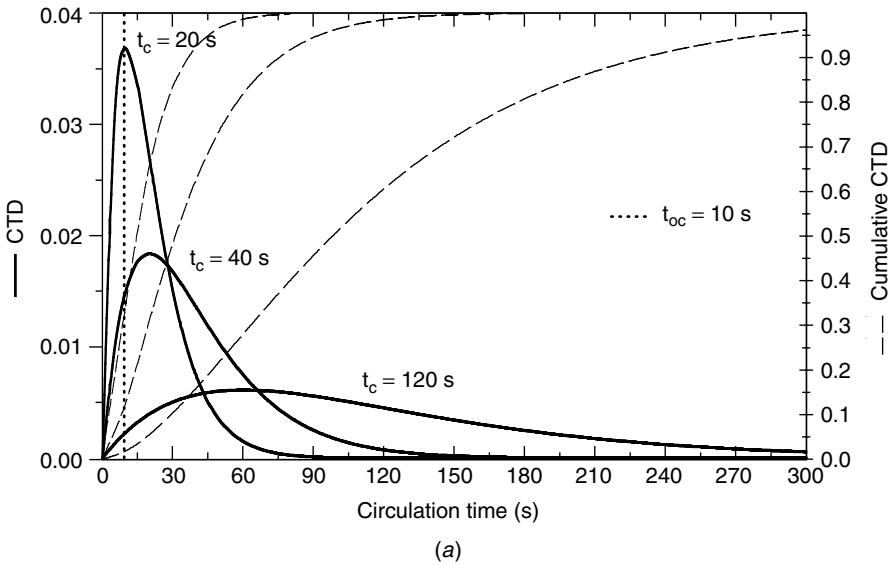
**Figure 18-3**   (*a*) Calculated CTD [using eqs. (18-53)–(18-55)] and cumulative CTD at mean circulation times of 20, 40, and 120 s using a standard deviation of 8.9 s. Also shown as an example is a line of dots representing an oxygen consumption time of 10 s, which can be used to estimate the percent of oxygen depleted cells for a given circulation time (see Figure 18-3*b*). (*b*) Effect of mean circulation time on the percentage of cells subjected to oxygen depletion at different oxygen consumption times ($t_{oc}$).

cells exposed to oxygen-depleted conditions at different oxygen consumption times can be made, and the results are shown for $t_{oc} = 5$, 10, 30, and 120 s in Figure 18-3*b*. From this figure it is clear that as the mean circulation time increases, the percentage of cells exposed to oxygen-depleted conditions increases, and as the oxygen consumption time increases, the percentage of oxygen-deprived cells decreases. These calculations do not account for oxygen mass transfer, which would decrease the percentage of oxygen-deprived cells. Nevertheless, the concept of combining the CTD with oxygen uptake kinetics is very useful in analyzing the effects of nonhomogeneous DOT on cell metabolism.

## 18-2.5 Scale-down Approach

Scale-down is used to try to model physically at the laboratory scale the environmental conditions that microorganisms experience at the large scale. Oosterhuis and Kossen (1984) suggested that for a more realistic approach to scale-up, the rate-limiting step has to be determined first. The laboratory scale process is then designed by optimizing the rate-limiting step. The results of the optimization are then applied to the production scale, although this step has rarely been implemented. The most important requirement for experiments on the small scale is that they have to be representative of the conditions at the large scale. This obviously determines the possibilities and limits of the scale-down approach. A knowledge of the reaction kinetics and metabolic pathways is essential, and these have to be measured. Figure 18-4 shows the scale-down procedure as proposed by Oosterhuis and Kossen (1984). Scale-down strategies are based on actual or calculated measurements at the large scale and are designed on the individual characteristic features of the actual process (see Section 18-2.7.1 for details of scale-down studies).
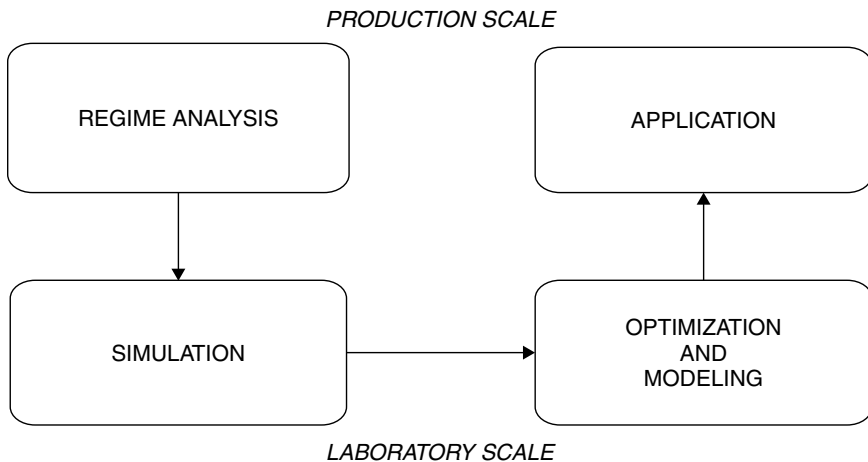
*PRODUCTION SCALE*



*LABORATORY SCALE*

**Figure 18-4**    Scale-down procedure. (From Oosterhuis and Kossen, 1984.)

## 18-2.6 Regime Analysis

The rate-limiting step in a bioprocess can be determined by carrying out a regime analysis. This analysis is based on a comparison of the characteristic times of various mechanisms in a process. Characteristic times can be defined as a ratio of capacity to flow. The comparison of times, in terms of orders of magnitude, can be made experimentally, or theoretically, qualitatively, or quantitatively. A low value of a characteristic time means a fast mechanism; a high value indicates a slow mechanism. Regime analysis can also be used to quantify the effects of changes from the well-mixed conditions at the small scale to the possible inhomogeneities arising at the large scale. It can also be used to determine whether there is a single rate-limiting mechanism (pure regime) or whether more than one mechanism (mixed regime) is responsible. Besides regime analysis, it is also important to use dimensional analysis and the principles of similarity to devise small scale experiments (Sweere et al., 1987). The use of regime analysis in conjunction with scaled-down optimization techniques has been reviewed by Sweere et al. (1987). Regime analysis of baker's yeast and *B. subtilis* fermentations can be found in Sweere et al. (1987) and Amanullah (1994). Oosterhuis (1984) conducted a regime analysis for the gluconic acid fermentation in a 25 m$^3$ fermenter. The results of the analysis are shown in Table 18-2, from which the following conclusions can be made:

1. The characteristic times for oxygen consumption and transfer to the liquid phase are of the same order of magnitude, and therefore oxygen limitation can occur. Also, the liquid circulation time is on the same order of magnitude, and hence oxygen gradients are likely to occur.

**Table 18-2** Regime Analysis of a 19 m$^3$ Gluconic Acid Fermentation

|  | Time (s) |
|---|---|
| *Transport Phenomena* | — |
| Oxygen transfer | 5.5 (noncoalescing) |
|  | 11.2 (coalescing) |
| Liquid circulation | 12.3 |
| Heat transfer | 330–650 |
| *Conversion* | — |
| Oxygen consumption | 16 (zero order) |
|  | 0.7 (first order) |
| Growth | $1.2 \times 10^4$ |
| Substrate consumption | $5.5 \times 10^4$ |
| Heat production | 350 |

*Source*: Oosterhuis (1984).

2. Growth and substrate consumption are unlikely to influence the perfor-
   mance of the process since the time constants for these processes are much
   larger compared to those for oxygen consumption and oxygen transfer.

3. From a comparison of the times for heat transfer and heat production, it
   is possible to say that heat transfer will not be a problem at this scale,
   and temperature gradients should not be present since the liquid circulation
   time is relatively small compared to the time constant for heat production.

## 18-2.7  Effects of Fluctuating Environmental Conditions on Microorganisms

Most of the studies in the literature are limited to investigating the effects of
substrate and dissolved oxygen inhomogeneities on microorganisms, although
more recently the effects of pH gradients have also been reported using
*B. subtilis* as a model system (Amanullah et al., 2001b) and using GS-NSO
myeloma cells (Osman et al., 2002). It should be pointed out that very few
studies have been reported in animal cell culture systems, and therefore the
review in the following sections has been limited to microbial systems. In
investigating the influence of a changing environment on cells, a distinction
has to be made between a single change (step signal or impulse) and continuous
changes. The latter can be divided into periodic and nonperiodic. The response
of microorganisms to forced variations in dissolved oxygen and substrate
concentration has been used to study the effects of (1) periodic operation of both
fed-batch and continuous culture fermentations as a method of improving culture
performance, (2) transient conditions on the biochemistry of microorganisms
in order to gain insight into microbial regulatory and control mechanisms,
(3) determination of environmental fluctuations to which microorganisms will
be exposed on scale-up, (4) verification of scale-down performance as an
indicator of large scale performance, and (5) improvements to large scale
fermentation processes.

Many of the inhomogeneities encountered in production scale fermenters are
cyclic in nature and can be approximated by forced sine- or square-wave func-
tions. Such periodic fluctuations lead to every point on the sine or square wave
describing a change in pressure, dissolved oxygen, or substrate concentration as
a function of time (Vardar and Lilly, 1982). Therefore, each point represents a
different region in a mechanically agitated vessel or a discrete element of fluid in
circulation through the micro- and macromixed regions of the vessel. Experimen-
tal small scale simulations of mixing and mass transfer limitations in large scale
bioreactors have been made in several ways: by cyclic feeding of the limiting
nutrient, by cyclic changes in the fermenter head pressure, by creating artificial
dead zones, and by adding viscosity-enhancing agents. These studies are reviewed
in the following sections and have been divided primarily into the effects of fluc-
tuations in substrate and dissolved oxygen concentrations on microorganisms,
although pH gradients are discussed in Section 18-2.11.

***18-2.7.1 Scale-down Models to Simulate Substrate Inhomogeneities at the Large Scale***. An example of a microorganism that is particularly sensitive to glucose concentrations is *Saccharomyces cerevisiae*, which may alter its metabolism from oxidative to oxido-reductive, depending on the glucose level. A large number of investigations have been carried out using this microorganism, not only because of its commercial importance as baker's yeast, but also due to its sensitivity to the glucose effect. The primary goal in the baker's yeast process is to direct the glucose availability to biomass formation and prevent the formation of ethanol. Another industrial microorganism that is commonly used to produce recombinant proteins (Bylund et al., 2000) is *E. coli.* In this case, acetate formation due to overflow metabolism of glucose is undesirable. Thus, fed-batch strategies are commonly applied in industrial fermentations involving these microorganisms. Glucose feed concentrations of 500 to 600 g/L are generally used. However, the glucose saturation concentrations for *E. coli* and *S. cerevisiae* are 5 and 150 mg/L, respectively (Larsson et al., 1996). On a macroscale with respect to liquid-phase nutrients, it is reasonable to assume that higher concentrations of the substrate exist locally in the entry region of even well-mixed systems. Exposure of cells to this feed zone may affect their biological performance and the degree and duration of the perturbation will depend on the sensitivity of the microorganism to the change. The most comprehensive experimental evidence for such elevated concentrations in large bioreactors have been reported by the groups of Larsson and Enfors (Royal Institute of Technology, Stockholm, Sweden).

Larsson et al. (1996) measured spatial concentrations of glucose in fed-batch fermentations of *S. cerevisiae* at a scale of 30 $m^3$ (19.8 to 22 $m^3$ working volume) at the top (0.5 m below the liquid surface, where about 600 g/L glucose was added), middle and bottom of the bioreactor (close to the well-mixed region of the lowest impeller). Rapid sampling (0.15 s/sample) and inactivation allowed the determination of transient concentrations of glucose. At the top location glucose varied in the range of about 40 to 80 mg/L, whereas at the bottom location the level was relatively constant at about 22 mg/L. Given that the saturation constant is about 150 mg/L and Monod kinetics apply, these measurements suggest significant variations in cell metabolism, depending on the cellular spatial location in the bioreactor. Interestingly, the measured glucose variation was lower (about 16 to 36 mg/L) when glucose was fed near the bottom impeller.

The effects of glucose gradients in a 12 $m^3$ bioreactor on the production of recombinant protein by *E. coli* was also reported by Bylund et al. (1999). These authors measured spatial concentrations in the constant glucose feed (550 g/L) phase using the technique described by Larsson et al. (1996) except that the measurement location was altered such that samples were withdrawn 3 cm below the addition point and at 180° from the feed point. More significant variations in glucose levels were measured than those reported by Larsson et al. (1996); in the 180° position, the variation in glucose levels was in the range 70 to 4500 mg/L (Figure 18-5A). Of course, if it were possible to measure instantaneously from an infinitesimally small volume, the upper range in measured glucose levels

would approach that in the feed solution. Such measurements also raise questions about feedback control strategies in large scale bioreactors based on point measurements using online probes.

A particularly interesting study of the physiological response of *E. coli* to glucose gradients in large scale bioreactors was reported by Enfors et al. (2001). Fed-batch cultivations were conducted at a 22 m$^3$ scale (30 m$^3$ bioreactor) equipped with either four radial flow Rushton turbines or four Scaba impellers in a radial/axial flow combination (see Section 18-4 for details of such impellers). Measurements of glucose concentration were made at three locations, including the glucose addition zone (top position), mid-liquid height, and in the plane of bottom impeller. The values of glucose measured were 57, 34, and 27 mg/L at the top, middle, and bottom positions, respectively. These differences were largely absent when the Scaba impellers were used. Spatial variations in glucose concentration with increasing distance from the feed point has been demonstrated in previous large scale studies (Larsson et al., 1996; Bylund
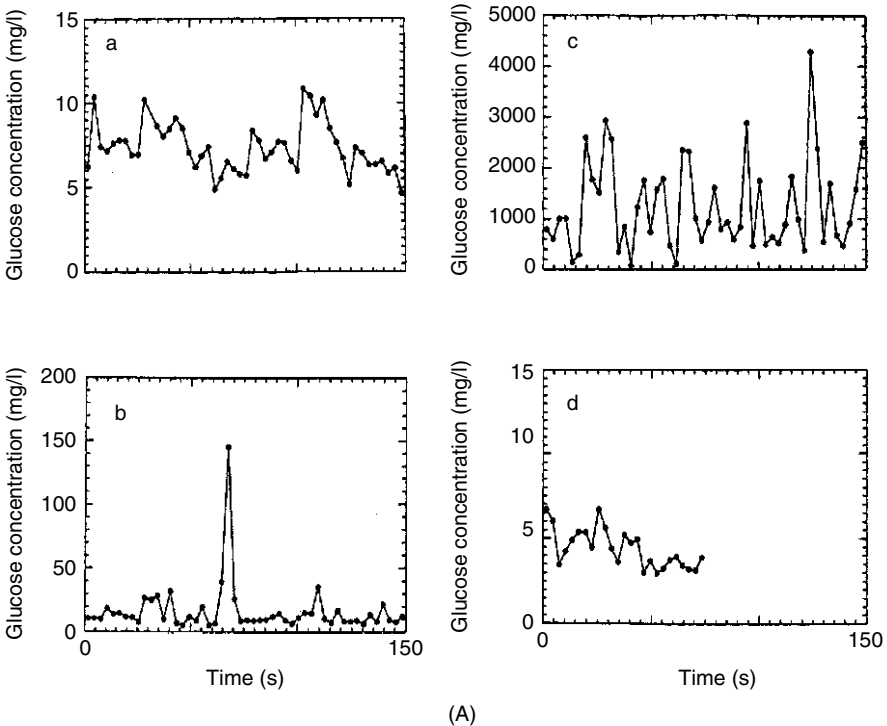


**Figure 18-5**    (A) Glucose sampling with a frequency of 3 s in a 12 m$^3$ *E. coli* fermentation. Glucose was fed to the top surface of the liquid at a concentration of 552 g/L and sampled at different locations: (*a*) 3 cm below feed point; (*b*) 30 cm below feed point; (*c*) 180° from feed point; (*d*) at the bottom of the bioreactor. (From Larsson et al., 1996.) (*Continued*)
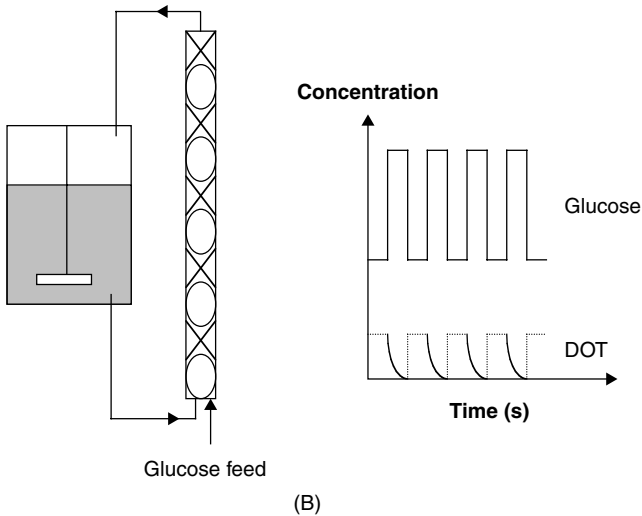
(B)

**Figure 18-5**   (B) Scale-down model (STR + PFR) to simulate the effects of a high glucose concentration feed zone coupled to low dissolved oxygen (DOT) effects in large scale bioreactors. The scale-down model consists of an aerated STR and a PFR in series. The nonaerated PFR contains static mixers to promote plug flow and high oxygen mass transfer rates, DOT probe at the outlet, and a number of sampling points along its length. With glucose fed to the PFR it is possible to measure the physiological response of cultures subjected to high glucose levels at the addition point with low levels of DOT and low and high levels of glucose and DOT, respectively, in the bulk (represented by the STR). (From George et al., 1993.)

et al., 1998). The mixing time was measured between 1 and 2 min. Thus, cells circulating in the bioreactor encountered spatial variations in glucose concentrations. The consequence of this was formate accumulation, highlighting the effects of localized oxygen limitation in zones of high glucose concentrations. The reduced biomass yield compared to small scale cultivations (Bylund et al., 1998) was attributed to the repeated production/assimilation of acetate from overflow metabolism of glucose.

A two-compartment scale-down model, stirred tank reactor (STR) in combination with a plug flow reactor (PFR), was also used to model the presence of glucose gradients (Figure 18-5B). The PFR was fitted with static mixers to provide high oxygen transfer rates ($k_L a = 600$ to $1000$ h$^{-1}$) as described by George et al. (1993). In this manner the cells were repeatedly exposed to high glucose levels with decreasing oxygen availability with increasing cell density. The mean residence times in the PFR and STR were 56 s and 9 min, respectively. Glucose was fed at the entrance of the PFR and samples were withdrawn at different locations in the PFR after 14, 28, 32, and 56 s. Acetate, lactate, and formate appeared in the oxygen-insufficient PFR whereas only formate accumulated in the oxygen-sufficient STR, indicating that acetate and lactate were readily

assimilated there. Measurement of the mRNA levels of stress-induced genes showed increased levels with increasing residence time in the PFR, whereas very low levels were measured in the STR. Flow cytometric analyses of cells for viability and membrane potential from the scale-down model and the large scale bioreactor were in good agreement and significantly higher than when conducted in a STR without gradients in glucose levels. These results suggest that glucose heterogeneity in the large scale bioreactor was actually beneficial to the cells with respect to viability, although the biomass yield was lower.

Several other publications have described the use of two-compartment systems to investigate the influence of fluctuations in glucose concentration on a fed-batch baker's yeast production (Sweere et al., 1986, 1988c; Namdev et al., 1991; George et al., 1998) and *E. coli* fermentations (Hewitt et al., 1999; Bylund et al., 2000). The reader is referred to these studies for further details. In general, using baker's yeast, the studies showed that increasing circulation times caused a reduction in the biomass production and an increase in the product formation, especially ethanol. They concluded that the fluctuations in glucose concentrations at relatively rapid circulations was likely to have a distinct influence on the fed-batch production of baker's yeast.

### 18-2.7.2   Scale-down Simulations of Dissolved Oxygen Inhomogeneities at the Large Scale.
One of the most important aspects in the scale-up of any aerobic biochemical process is to maintain an adequate supply of oxygen to the microorganisms. As a result, many investigations have been devoted to the optimization of microbial growth and product formation with respect to dissolved oxygen tension concentrations. Several scale-down configurations (Figure 18-6) have been used, including well-mixed single-compartment (STR) and two-compartment systems (STR + STR and STR + PFR). In this section we review the studies conducted in scale-down models to simulate DOT gradients at large scales of operation.

*Well-Mixed Single-Compartment Model (STR).* Using such models, the dissolved oxygen can be fluctuated with a fixed frequency in a square- or sine-wave fashion by either varying the inlet gas composition or the fermenter head pressure to alter the liquid-phase dissolved oxygen concentration. A number of studies have implemented such strategies (Vardar and Lilly, 1982; Sokolov et al., 1983), and the reader is referred to these papers for further details. An easier setup to simulate dissolved oxygen gradients using a single well-mixed compartment would be to use timed pulsing of mixtures of nitrogen and oxygen (Oosterhuis, 1984; Sweere et al., 1988a,b; Namdev et al., 1991).

Namdev et al. (1991) simulated the fluctuating dissolved oxygen concentrations in large bioreactors in a 2 L vessel using a Monte Carlo approach. A lognormal distribution, described by a mean circulation of 20 s and a standard deviation of 8.9 s, was discretized into $n$ elements of equal probability, each with a corresponding circulation time. A uniform random number was then used to select a circulation time. Therefore, a random circulation time was selected
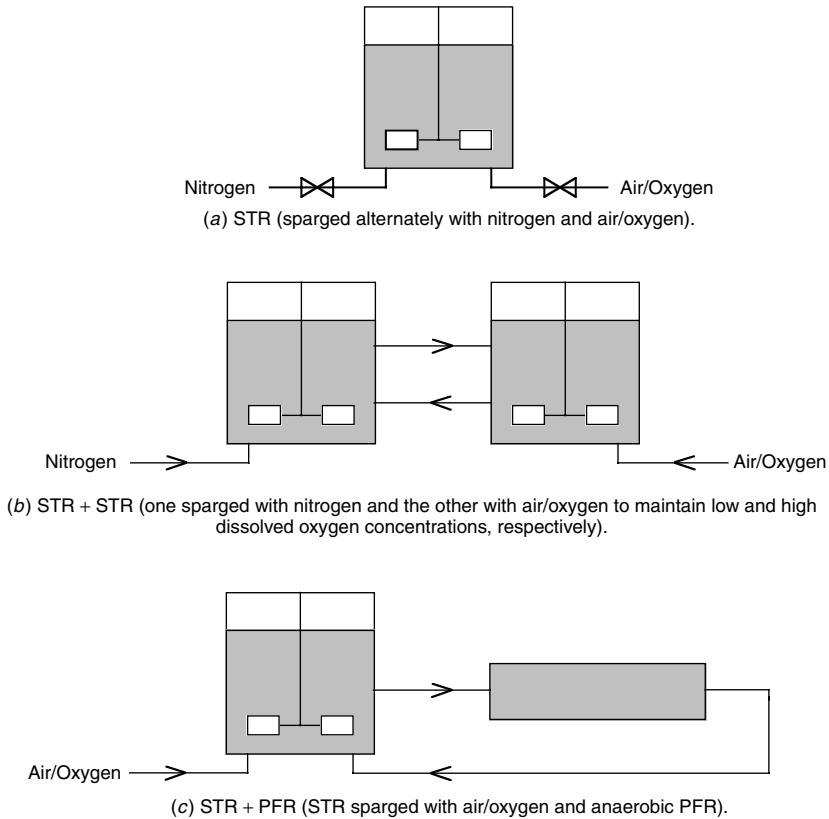
(*a*) STR (sparged alternately with nitrogen and air/oxygen).



(*b*) STR + STR (one sparged with nitrogen and the other with air/oxygen to maintain low and high dissolved oxygen concentrations, respectively).



(*c*) STR + PFR (STR sparged with air/oxygen and anaerobic PFR).

**Figure 18-6**    Different scale-down configurations to simulate dissolved oxygen gradients in large scale bioreactors.

within the bounds of the CTD. This method was used to control the aerated and nonaerated cycles to mimic the circulation time distribution of a production scale bioreactor. The results of the simulation were not sensitive to the order of the cycles since the circulation times used were much shorter than the growth rate of the cells. Due to the randomness of the circulation time selected, no single circulation time would be dominant, unlike the case for periodic oscillations. Using a culture of *S. cerevisiae* in a complex medium, they found that the biomass production decreased by 20% compared to experiments with continuous aeration. A 30% reduction in biomass level was found when the culture was subjected to periodic fluctuations, with 5 s of aeration and 15 s without aeration.

Yegneswaran et al. (1991) used a Monte Carlo method and CTD similar to those of Namdev et al. (1991) to investigate the effects of dissolved oxygen on a culture of antibiotic producing *Streptomyces clavuligerus*. They found that the yield of cephamycin C was suppressed by almost 44% due to the Monte Carlo simulation as compared to constant period cycling. One limitation in the

studies of Namdev et al. (1991) and Yegneswaran et al. (1991) arises from the use of conditions producing relatively small $k_L a$ values to alter the liquid-phase dissolved oxygen level by varying the composition of oxygen in the gas phase. Therefore, only the effects of relatively slow fluctuations can be studied, since the lowest value of the fluctuating cycle time cannot be less than the time constant for oxygen transfer $(1/k_L a)$ from the gas to the liquid phase. Another limitation of the methods of fluctuating head pressure or gas composition as a means of varying the liquid-phase dissolved oxygen concentration can be identified; only a mean circulation time is simulated and no information regarding the combined effects of poor oxygen transfer and liquid phase mixing is obtained. In practice, the microorganisms in production scale vessels will be subjected to a mean circulation time as well as a circulation time distribution. For more accurate scale-down modeling, the following should also be considered: (1) realistic values of the mean circulation time (typically, <60 s and preferably, <30 s), (2) the circulation time distribution in the model system resembles that measured on the production scale, and (c) the relative compartment volumes in the model should be correlated to those measured or calculated at the large scale.

*Two-Compartment Systems: Two Well-Mixed Stirred Tanks Model (STR + STR).* A two-compartment model, consisting of two well-mixed tanks (maximum working volumes of 0.6 and 1.6 L) with an exchange flow was presented by Oosterhuis et al. (1983, 1985) to model the scaling down of a circulation time distribution. This was based on experimental determinations of the local dissolved oxygen concentration in a production scale fermenter (Figure 18-2). From those results it could be concluded that it was possible to consider the reactor to consist of two parts: (1) high dissolved oxygen levels in the vicinity of the impeller, where maximum product formation can occur, and (2) dissolved oxygen concentrations close to the saturation constant of the microbial kinetics for oxygen in the other parts of the vessel. The exchange flow between the compartments was determined from radio pill flow follower experiments, which were also used to measure the CTD at the large scale. Close agreement was found between the experimental CTD measured in the production scale reactor and the CTD in the two-stirred-tanks system, as suggested by Levenspiel (1972). The mean circulation time and therefore the circulation time distribution could be varied by changing the liquid volumes in each vessel and/or by changing the circulation rate between the compartments. Air was sparged in to the smaller vessel, with agitator speed-controlled dissolved oxygen level, to simulate the small well-mixed highly oxygenated zone around the impeller. Nitrogen was sparged into the larger vessel to mimic the relatively poorly aerated areas away from the impeller. Such a model could therefore be used to model both the effects of gradients in dissolved oxygen and the bulk flow on microorganisms.

*Two-Compartment Model: Well-Mixed and Plug Flow Reactors Combination (STR + PFR).* Studies using a two-compartment model, consisting of a well-mixed stirred tank and a plug flow reactor to investigate the effects of glucose and dissolved oxygen gradients on cellular metabolism have been described

(Purgstaller and Moser, 1987; Larsson and Enfors, 1985, 1988; Amanullah et al., 1993a, 1993b, 2001).

It has been shown that various small scale models consisting of idealized reactor types can be used to simulate large scale fermentation processes, with respect to dissolved oxygen inhomogeneities. The reaction kinetic expressions, material balances on substrates, and products have to be formulated and solved in the context of the combined model network. The choice of the model configuration depends on (1) the system that has to be simulated, (2) knowledge of the hydrodynamics of the system, and (3) the equipment available and financial resources.

## 18-2.8   Required Characteristics of a Model Culture for Scale-down Studies

Two requirements can be stated for a reacting system to exhibit mixing sensitivity. First, there must be an inhomogeneous reactant distribution, such that the distribution is affected by the mixing intensity. Second, for the response to different mixing intensities to be appreciable, it is necessary for the characteristic reaction time to be less than the total time spent in regions where inhomogeneities exist. In other words, the Damkohler number, defined as the ratio of the system residence time to the characteristic reaction time, must be greater than unity (Fowler and Dunlop, 1989) (see also Chapter 13). The sensitivity of microorganisms to substrate concentrations can be used as a tool for studying mixing and transport effects in fermenters. However, sensitive instrumentation is required to detect instantaneous variations such as a membrane probe coupled to an online mass spectrometer to measure low boiling point volatiles in the liquid phase (Griot et al., 1987). The rapid secretion of low-molecular-weight products in response to substrate variations would be a desirable characteristic. Rapid growth and response would also be desirable.

*S. cerevisiae* possesses some of the desirable characteristics. It grows rapidly under aerobic conditions and responds rapidly to variations in glucose and oxygen (Furukawa et al., 1983). Einsele (1978) has shown that the response time of this organism to glucose pulses is approximately 4 s. Ethanol is produced under conditions of high glucose concentration and is independent of the oxygen concentration. However, it is also produced under low concentrations of glucose and oxygen. The interactive effect of glucose and oxygen make the interpretation quite difficult. The response is not reversible, and adaptation effects with respect to oxygen have been observed (Furukawa et al., 1983). Moes et al. (1985) reported the use of a *B. subtilis* culture with an oxygen-sensitive product distribution to characterize mixing and mass transfer in bioreactors. The claimed desirable characteristics of this culture included (1) extreme sensitivity with respect to oxygen supply and changes in reactor operating variables such as impeller speed and aeration rate, and (2) rapid and reversible response, allowing a number of investigations to be carried out within a single batch fermentation. However, in practice, the choice of the microorganism is dictated by the scale-up process of interest.

## 18-2.9  Use of *Bacillus subtilis* as an Oxygen- and pH-Sensitive Model Culture

In this *B. subtilis* strain (AJ 1992 from Ajinomoto, Japan) glucose is utilized to form pyruvate, which in the presence of excess oxygen is completely oxidized to carbon dioxide and water via the trichloroacetic and (TCA) and respiratory cycles. At low oxygen levels, pyruvate is used to produce acetoin, which in turn can be reduced by nicotinamide adenine dinucleotide (NADH) to form butanediol. Lactate is also formed from pyruvate at low levels of oxygen. Acetoin is produced primarily at oxygen levels above 150 parts per billion (ppb) and butanediol below 80 ppb. Moes et al. (1985) demonstrated the extreme sensitivity of the culture in the range 80 to 90 ppb. Using a complex medium, batch fermentations could be completed within 8 h with a biomass concentration between 2 to 3 g/L, using approximately 11 g/L of glucose. For oxygen concentrations above 100 ppb, typical values of acetoin and butanediol concentrations were in the range 0 to 3 and 0 to 0.5 g/L, respectively. At low oxygen concentrations (50 ppb), values of acetoin and butanediol were in the range 0 to 5 and 0 to 3 g/L, respectively. In batch fermentations, switching from one oxygen level to another caused one already accumulated product to be converted to the other in a reversible manner. The high rates of change of 0.5 to 1.0 g/L per hour enabled detection within 10 min.

Griot et al. (1986, 1987) showed that this strain changed the selectivity of excretion of metabolites in response to variations in dissolved oxygen levels in less than 1 s. The response time of the culture to a change in gas phase oxygen concentration was shown using mass spectrometry to be a total of 7.7 s. After subtracting the response of the gas–liquid transfer (3.2 s) and the acetoin detection (4 s), the response time of the culture was estimated to be of the order of 0.5 s. In addition to its sensitivity to dissolved oxygen levels, the production of the metabolites acetoin (Ac) and 2,3-butanediol (Bu) is sensitive to pH values between 6.5 and 7.2, with the total metabolite (Ac + Bu) concentration 3.5 times greater at pH 6.5 than at 7.2. Also, the acetic acid concentration was 0.56 g/L at pH 6.5, whereas its value diminished to zero at pH 7.2 (Amanullah et al., 2001b). In conclusion, the *B. subtilis* culture is a very useful tool to study the effects of mixing due to its unusual sensitivity to oxygen supply and pH. However, use of a well-defined medium is essential.

In the next two sections of this chapter we describe by way of examples, detailed practical designs of scale-down bioreactors for investigating the effects of dissolved oxygen and pH gradients and the results obtained. *B. subtilis* is employed as the model culture given its sensitivity to dissolved oxygen and pH.

## 18-2.10  Experimental Simulations of Dissolved Oxygen Gradients Using *Bacillus subtilis*

Given that significant oxygen gradients have been identified even at a 25 m$^3$ (19 m$^3$ working volume) scale (Oosterhuis et al., 1985), one approach has been to use two interconnected stirred tanks (STR + STR), one (well oxygenated)

to represent the active (well mixed, oxygenated) zone and the other (with low oxygen levels), the quiescent zone. Both STR + STR and STR + PFR scale-down models are described here using an oxygen-sensitive culture of *B. subtilis* (see Section 18-2.9) to identify relationships between mixing and biological performance parameters and to compare the performance of each scale-down configuration. For successful scale-down, both mean and distribution of circulation times (CTDs) at the large scale have to be replicated within the scale-down configuration (Amanullah et al., 1993a; Amanullah, 1994). The CTD in the two stirred tanks scale-down configuration can be described by the following equation given by Levenspiel (1972) for a tanks-in-series model:

$$t_c C = e^{-t/t_c} \sum_{m=1}^{\infty} \frac{(t/t_c)^{mN-1}}{(mN-1)!} \tag{18-54}$$

where C is the tracer concentration at time t, $t_c$ the mean circulation time, m the number of circulations, and N the number of tanks. For a single circulation or one complete recirculation (m = 1) in the STR + STR model, eq. (18-54) reduces to

$$C = \frac{e^{-t/t_c}}{t_c^2} t \tag{18-55}$$

Oosterhuis et al. (1985) reported a mean circulation time of approximately 12 s in an unaerated 19 m³ fermenter using a radio pill flow follower. The experimental cumulative CTD associated with this mean is shown in Figure 18-7. This is the distribution of the residence time of the liquid outside the impeller region. If it is
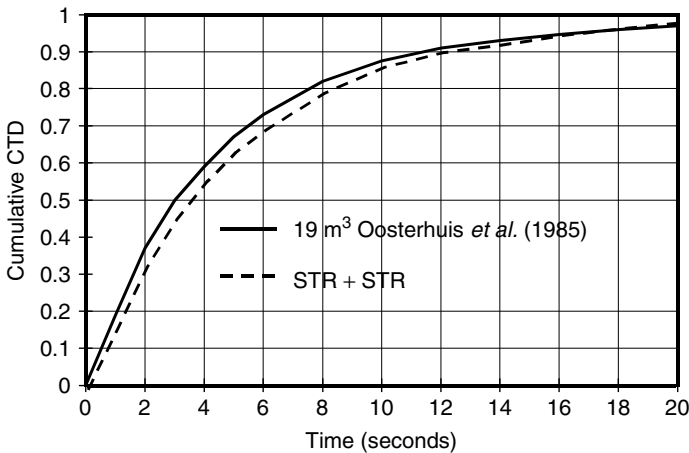


**Figure 18-7** Comparison of the experimental (Oosterhuis et al., 1985) and calculated cumulative CTDs for a single circulation in the STR + STR scale-down model (Amanullah et al., 1993a; Amanullah, 1994) and that at a scale of 19 m³. The mean circulation time in both cases is 12 s.

assumed that the residence time in the impeller region is relatively small and that the remainder of the vessel behaves like a well-mixed tank with a much longer residence time, eq. (18-55) can be used to describe the CTD. Figure 18-7 also shows the cumulative CTD calculated using eq. (18-55), with a mean circulation time of 12 s, for a single circulation in the STR + STR model. Comparison of the experimental and calculated cumulative CTDs shows that eq. (18-55) is fairly accurate in predicting the experimental CTD, and this is especially the case for the tail of the distributions. Therefore, the STR + STR model is well suited to study the effects of cell residence in the poorly oxygenated bulk regions, alternated by residence in the well-aerated impeller region.

Detailed descriptions of the scale-down models and their operation are provided in Amanullah et al. (1993a) and Amanullah (1994). Figure 18-8$a$ depicts the scale-down STR + STR configuration in the laboratory. Two interconnected stirred vessels 6 L (2.8 or 4.8 L working volumes) and 2 L (1.2 L working volume) in capacity were used. Two variable speed pumps with a maximum estimated pumping capacity of 16 L/min, enabling a minimum mean circulation time of 15 s, were employed to provide the flow between the vessels. Dissolved oxygen tension (DOT) was measured and controlled at 5% ± 0.5% of air saturation in the smaller vessel by means of gas blending, keeping the total flow of gas constant at 1 vvm. Nitrogen was sparged at a rate of 0.5 vvm into the larger vessel to maintain a DOT level close to zero.

The mean circulation time ($t_c$) was varied in the range 15 to 300 s at $V_a/V_q$ of 0.25 and 0.43, where $V_a$ and $V_q$, are volumes of the active (small bioreactor with DOT at 5%) and quiescent (large bioreactor with DOT close to zero) zones, respectively. In the STR + PFR model (Figure 18-8$b$), the dissolved oxygen was maintained at 10% by gas blending in the STR. The plug flow volume was either 2 or 4 L, resulting in $V_a/V_q = 0.5$ and 0.25, respectively. The results from both the STR + STR and STR + PFR models were compared against a control batch fermentation with DOT = 10%. This control represented the ideal mixing situation in terms of oxygen supply and corresponded in effect to a zero-mean circulation time. The control experiment yielded maximum values of both final biomass concentration (6.44 g/L) and specific growth, rate ($\mu$) at 0.31 h$^{-1}$. Acetoin (Ac) production rate was also a maximum at 0.36 g/L per hour, while the 2,3-butanediol (Bu) production rate, as expected, was zero. The biological performance of the culture in the experiments conducted for $0 < t_c < 300$ s at $V_a/V_q = 0.25$ and 0.43 have been expressed in Figure 18-9$a-c$ in terms of both maximum biomass ($x_{max}$) and metabolite concentrations, specific growth, and the Ac/Bu concentration ratio, which is dependent on the supply of dissolved oxygen. The values of $x_{max}$ and $\mu$ decreased with increasing mean circulation times, while the total metabolite concentration increased (Figure 18-9$a$ and 18-9$b$). Although the percentage reduction in $x_{max}$ relative to the control was similar (10 to 15% for $t_c = 30$ s) for both ratios, the percentage reduction in $\mu$ for the 0.25 ratio was significantly higher than for the 0.43 ratio. This implies that although the potential for biomass formation remained unaffected at the different $V_a/V_q$ ratios, the fermentation time required to attain similar biomass concentrations was longer
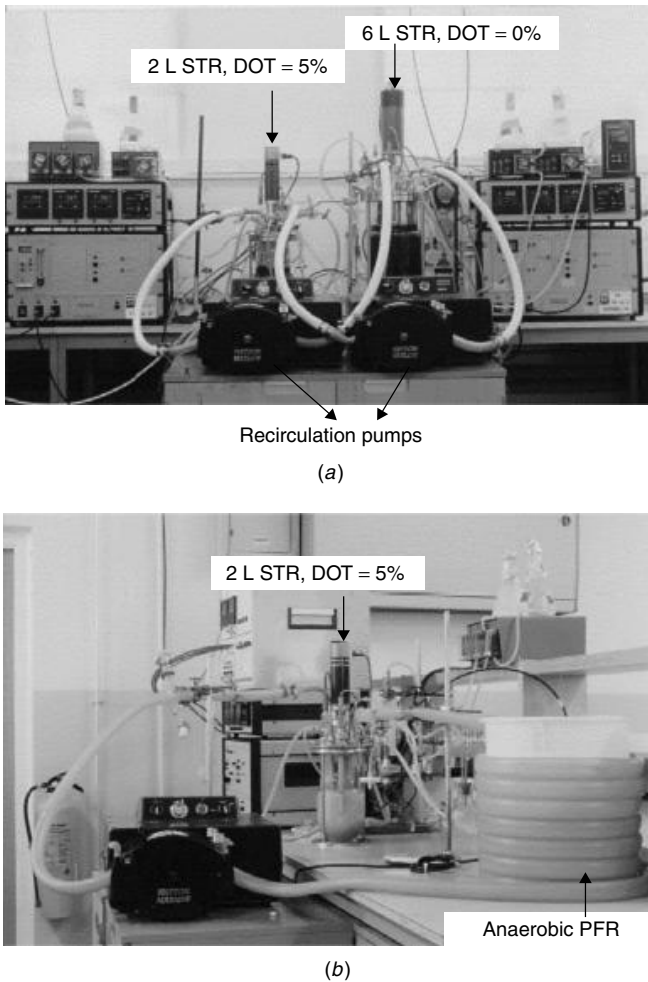
(a)



(b)

**Figure 18-8** (a) Laboratory scale-down model consisting of two interconnected stirred tanks (STR + STR) at different DOT levels to simulate dissolved oxygen levels at large scales of operation. The mean circulation time can be altered by manipulating the exchange flow rate via the recirculation pumps. (From Amanullah, 1994.) (b) Laboratory scale-down model consisting of an interconnected stirred tank and unaerated plug flow reactor (STR + PFR) to simulate dissolved oxygen levels at large scales of operation. The DOT level in the STR was controlled at 5% of air saturation. Different residence times in PFR could be imposed by altering the speed of the recirculation pump. (From Amanullah, 1994.)

at the 0.25 ratio. Figure 18-9c shows the Ac/Bu ratio as a function of the mean circulation time at $V_a/V_q = 0.25$ and 0.43 at a biomass concentration of 4 g/L. In both cases, the Ac/Bu ratio decreased sharply in the range $0 < t_c < 120$ s. In each case (increasing $t_c$ and lower $V_a/V_q$), the biological response of the culture
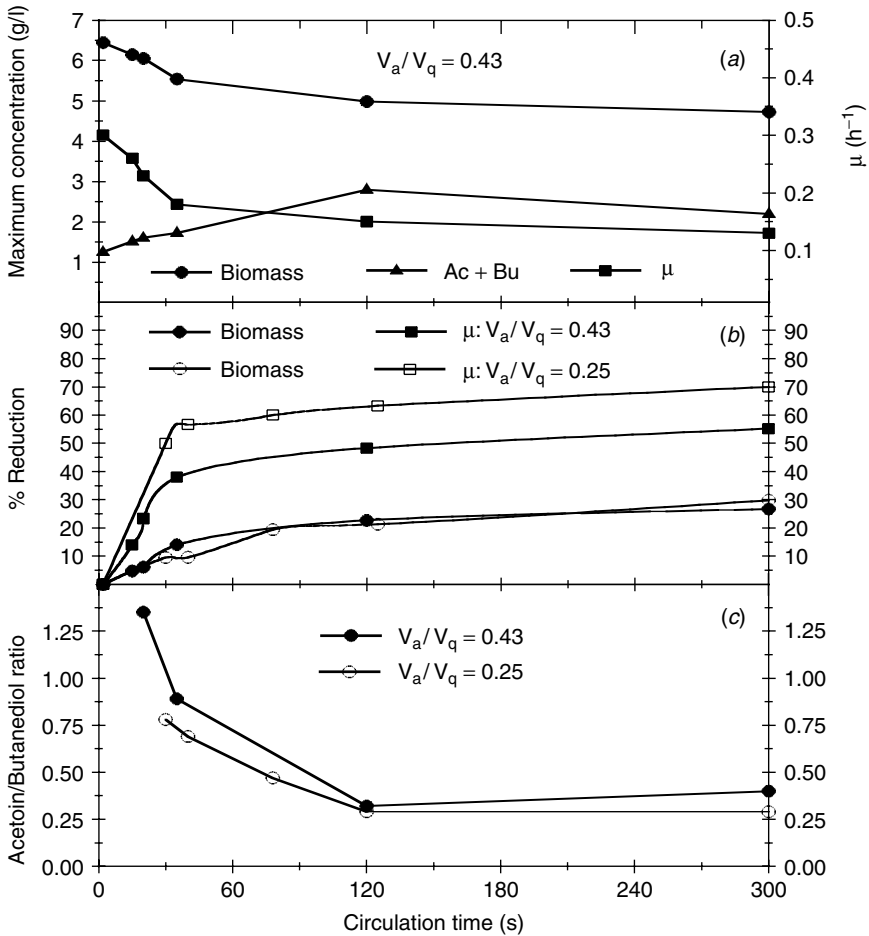
**Figure 18-9** (*a*) Maximum biomass, metabolites concentration, and specific growth rates as a function of mean circulation time. (*b*) Maximum biomass and specific growth rates expressed as percentage changes relative to performance under ideal conditions of oxygen supply for $V_a/V_q = 0.43$ and 0.25. (*c*) Metabolite concentration ratios at a biomass concentration of 4 g/L at $V_a/V_q = 0.43$ and 0.25 as a function of mean time circulation time. (From Amanullah, 1994.)

can be explained by an increase in the percentage of cells subjected to oxygen depletion with increasing mean circulation times (see Figure 18-3*b*).

The percentage reduction in $x_{max}$ for $V_a/V_p = 0.25$ for the different scale-down models is shown in Figure 18-10. For similar mean circulation times the percent reduction in maximum biomass concentration for the STR + STR model was significantly lower than for the STR + PFR model. One reason for this may due to the fact that in the STR + STR model there was always some oxygen available to the microorganisms in the quiescent zone due to the entrainment of
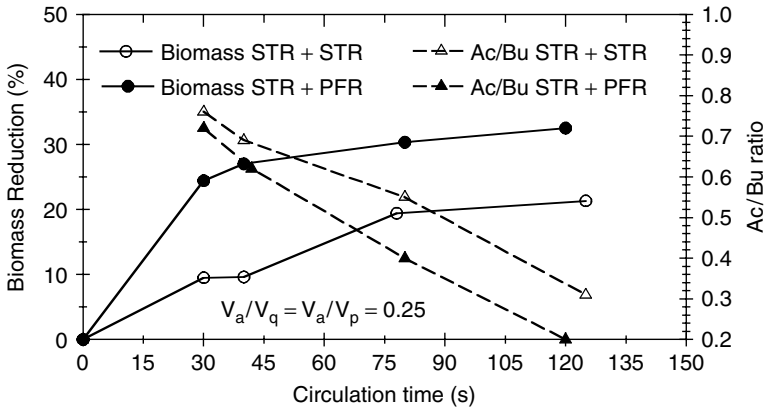
**Figure 18-10**   Effects of mean circulation time on the percent reduction in maximum biomass concentration and product ratio, relative to ideal conditions of oxygen supply, for different scale-down models. (From Amanullah, 1994.)

air in the exchange flow. In contrast, the cells in the STR + PFR system were truly subjected to anaerobic conditions once the oxygen was consumed in the PFR. The Ac/Bu ratio at a specific biomass concentration of 4 g/L is shown in Figure 18-10 as a function of mean circulation time for the two-model configurations for $V_a/V_p = 0.25$. The Ac/Bu ratio for the STR + PFR model was $\approx 27\%$ lower than for the STR + STR model for $t_c \geq 80$ s.

The results presented also highlight the importance of the choice of the scale-down configuration when studying the impact of large scale dissolved oxygen inhomogeneities on microorganisms. The difference in biological performance between the two configurations can be explained in terms of the flow characteristics and oxygen availability in each system. The STR + STR model is more appropriate for use when the region outside the impeller zone, with a low dissolved oxygen concentration, behaves like a well-mixed tank characterized by mean circulation times with relatively large standard deviations. The STR + PFR model may be more suitable for situations where the motion of the fluid outside the impeller zone nearly resembles plug flow and may be characterized by relatively smaller standard deviations for a given mean circulation time. The results also suggest the fact that for successful scale-up or scale-down, apart from the CTD, both mean circulation times and relative compartment volumes have to be replicated at the different scales. In addition, use of the relative volume of the compartments or ratio of the residence times in each compartment is not suitable as a scale-up or scale-down criterion.

Significant changes in biological performance are likely to occur upon scale-up of this fermentation, due to the circulation of cells through oxygen-deprived regions. The performance can be enhanced if the microorganisms are circulated through the impeller region at a high enough frequency (small mean circulation times) such that the concentration of oxygen is kept above the critical value along

all circulation paths or if the relative size of the well-mixed region is increased. However, increases in the flow capacity have to be balanced against cost of the higher power input. Although unicellular bacteria are generally thought to be insensitive to hydrodynamic stress in the range employed in bioreactors (Hewitt et al., 1998), the influence of increased agitation intensities may be important in other biological systems, especially mycelial fermentations (Jüsten et al., 1996; Amanullah et al., 2000), where increased hyphal fragmentation can occur.

## 18-2.11    Experimental Simulations of pH Gradients Using *Bacillus subtilis*

Studies simulating the effects of pH gradients on microbial growth and product formation are scarce, yet it is a fundamental parameter in the regulation of cellular metabolism, particularly in processes characterized by multiple end products. The first laboratory scale two-compartment system used to investigate the effects of pH fluctuations consequent of large scales of operation on microorganisms was reported by Amanullah et al. (2001b). *B. subtilis* was used as a model culture since in addition to its sensitivity to dissolved oxygen levels, production of the metabolites acetoin and 2,3-butanediol is sensitive to pH values between 6.5 and 7.2 (see Section 18-2.9).

The basis of industrial pH control (Figure 18-11*a*) is the point measurement by a pH probe (typically, near an impeller) and the subsequent on–off pulse injection of acid or base typically near the top surface in response to a deviation from the set point. Thus, the local pH values near the addition point may deviate from the bulk pH. In the study reported by Amanullah et al. (2001b), it was assumed that acid or base in production scale vessels was added at the broth surface, in response to a point measurement of a pH probe in the vicinity of the impeller region. This large scale situation can then be simulated experimentally by a stirred tank reactor + plug flow reactor (STR + PFR) configuration shown in Figure 18-11*b*. The STR represents the well-mixed impeller region, while the residence time in the PFR mimics the time spent by cells outside this region in the higher-pH zone. Figure 18-12 shows by way of example the transient pH probe response to a pulse injection of base to a 0.01 $M$ $KH_2PO_4$ buffer solution in a 4.4 $m^3$ bioreactor under unaerated conditions (Singh et al., 1986). Two pH probes were used, one near each of the two impellers used. The response is typical of that of a tracer injection at the liquid surface. Although mixing times give information about the rate of mixing of acid and/or base, it is not sufficient to characterize the mixing process because it does not provide any information on fluid segregation in the vessel for which the CTD is necessary to describe the microenvironment experienced by cells (Oosterhuis and Kossen, 1984; Amanullah et al., 1993a; Amanullah, 1994).

The experimental design of the scale-down experiments reported by Amanullah et al. (2001b) was based on the concepts proposed by Namdev et al. (1992) to evaluate the effects of glucose feed zone in fed-batch fermentations of *S. cerevisiae*. They represented the mixing process in a large scale fed-batch fermentation by a three-zone mixing model consisting of feed, bulk, and impeller
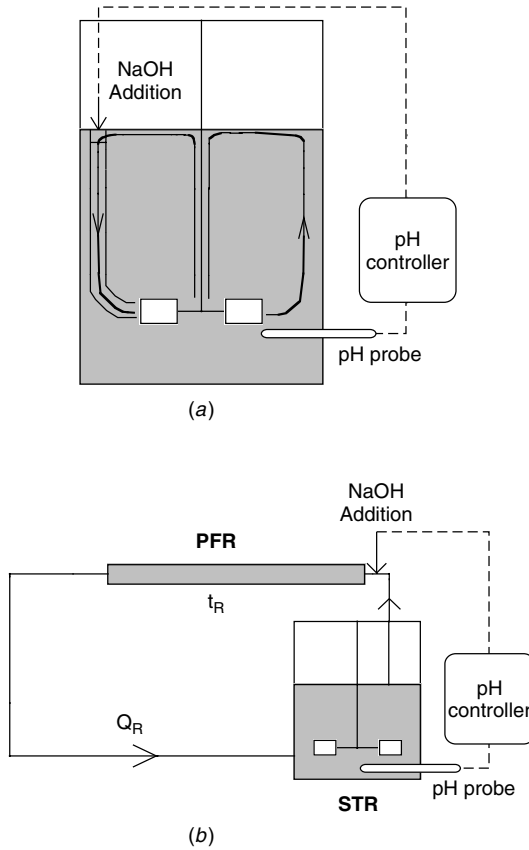
Figure 18-11   (*a*) Typical pH control in a production scale bioreactor and (*b*) scaled-down model to simulate pH spatial fluctuations found in production scale bioreactors.
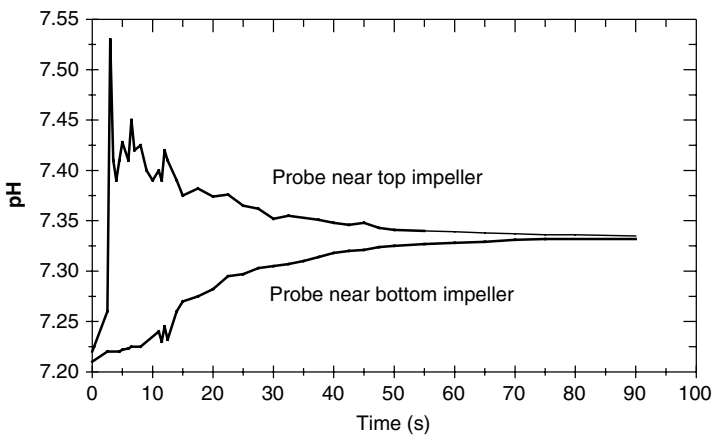


**Figure 18-12**   Unaerated pH probe response in a 4.5 m$^3$ fermenter using a buffer solution. (From Singh et al., 1986.)

zones. Following the lognormal CTD suggested by Bajpai and Reuss (1982) for a 100 m$^3$ fermenter, Namdev et al. (1992) used a lognormal CTD based on the "network of zones" model of Mann et al. (1981) with a mean of 20 s and a standard deviation of 8.9 s to simulate glucose feeding in bioreactors of such scales. A recycle flow model was used which consisted of a stirred tank and a plug flow loop with a recirculation rate. The CTD of the recycle flow model is given by (Levenspiel, 1972)

$$F(t) = F \exp[-F(t - t_R)] \tag{18-56}$$

where

$$F = \frac{Q_R}{V_{STR}} \tag{18-57}$$

$$t_R = \frac{V_{PFR}}{Q_R} \tag{18-58}$$

The recirculation rate, $Q_R$, determines the frequency of cells entering the PFR, F, from a given scale-down STR, $V_{STR}$ and $V_{PFR}$ are volumes of the STR and PFR, respectively, and $t_R$ is the residence time in the PFR. The residence time of a fluid element in the PFR is considered to be analogous to the time that it would spent in the acid or alkali addition zone in a production scale fermenter. The STR represents the well-mixed impeller region.

Since an estimate of the volume of the addition zone was not available, the volume of the loop was estimated as 5% of the total fermenter volume [similar to the volume fraction used by Namdev et al. (1992) and George et al. (1993)] at 50 mL. Using this PFR volume, the recirculation rate was varied to obtain different residence times in the PFR. For simulating pH fluctuations, the pH in the STR was controlled by the addition of 5 $M$ NaOH into the PFR via a mixing bulb which incorporated the incoming broth from the STR with the NaOH at the entrance of the PFR. The mixing bulb was essential to segregate the addition zone in compliance with the three-zone mixing model (zone 1: base addition (or feed) point; zone 2: circulation volume affected by the high pH; and zone 3: well-mixed impeller region). Since the culture was sensitive to dissolved oxygen, for each experiment with pH control by adding base into the PFR, equivalent experiments were conducted with pH control by addition of base into the STR, thus ensuring that any dissolved oxygen effects were common to both types of experiments. Residence times in the PFR was varied from 30 to 240 s. The results showed that without pH fluctuations in the PFR, there were no differences in performance between the batch STR and STR + PFR due to variations in dissolved oxygen or indeed any other parameters.

Since identical conditions (e.g., dissolved oxygen) were used for the STR + PFR controls with constant pH and STR + PFR scale-down model apart from the imposition of pH fluctuations in the latter case, the increase in acetic acid concentration, with a corresponding decrease of up to 27% in Ac + Bu concentration at a residence time of 240 s, must have been due to the increased exposure

of cells to alkaline conditions at higher residence times in the PFR. Exposure of cells to the higher-pH environment did not affect the growth of the culture. The results from the scale-down studies clearly showed that cellular metabolism of this culture was affected by pH fluctuations at PFR residence times of 60 s or higher. It was proposed that these changes in metabolism may be linked to both the sensitivity of the acetoin and 2,3-butanediol forming enzymes to pH and to the inducing effects of dissociated acetate on the acetolactate synthase enzyme (Amanullah et al., 2001b).

It is well recognized that the optimum location for the addition and subsequent dispersion of any inlet feed, such as acid or base for pH control or glucose in fed-batch fermentations, is in the impeller region due to the prevailing high turbulence. (See Chapter 13 for further discussion of local mixing effects.) This would also reduce any overshoot from the set point, since the pH probe is generally in the close vicinity of this region. It is recommended to locate any pH feed near an impeller, perhaps employing several feeding points in order to eliminate or reduce pH fluctuations and their effect on microbial metabolism. A recent study of large scale free-suspension animal cell culture has shown such a change to be necessary and effective (Langheinrich and Nienow, 1999). Also, a comparison of the performance of large scale and scale-down experiments with respect to glucose feeding in *E. coli* fermentations for recombinant protein production also concluded that a two-feed-point glucose addition was superior to a single feed addition in preventing unwanted acetate formation at the large scale (Bylund et al., 1999).

## 18-3   POLYSACCHARIDE FERMENTATIONS

The large scale production of microbial polysaccharides exemplifies a fermentation industry with global markets representing hundreds of millions of dollars. One of the most challenging tasks in the fermentation industry today is the design of bioreactors for the production of rheologically complex polysaccharides at high concentrations of consistent high quality. Quality in this context refers to the molecular weight of the biopolymer, which in turn determines its viscosifying properties. These include commercially important polysaccharides such as xanthan, gellan gum, pullulan, alginate, curdlan, and glucan.

Traditionally, strain selection and more recently, genetic engineering have been used to potentially dramatically increase the maximum productivity and product concentration achievable in such processes. However, whether this potential is fully realized also depends on bulk mixing and oxygen mass transfer, which in turn are governed primarily by vessel design, impeller type, and fluid properties (rheological and chemical composition). These generic problems inherent in viscous fermentations, including those used to manufacture gellan gum (Dreveton et al., 1996), pullulan (Wecker and Onken, 1991), curdlan (Lee et al., 1999), and alginate (Peña et al., 2000) have been investigated and reported here using xanthan gum as a model polysaccharide fermentation system. For details of

the other polysaccharide fermentations, the reader is referred to the aforementioned publications. Xanthan gum is an extracellular polysaccharide produced by *Xanthomonas campestris* and is commercially the most important bacterial polysaccharide. It has widespread applications as a viscosity-enhancing agent and stabilizer in the food, pharmaceutical, and petrochemical industries (Jeanes et al., 1976; Norton et al., 1981). Since the cost of downstream processing determines whether or not the manufacture of the gum is commercially feasible, a high product concentration (>25 g/L) is essential (Pace and Righelato, 1980; Galindo, 1994).

Ever since xanthan gum was reported by Rogovin et al. (1961), considerable research has been devoted to addressing the problems of poor bulk mixing and low oxygen transfer rates in xanthan gum fermentations (Moraine and Rogovin, 1973; Nienow, 1984; Funahashi et al., 1987a,b,c, 1988a,b; Nienow and Elson, 1988; Peters et al., 1989a,b, 1992; Galindo and Nienow, 1992, 1993; Herbst et al., 1992; Flores et al., 1994; Zhao et al., 1991, 1994). It is generally agreed in the literature that the process bottleneck in highly productive xanthan fermentations is related to these two parameters. However, the interpretation of experimental results in relation to these problems is difficult, due to the inability to separate the variable of oxygen transfer from that of vessel inhomogeneity. Accumulation of the extracellular gum also induces rheological complexities such that zones of significant motion (called a *cavern*) around impellers are formed (Figure 18-13), with essentially stagnant regions elsewhere (Nienow and Elson, 1988; Amanullah et al., 1998a,b). Cavern size is governed by the properties of the fluid, power input, and agitator design and is regarded as one of the limiting factors in the fermentation process. Thus, homogeneity of the broth is important to maintain optimal levels of dissolved oxygen, temperature, and pH and to prevent gradients in these parameters. In addition, oxygen transfer becomes increasingly difficult in these highly viscous broths.

## 18-3.1    Rheological Characterization of Xanthan Gum

During the course of the fermentation, the excretion of the polysaccharide increases the apparent viscosity of the broth by over three orders of magnitude. Initially, the broth is Newtonian and in turbulent flow. However, with increasing gum accumulation, it becomes increasingly viscous and non-Newtonian with Reynolds numbers in the transitional regime. The highly viscous and extremely shear thinning behavior of the gums, which also typify good-quality gums, can be characterized using the power law model with values of fluid consistency (K) and flow behavior (n) indices in the range 0 to 70 $N/m^2 \cdot s^n$ and 1 to 0.1, respectively. Typically, the flow behavior index remains constant (<0.2) at concentrations above 20 g/L. In addition, concentrations of xanthan in excess of 10 g/L generally possess a yield stress that can be obtained by fitting the Casson model (refer to Section 18-3.3) to data over the shear rate range 0.1 to 0.2 $s^{-1}$ (Amanullah et al., 1998b).
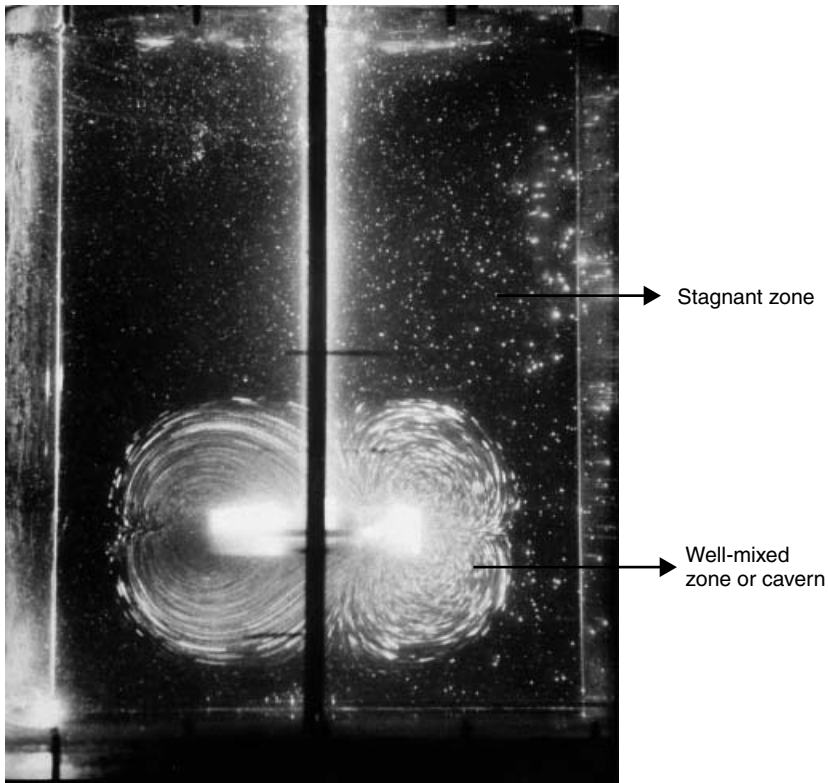
**Figure 18-13**  Cavern formation in shear thinning fluids. A well-mixed region exists in regions of high shear rate, while stagnant regions form in regions of low shear rate.

## 18-3.2   Effects of Agitation Speed and Dissolved Oxygen in Xanthan Fermentations

***18-3.2.1   Agitation Speed***.  Agitation speed affects both the extent of motion in xanthan fermentation broths because of their rheological complexity and the rate of oxygen transfer. The combination of these two effects causes the dissolved oxygen concentration and its spatial uniformity to change with agitator speed. Separating these complex interactions was achieved in the following way (Amanullah et al., 1998c). First, the influence of agitation speeds of 500 and 1000 rpm using three Rushton turbines (D/T = 0.5) at a 6 L scale was investigated at a constant nonlimiting dissolved oxygen concentration of 20% of air saturation using gas blending. Under these controlled dissolved oxygen conditions, the results demonstrated that the biological performance of the culture was independent of agitation speed (or shear stress) as long as broth homogeneity could be ensured. No difference in biological performance could be measured at different agitator speeds up to a xanthan concentration of 20 g/L. At higher gum concentrations, it was shown that the superior bulk mixing led to higher

microbial oxygen uptake rates at 1000 rpm compared to 500 rpm, which in turn is responsible for enhanced performance at the higher speed. With the development of increasing rheological complexity lending to stagnant regions at xanthan concentrations greater than 20 g/L, it was shown that the superior bulk mixing achieved at 1000 rpm compared to 500 rpm, leading to an increased proportion of the cells in the fermenter to be metabolically active and hence higher microbial oxygen uptake rates, was responsible for the enhanced performance. Thus, for a given cavern size with equivalent dissolved oxygen levels, the specific xanthan production rate remained similar, independent of impeller speed.

The phenomenon of decreased specific xanthan production rate in the production phase is expected since it is partly growth associated. However, in many instances there is a continual decrease throughout the production phase, where the biomass concentration is approximately constant. Peters et al. (1989a) concluded that provided that oxygen limitation could be avoided (either by increased speed or by using oxygen enriched air), the specific xanthan production rate was not influenced by agitation speed or the shear stress related to it. It is important to point out that in that study, xanthan concentrations did not exceed 16 g/L, and as a result, stagnant zones did not develop in the moderately viscous broths. Their conclusions, however, were confirmed by Amanullah et al. (1998b) at much higher xanthan concentrations of 25 to 35 g/L, typical of those generally desired for commercial production of xanthan gum.

***18-3.2.2   Dissolved Oxygen***.  The effects of varying dissolved oxygen were compared to a control in each case with an agitator speed of 1000 rpm to ensure full motion, but with a fixed nonlimiting dissolved oxygen of 20% of air saturation (Amanullah et al., 1998c). The specific oxygen uptake rate of the culture in the exponential phase, determined using steady-state gas analysis data, was found to be independent of dissolved oxygen above 6% of air saturation, whereas the specific growth rate of the culture was not influenced by dissolved oxygen even at levels as low as 3%, although a decrease in xanthan production rate could be measured. In the production phase, the critical oxygen level was determined to be 6 to 10%, so that below this value, both specific xanthan production rate as well as specific oxygen uptake rate decreased significantly. In addition, it was shown that the dynamic method of oxygen uptake determination was unsuitable even for moderately viscous xanthan broths, due to the presence of very small bubbles that act as an oxygen sink.

### 18-3.3   Prediction of Cavern Sizes in Xanthan Fermentations Using Yield Stress and Fluid Velocity Models

As discussed earlier, agitation of fluids with $n \leq \sim 0.3$ results in the formation of a cavern, a region of relatively rapid motion around the impeller (Wichterle and Wein, 1975) where high shear rates prevail with essentially stagnant regions elsewhere in the vessel. It is essential for the correct design and operation of bioreactors for highly viscous fermentations to determine the size of the region

of motion as a function of the fluid rheology and agitation conditions. Two approaches have been employed for the estimation of cavern sizes. The first model [the Elson and Nienow (EN) model] is based on the concept of a yield stress that is defined as the minimum shear stress required to induce fluid motion and can be estimated using rheological models such as the Herschel–Bulkley or Casson equations applied at low shear rates.

The Herschel–Bulkley (HB) equation is given by

$$\tau_{HB} = (\tau_y)_{HB} + K_{HB}\dot{\gamma}^{n_{HB}} \tag{18-59}$$

the Casson equation is given by

$$\tau^{0.5} = (\tau_y)_C^{0.5} + K_C\dot{\gamma}^{0.5} \tag{18-60}$$

where $\tau$ is the fluid shear stress, $\tau_y$ the fluid yield stress, $\dot{\gamma}$ the fluid shear rate, and K and n are fluid consistency and flow behavior indices, respectively.

Solomon et al. (1981a) proposed a physical model to estimate cavern sizes based on a torque balance to predict its diameter, $D_c$. They assumed that the cavern was spherical, that the predominant motion at the cavern boundary was tangential in nature (applicable to radial flow impellers), and that the stress imparted by the impeller at the cavern boundary was equal to the fluid yield stress. This model was later modified by Elson et al. (1986) assuming the cavern to be a right circular cylinder with height, $H_c$, centered on the impeller to give

$$\left(\frac{D_c}{D}\right)^3 = \frac{1}{\pi^2[(H_c/D_c + \frac{1}{3}]}Po_t\left(\frac{\rho N^2 D^2}{\tau_y}\right) \tag{18-61}$$

where $Po_t$ is the power number in the turbulent regime and $H_c/D_c = 0.4$ for radial flow Rushton turbines. Equation (18-61) can be used to calculate the size of the cavern assuming that a yield stress can be determined for highly shear thinning fluids. However, Barnes and Walters (1985) point out that if sufficiently low shear stress and shear rates could be measured, these fluids would not exhibit a yield stress, but instead, a very high constant zero shear rate viscosity would be obtained. In addition, many highly shear thinning fluids for which $\sim\leq 0.3$ appear to indicate a yield stress when their flow curves are plotted on linear coordinates. Yet the rheological data could be modeled using a power law equation [eq. (18-62)] equally well:

$$\tau = K\dot{\gamma}^n \tag{18-62}$$

An alternative model was developed to address the problem of estimating fluid yield stress and is based on a fluid velocity approach (Amanullah et al., 1998a). This model considers the total momentum imparted by the impeller as the sum of both tangential and axial components and assumes a torus-shaped cavern. It combines torque and axial force measurements (for axial flow impellers) with the simple power law equation to predict the cavern diameter with the cavern

boundary defined by a limiting velocity. The proposed new model is capable of predicting the measured cavern diameters for Re > 20 using both radial and axial flow impellers and is valid for sizes greater than the impeller diameter but less than the vessel diameter. This approach is also shown to be superior to the traditional EN yield stress model in extremely shear thinning fluids whose flow curve can be well fitted by the power law equation. Thus, the radius of a torus-shaped cavern ($r_c$) for a power law fluid is given by

$$r_c^{\,1-2/n} = v_o \left[ \left( \frac{2}{n} - 1 \right) \left( \frac{4\pi^2 K}{F} \right)^{1/n} \right] + b^{1-2/n} \tag{18-63}$$

where $r_c = D_c/4$, $b = T/4$, $v_o$ is the fluid velocity at the cavern boundary (estimated at $1 \times 10^{-3}$ m/s; Amanullah et al., 1998a), and F is the total force imparted by the impeller (radial and axial) defined by

$$F = \rho N^2 D^4 \sqrt{N_f^{\,2} + \left( \frac{4Po}{3\pi} \right)^2} \tag{18-64}$$

Just as torque measurements can be made dimensionless through the power number, so the axial force measurements can be described in terms of a dimensionless axial force number, $N_f$, where

$$N_f = \frac{F_a}{\rho N^2 D^4} \tag{18-65}$$

The concept of an axial force number, $N_f$, is new. It has been shown that $N_f$ is a scale-independent parameter like Po for geometrically similar vessels (Amanullah et al., 1998a), although it would expected to depend on the Reynolds number and the impeller configuration. Axial force ($F_a$) measurements in a study by Underwood (1994) gave values too low to be detected for radial flow impellers ($N_f = 0$), while axial flow impellers gave significant and easily measured values. Therefore, for a given impeller $N_f$ can be determined as a function of Re and used in a scale-independent manner. Although eq. (18-63) is superior to (18-61) for estimating cavern diameters (Amanullah et al., 1998a) and can be used for both radial and axial flow impellers, it is more complex in its use. Consequently, eq. (18-61) has been used for the purposes of estimating cavern sizes in xanthan fermentations (Amanullah et al., 1998b). The yield stress model [eq. (18-61)] has been used successfully to predict cavern dimensions using model solutions of xanthan with a wide range of impeller designs (Elson et al., 1986; Nienow and Elson, 1988; Elson, 1988, 1990; Galindo and Nienow, 1992, 1993) in xanthan fermentations (Zhao et al., 1991, 1994) and in other yield stress fluids (Etchells et al., 1987). The gassed power consumption, $Po_g$, in eq. (18-61) can either be measured or estimated while the height/diameter ratio remains approximately constant at cavern diameters less than the vessel diameter. However, its value

depends on agitator type. Once the cavern reaches the vessel wall, impeller type has little influence on the vertical expansion of the fluid for further increases in impeller speed (Elson, 1990). The rate at which the height of the cavern increases with impeller speed thereafter can be expressed as

$$H_c \propto N^p \tag{18-66}$$

The values of $H_c/D_c$ and p are also impeller dependent (Amanullah et al., 1998b). For $N > N_w$, where $N_w$ is the agitator speed and $H_{cw}$ is the height of the cavern when $D_c = T$, the cavern height, $H_c$, can be calculated from

$$\frac{H_c}{H_{cw}} = \left(\frac{N}{N_w}\right)^p \tag{18-67}$$

By definition, $H_{cw} = (H_c/D_c)T$ and $N_w$ can be obtained by rearranging eq. (18-61) and replacing $D_c$ with T

$$N_w = \frac{\pi}{D} \left\{ \frac{[(H_c/D_c) + \frac{1}{3}](T/D)^3 \tau_y}{\rho Po_g} \right\}^{0.5} \tag{18-68}$$

## 18-3.4   Influence of Impeller Type and Bulk Mixing on Xanthan Fermentation Performance

Amanullah et al. (1998b) compared the physical and biological performance of four pairs of impellers: a standard Rushton turbine (SRT, D/T = 0.33), a large-diameter Rushton turbine (LRT, D/T = 0.42), a Prochem Maxflo T (PMD, D/T = 0.44), and a Scaba 6SRGT (SRGT, D/T = 0.54) in a 150 L fermenter. The reasons for the choice of impellers studied and their characteristics are described in Amanullah et al. (1998a). Dissolved oxygen was controlled using agitation speed with maximum agitation speeds of up to 700 rpm with the SRT and PMD and 600 rpm with the LRT and SRGT (because of motor limitations). Throughout the LRT and SRGT fermentations, this method successfully maintained DOT levels above the 15% set point. However, the culture became oxygen limited (<10%) in the SRT and PMD fermentations. The impeller power consumption (and hence the gassed power number, $Po_g$) of the impellers was monitored using online torque measurements throughout each 150 L fermentation. As a result of their diameters and power characteristics, the specific power inputs in the stationary phase of the LRT and SRGT fermentations could be maintained sufficiently high to keep the DOT above 15% of saturation. The total energy requirement for agitation could be calculated by integrating the specific power input with respect to fermentation time. The lowest energy requirement was obtained using the PMD at 270 Wh/kg. This was approximately 14% lower than with the SRT. The energy consumption with the SRGT and LRT was 7 and 28% greater than that with the SRT.

The results of the duplicate fermentations with each pair of impellers did not vary by more than $\pm 5\%$. Fifty g/L of glucose was added in a fed-batch mode to obtain high gum concentrations. Cell growth was limited by the supply of nitrogen. The highest concentration of gum was 34.8 g/L with the LRT, followed by 32.4 g/L using the SRGT with fermentations of 61 and 48 h, respectively. The highest overall productivity resulted with the SRGT at 0.68 g/L per hour. Fermentations using the SRT and PMD produced approximately similar quantities of gum at 29.7 and 29.0 g/L, respectively. On the basis of gum concentration and quality (as determined by measurement of viscosity), the best results were obtained with the LRT. The poorest quality of gum was obtained using the PMD. On the basis of energy consumption, the PMD was the most efficient. Xanthan productivity per unit energy input was 14% lower than with the SRT, which in turn was 11 and 1% lower than compared to the LRT and SRGT, respectively. Significantly, none of the criteria above favored the SRT. To elucidate the reasons for the very different performances obtained, a better understanding of the interaction between the bulk mixing and oxygen transfer was sought.

Equations (18-61), (18-66), (18-67), and (18-68) were used to estimate the cavern volume using each impeller. Since $N \geq N_W$ throughout the fermentation, the predicted diameter of caverns formed around each impeller was always greater or equivalent to the vessel diameter. Thus, adequate radial mixing could be achieved. However, mixing in the axial direction was poorer. The calculations demonstrated that the total height of the caverns was equivalent to the height of the broth for concentrations up to 16 g/L, ensuring complete homogenization. From 16 to 25.9 g/L, the caverns still interacted, although stagnant regions began to develop above the top and below the bottom impeller. At concentrations in excess of 27.3 g/L, the caverns did not interact and additional stagnant zones developed between the impellers. The calculated cavern volumes expressed as percentage of the total broth volume ($C_V/T_V$), plotted as a function of xanthan concentration for all four impellers, are shown in Figure 18-14. These results indicate that all impellers were equally effective in complete broth homogenization up to 16 to 18 g/L, although very different specific power inputs were necessary to achieve this. Differences in bulk blending were apparent only at higher concentrations; the volume of stagnant regions was greatest (45% at the end of the fermentation) with the SRT at a given gum concentration and least with the SRGT (19%).

The specific productivity in the stationary phase was correlated as a function of the well-mixed cavern region. The specific productivity decreased linearly from 0.36 to 0.04 g xanthan/g biomass per hour as the cavern volume decreased (Figure 18-15). It is proposed that the reduction in specific xanthan productivity was due to the oxygen limitation in the stagnant regions. This hypothesis was tested first, by plotting the measured oxygen transfer rates obtained with each impeller in the stationary phase as a function of the cavern volume. The linear relationship obtained suggested that oxygen transfer in these highly viscous fermentations predominantly occurs in the cavern. Therefore, with increasing fermentation time, the gas dispersion capability of all the impellers used was

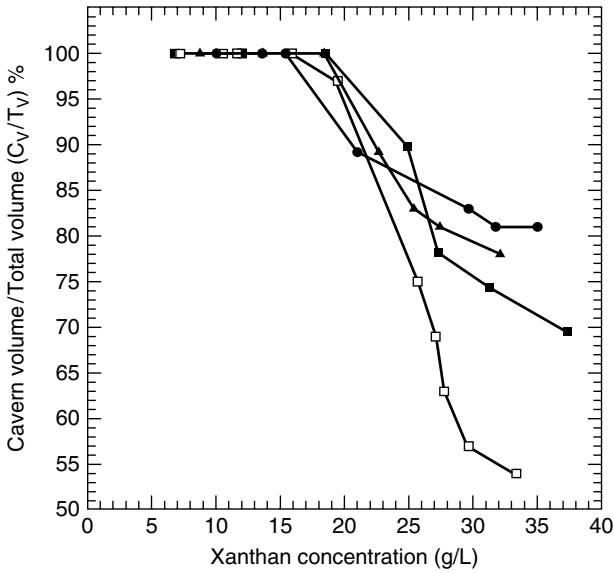**Figure 18-14**   Variation in the cavern volume (expressed as a percentage of the total broth volume) with xanthan concentration: (•) SRGT; (■) LRT; (▲) PMD; (□) SRT. (From Amanullah et al., 1998b.)
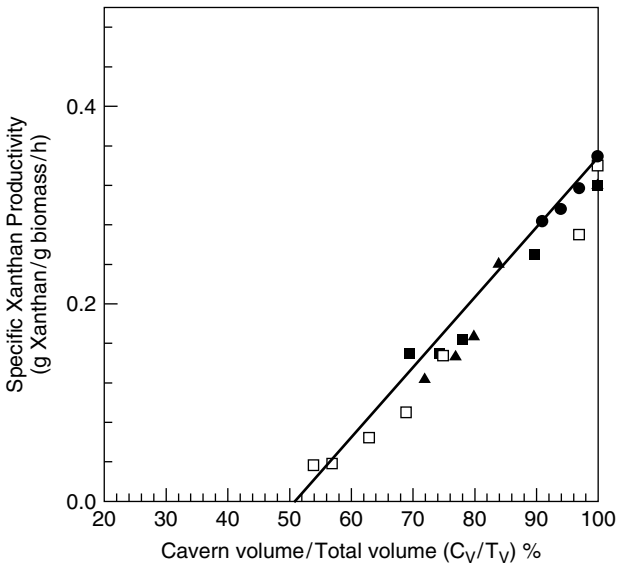


**Figure 18-15**   Effect of the cavern volume (expressed as a percentage of the total broth volume) on the specific xanthan productivity: (•) SRGT; (■) LRT; (▲) PMD; (□) SRT. (From Amanullah et al., 1998b.)

severely restricted to the reducing cavern size due to the increasing viscous and non-Newtonian behavior of the broth. Furthermore, a linear correlation of the specific productivity as a function of specific oxygen uptake rate was also obtained. Similar results were reported by Peters et al. (1989a).

It is clear from the previous discussion that it is necessary to reduce the stagnant regions to a minimum and therefore increase oxygen availability in xanthan fermentations to achieve high productivity. In this respect, the agitator design has an important role. The generally enhanced biological performance obtained with the LRT and SRGT impellers can be attributed to their relatively superior bulk blending and oxygen transfer characteristics, which results at the expense of increased torque and energy consumption. Importantly, it should be recognized that a large torque agitation system for a given power input gives a larger cavern (Nienow and Elson, 1988). Thus, it is the combination of the largest D/T ratio and moderately high aerated power number for the Scaba SRGT and the high aerated power number and moderately large D/T ratio for the LRT that leads to them having similar and better performances than the SRT.

Solomon et al. (1981b) showed that pairs of large-diameter impellers were superior when compared to standard Rushton turbines for the mixing of yield stress fluids in terms of power consumption and energy costs. Zhao et al. (1994) demonstrated reduced operating costs and higher yields when using larger-diameter Rushton turbines in xanthan fermentations. Although larger caverns ensure motion in more of the fermenter, it may still be necessary to consider gross recirculation to prevent compartmentalization. Large solidity ratio axial flow impellers may be better in this respect (Nienow, 1990), especially as they also produce large $H_c/D_c$ ratios. To retrofit 0.33 D/T-ratio Rushton turbines with larger D/T systems with higher torque is more expensive than equal torque, speed, and power retrofitting in nonyield stress broths (Nienow, 1990). This factor, too, needs to be considered when selecting the agitation system, and it is important to do a proper economic assessment, allowing for the time value of money (Muskett and Nienow, 1987).

Literature data on the performance of novel impellers in fermentations are relatively scarce. Retrofitting large-diameter PMD impellers in place of standard Rushton turbines at constant power input in a range of bioreactor sizes has been reported to improve the oxygen transfer efficiency (attributed to enhanced bulk blending) and product yield in viscous shear-thinning mycelial fermentations (Gbewonyo et al., 1987; Buckland et al., 1988a,b). Thus, it is still possible that if larger D/T-ratio PMD impellers had been used in the study reported by Amanullah et al. (1998b), their performance might have matched that of the LRT and SRGT impellers. The results of that study also show that improved agitator performance can be used either to reduce operating costs significantly or to obtain enhanced productivity and product quality (at the expense of energy input) in xanthan fermentations. These findings further the strong grounds already established from a mixing viewpoint using model fluids for retrofitting the traditionally used standard Rushton turbines with large diameter impellers of similar designs. The latter can be used to improve both liquid pumping and gas-handling

capacities (Nienow, 1990), thereby increasing the mass transfer potential. However, retrofitting of the standard with large diameter Rushton turbines in existing bioreactors may be difficult given the limitations of many motors and drive. An alternative is to use large diameter, low power number impellers such as the PMD and SRGT impellers, which can then be retrofitted for equal speed, torque, and hence power consumption.

## 18-3.5   Factors Affecting the Biopolymer Quality in Xanthan and Other Polysaccharide Fermentations

The quality of polysaccharide gums as determined by their mean molecular weight and molecular weight distribution is an important issue that in turn affects the rheological properties of the gum. A number of studies have reported that high DOT levels as well as good homogeneity of the broth result in xanthan gums of high molecular weight (Peters et al., 1989a,b). These studies demonstrated that as long as oxygen limitation could be overcome and homogeneous mixing conditions could be achieved, the hydrodynamics related to the use of different impellers or bioreactor design did not affect the quality of the gum produced. In a study reported by Amanullah et al. (1998a), mean molecular weight of xanthan using radial flow LRT and SRGT impellers was 8.8 and $9 \times 10^6$ kg/mol, respectively, while for the axial flow PMD impeller it was $8.1 \times 10^6$ kg/mol. The superior-quality gum obtained with the radial flow impellers was attributed to their enhanced bulk mixing and oxygen transfer characteristics.

Lawford and Rousseau (1991) reported that replacement of Rushton turbines with axial flow impellers under non-DOT-limiting conditions resulted in higher-quality (water-insoluble) curdlan. The authors suggested that the quality of the gum degraded at the higher shear rates imposed by the Rushton turbines, although bulk mixing characteristics were not analyzed, and it is difficult to ascertain whether local DOT limitations in the case of the Rushton turbines (lower cell viability was measured compared to the axial flow impellers) may have resulted in a lower-quality gum. Interestingly, the apparent viscosity of the gum increased to a maximum before decreasing in all fermentations. The authors speculated the role of endoglucanase activity with cell death associated in later stages of the fermentations. Dreveton et al. (1994) reported that the mean molecular weight of gellan gum could be increased twofold under homogeneous mixing conditions (obtained with helical ribbon impellers and enriched oxygen supply) compared to heterogeneous mixing conditions obtained with Rushton turbines. The authors claimed that these differences arose due to differences in shear rates obtained with these impellers, which in turn determined whether oxygen diffusional limitations were imposed on cells. However, since these results were obtained without separating dissolved oxygen effects, it is not possible to ascertain whether the differences in gum quality were not simply due to oxygen limitations in the poorly mixed regions using the Rushton turbines.

In other polysaccharide fermentations such as alginate, curdlan, and pullulan gums, the effects of agitation speed and dissolved oxygen are more complex. Peña

et al. (2000) reported that at constant agitation speed of 300 rpm in a 1.5 L bioreactor, production of water-soluble alginate was enhanced at DOT levels of 5% compared to 0.5%. However, at DOT levels greater than 5%, the carbon source (sucrose) was utilized primarily for biomass formation rather than gum production. At a constant DOT of 3%, an increase in agitation speed to 700 rpm resulted in increased specific growth rate of the culture and alginate production, although the molecular weight of the polymer was nearly halved compared to 300 rpm. The authors stated that the measured alginate activity, controlled by the availability of oxygen to the cells (lower at lower speeds due to the formation of cell agglomerates), was responsible for degradation of the alginate. However, differences in alginase activity at the low and high agitation speeds were not reported, and in addition, higher leakage rates of alginase at higher agitation speeds cannot be ruled out either as the cause of the lower mean molecular weight of the alginate. On the other hand, Lee et al. (1999) found that the molecular weight of curdlan did not change with agitation speed in the range 300 to 700 rpm using a 5 L fermenter. Wecker and Onken (1991) showed that in the case of the water-soluble biopolymer, pullulan, production of the biopolymer by *Aureobasidium pullulans* was enhanced at 150 rpm compared to 500 rpm at a constant dissolved oxygen level of 100% in 6- and 50 L bioreactors. In addition, it was also shown that enhanced gum formation occurred at a DOT level of 50% compared to 100% at a constant agitation speed of 500 rpm. On the other hand, Gibbs and Seviour (1996) showed that pullulan production was reduced at high agitation speeds above 750 rpm using a 10 L bioreactor due to high dissolved oxygen. When operated at 1000 rpm at constant DOT, pullulan production was not affected.

## 18-4   MYCELIAL FERMENTATIONS

The industrial importance of filamentous fungi is illustrated by applications ranging across the production of antibiotics, organic acids, proteins, and food. The best known examples of the use of filamentous fungi are for production of penicillin by *Penicillium chrysogenum*, citric acid by *Aspergillus niger*, and recombinant proteins by *A. oryzae*. However, during the last two decades, filamentous fungi have been used increasingly as eukaryotic hosts for foreign gene expression, for which they have several attractions (Jeenes et al., 1991). First, due to their saprophytic life they are capable of secreting large quantities of proteins (van Brunt, 1986). Posttranscriptional modifications of proteins such as glycosylation are important capabilities offered by these hosts (Mackenzie et al., 1993). In addition, many species are generally regarded as safe by regulatory authorities. Despite the widespread industrial use and potential of fungal strains for secondary metabolite, organic acid, and heterologous protein production, relatively little is known about the influence of engineering variables such as agitation conditions upon the morphology of such organisms in submerged cultures. In many fungal fermentations, the high apparent viscosities and the non-Newtonian behavior of the broths necessitate the use of high agitation speeds to provide adequate mixing

and oxygen transfer. However, mycelial damage at high stirrer speeds (or power input) can limit the acceptable range of speeds, and consequently, the oxygen transfer capability and the volumetric productivity of the fermenter. The effects of hydrodynamic forces ("shear") on fungal physiology are poorly understood. An understanding of how agitation affects mycelial morphology and productivity ought to be valuable in optimizing the design and operation of large scale fungal fermentations for the production of secondary metabolites and recombinant proteins. Here the effects of agitation intensity on hyphal morphology and product formation in two fungal fermentations (*P. chrysogenum* and *A. oryzae*) are considered. *A. oryzae* was used to produce two proteins: α-amylase (homologous protein) and amyloglucosidase (heterologous protein).

Fungal morphology can be classified as dispersed or pelleted (Figure 18-16). The dispersed form is generally of greater importance, with the exception of some pelleted citric acid (*A. niger*) fermentations. Characterization of mycelial morphology is important for physiological and engineering studies of fungal fermentations and in the design and operation of such fermentations. The dispersed form of filamentous organisms in submerged cultures consists of branched and unbranched hyphae (freely dispersed) and clumps or aggregates (Tucker et al., 1992) and is most common in industrial filamentous fermentations. Although this classification does not have a physiological basis, it is nevertheless very useful when comparing relative changes in mycelial morphology. Morphological parameters of interest for the freely dispersed mycelia are mean total hyphal length, mean projected area, and the number of tips per hypha. Clump morphology can be quantified in terms of mean projected area (Tucker et al., 1992). The mean projected area of all elements was taken as a measure of the total
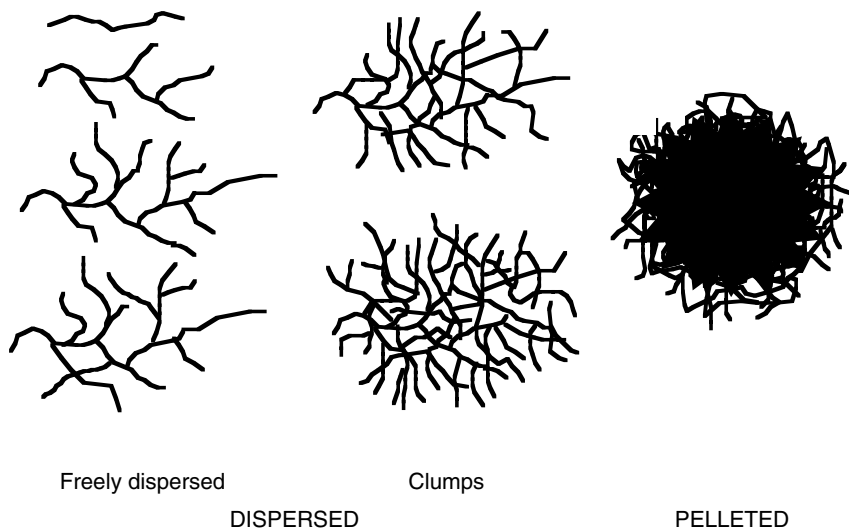


Freely dispersed          Clumps
          DISPERSED                              PELLETED

**Figure 18-16**   Classification of fungal morphology.

biomass (Packer and Thomas, 1990). Although the dispersed form of morphology is most commonly encountered in fungal fermentations, there are distinct benefits of operating with a pelleted morphology. Gbewonyo et al. (1992) demonstrated that in pilot scale Lovastatin fermentations using *Aspergillus terreus*, the pelleted form of morphology led to a fourfold lower apparent viscosity of the fungal broth compared to dispersed morphology fermentations. Although the oxygen uptake rate (and hence biomass concentration) was similar in the growth phase, significantly higher mass transfer and oxygen uptake rates were measured in the stationary phase, although overall product titers were similar. These results could therefore also be used to significantly lower power input (and hence operating costs) in pelleted fermentations [$k_L a = 77.4 P/V)^{0.6}$] and obtain similar mass transfer rates as dispersed morphology fermentations [$k_L a = 16.7(P/V)^{0.8}$].

Considering the importance of these complex morphologies on fermentation performance, and reports that changes in the morphology of *P. chrysogenum* can be caused by mechanical forces (Dion et al., 1954; Metz et al., 1981; van Suijdam and Metz, 1981; Smith et al., 1990; Nielsen, 1992; Makagiansar et al., 1993; Ayazi Shamlou et al., 1994; Jüsten et al., 1996, 1998a), the direct effect of agitation on morphology in submerged fermentations requires attention. As well as the total power input, the choice of impeller geometry determines the hydrodynamic forces that might affect the morphology (Jüsten et al., 1996; Amanullah et al., 1999) and differentiation (Jüsten et al., 1998a) of filamentous species, thereby influencing growth or production (König et al., 1981; Buckland et al., 1988a; Jüsten et al., 1998a; Amanullah et al., 1999). Other environmental factors, such as pH and spore concentration (in cases where spores are used as inoculum), also significantly influence mycelial morphology (Metz and Kossen, 1977). However, provided that these factors can be controlled and optimized, agitation-induced fragmentation, apart from growth, is considered to be one of the most important factors influencing mycelial morphology (especially in the design, operation, and scale-up of fungal fermentations). Although many studies have been conducted to investigate the effects of hydrodynamic forces on mycelial morphology and productivity (Dion et al., 1954; Ujcova et al., 1980; Metz et al., 1981; van Suijdam and Metz, 1981; Reuss, 1988; Smith et al., 1990; Makagiansar et al., 1993; Ayazi Shamlou et al., 1994; Nielsen et al., 1995), they generally suffer from two limitations. First, due to the lack of suitable methods for characterizing clumps (Tucker et al., 1992), only the freely dispersed form has been considered, although it may only account for only a small fraction of the biomass (Tucker et al., 1992; Jüsten et al., 1996). Second, it has not been possible to dissociate the influence of agitation from mass transfer effects. The dependence of product formation rates on impeller-generated fluid dynamic stresses has been observed for a wide variety of filamentous fungi (Ujcova et al., 1980; Vardar and Lilly, 1982; Smith et al., 1990; Braun and Vecht-Lifshitz, 1991; Märkl et al., 1991; Merchuk, 1991). There are also reports that mycelial fragmentation depends on the physiological state of the microorganisms (Smith et al., 1990; Paul et al., 1994).

## 18-4.1   Energy Dissipation/Circulation Function as a Correlator of Mycelial Fragmentation

Smith et al. (1990) and Makagiansar et al. (1993) proposed that the breakup frequency of mycelia would depend on $(P/D^3)(1/t_c)$, where P is the power input, D the impeller diameter, and $1/t_c$, the circulation frequency. This adaptation correlated the production rate and the morphology of the freely dispersed mycelia well at different scales up to 100 L and up to 1000 L, respectively. Unlike Smith et al. (1990) and Makagiansar et al. (1993), Jüsten et al. (1996) allowed for impeller designs other than Rushton turbines. Using well-established image analysis methodologies (Tucker et al., 1992; Paul and Thomas, 1998), Jüsten et al. (1996) were able to make quantitative measurements on the breakage of clumps and therefore to take into account the influence of realistic agitation conditions on the whole of the biomass. In off-line agitation studies it was demonstrated that *P. chrysogenum* morphological data using both radial and axial flow impellers of very different geometries and power numbers could be correlated with an energy dissipation/circulation function developed from the earlier work of Smith et al. (1990) and Makagiansar et al. (1993).

   The percentage of clumps in a fungal fermentation depends not only on the strain, the specific set of operating conditions, but also on the physiological state of the microorganisms. For instance, the percentage of clumps in the rapid growth phase is much greater than in the fed-batch stage of such fermentations. The value of 80% is quoted as an example specifically for *P. chrysogenum* in the rapid growth phase of a fed-batch fermentation. Nevertheless, it is still clearly necessary to include clump measurements for a proper representation of the total biomass. The energy dissipation/circulation (EDC) function was defined by Jüsten et al. (1996) as $(P/kD^3t_c)$, where P is the power input, D the impeller diameter, $t_c$ the mean circulation time, and k a geometric constant for a given impeller and is derived from a calculated impeller swept volume. This function arises from consideration of the energy dissipation in the impeller swept volume and the frequency of mycelial circulation through that volume. Although other correlating parameters, such as impeller tip speed and specific power input, were also considered, they were inferior to the energy dissipation/circulation function. The broader validity of these correlations was also verified in fragmentation studies at scales up to 180 L (Figure 18-17). The implications for the EDC function using tip speed and specific power input as scale-up criteria are interesting. Assuming that the flow number (Fl) and power number ($P_o$) are independent of scale (which is a reasonable assumption), for geometrically similar systems

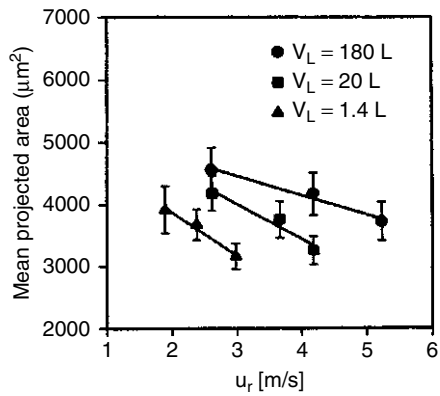$$\frac{P}{kD^3}\frac{1}{t_c} \propto N^4D^2 \tag{18-69}$$

At equal tip speed, $N \propto D^{-1}$ and therefore

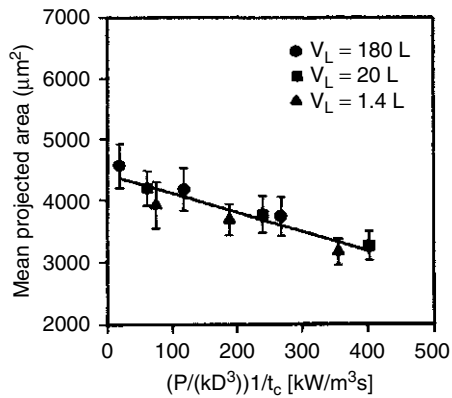$$\frac{P}{kD^3}\frac{1}{t_c} \propto D^{-2} \tag{18-70}$$
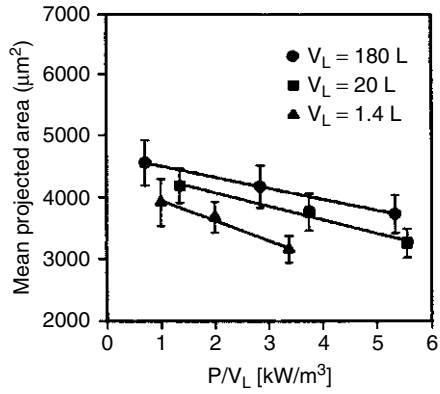
**Figure 18-17** Comparison of different scale-up criteria to correlate hyphal fragmentation in *P. chrysogenum:* (*a*) power per unit volume; (*b*) impeller tip speed; (*c*) the energy dissipation/circulation function. (From Jüsten et al., 1996.)

At equal P/V, $N \propto D^{-2/3}$ and therefore

$$\frac{P}{kD^3} \frac{1}{t_c} \propto D^{-2/3} \qquad (18\text{-}71)$$

Therefore, using both impeller tip speed and P/V as scale-up criteria, the value of the EDC function should decrease significantly on scale-up. This was confirmed in the study of Jüsten et al. (1996). Jüsten et al. (1998b) modeled the results of Jüsten et al. (1996) and suggested that clump fragmentation was the main cause of morphological changes and that the freely dispersed form was dominated by short fragments originating from clumps. It should be recognized that these studies were conducted in off-line vessels under nongrowing conditions, although it was subsequently shown that this function could also correlate the growth, morphology, vacuolation, and productivity in fed-batch penicillin fermentations (Jüsten et al., 1998a). It should also be noted that there is no fundamental understanding of how clumps might be broken by agitation.

   The broader validity of the EDC function to correlate hyphal fragmentation of fungal cultures other than *P. chrysogenum* was reported for *Aspergillus oryzae* using different agitation intensities and different impellers under nongrowing conditions in stirred tanks (Amanullah et al., 2000), chemostats (Amanullah et al., 1999), and fed-batch cultures (Amanullah et al., 2002). The study by Amanullah et al. (2000) demonstrated that the EDC function could correlate hyphal fragmentation for both *P. chrysogenum* and *A. oryzae*. Samples for fragmentation studies were obtained from chemostat cultures. Details of the impeller type, geometry, and operating conditions are shown in Tables 18-3 and 18-4 for *A. oryzae* and *P. chrysogenum*, respectively.

**Table 18-3**  Details of Agitator Type, Geometry, and Operating Conditions in Off-line Fragmentation Experiments Using *Aspergillus oryzae*

| Impeller | Impeller Diameter/Tank Diameter Ratio, D/T | Agitation Speed (rpm) | Power Number, Po[a] | Flow Number, Fl | Reynolds Number, Re |
|---|---|---|---|---|---|
| Rushton | | 540 | | | 14 100 |
| (radial flow) | 0.33 | 1200 | 3.90 | 0.78 | 31 400 |
| | | 1470 | | | 38 400 |
| Rushton | | 290 | | | 29 400 |
| (radial flow) | 0.65 | 330 | 4.2 | 0.87 | 33 500 |
| Prochem Maxflo T | | 120 | | | 11 400 |
| (axial flow) | 0.63 | 500 | 1.65 | 1.01 | 47 600 |
| Pitched blade | | 1210 | | | 46 500 |
| (axial flow) | 0.40 | 1500 | 0.60 | 0.61 | 57 600 |

[a] Off-bottom clearance: $0.25 \times T$.
*Source*:  Amanullah et al. (2000).

**Table 18-4**   Details of Agitator Type, Geometry, and Operating Conditions in Off-Line Fragmentation Experiments Using *Penicillium chrysogenum*

| Impeller | Symbol in Figures | Impeller Diameter/Tank Diameter Ratio, D/T | Speed Range (rpm) | Reynolds Number, Re[a] | Flow Number, Fl | Power Number, Po[b] |
|---|---|---|---|---|---|---|
| Paddle | ■ | 0.60 | 145–394 | 12 500–33 900 | 2.28 | 9.97 |
| (radial flow) | ● | 0.60 | 366–528 | 31 500–45 400 | 0.60 | 3.10 |
| Rushton turbine | ▼ | 0.65 | 238–407 | 24 000–41 100 | 0.87 | 4.52 |
| (radial flow) | ▲ | 0.40 | 548–1031 | 21 000–39 400 | 0.81 | 4.22 |
|  | ◆ | 0.33 | 767–1443 | 20 000–37 600 | 0.78 | 4.10 |
| Prochem Maxflow T | ☉ | 0.63 | 340–639 | 32 200–60 600 | 1.01 | 1.90 |
| (axial flow) | | | | | | |
| Propeller | ◇ | 0.50 | 745–2021 | 44 500–120 700 | 0.60 | 0.55 |
| (axial flow) | | | | | | |
| Pitched blade | □ | 0.60 | 359–676 | 30 900–58 200 | 1.03 | 1.97 |
| (axial flow) | △ | 0.40 | 776–1461 | 29 700–55 900 | 0.91 | 1.48 |
|  | ▽ | 0.40 | 1032–1943 | 39 500–74 300 | 0.63 | 0.61 |
|  | ○ | 0.40 | 1201–2054 | 45 900–78 500 | 0.53 | 0.40 |
| Intermig set (radial and axial flow) | ◇ | 0.65 | 423–795 | 42 700–80 300 | — | 0.81 |

[a] Viscosity = 0.001 Pa · s.
[b] Turbulent range with Reynolds number $> 10^4$ and no surface aeration. When surface aeration occurred, Po was reduced accordingly. The off-bottom clearance of the impellers was $0.7 \times D$.
*Source*: Jüsten et al. (1996); Amanullah et al. (2000).

Figure 18-18*a* shows the mean projected area of *A. oryzae* after 30 min of agitation normalized to a control (under nongrowing conditions). Details of impeller types and geometries are shown in Table 18-3. The control was taken as the mean of all the samples taken after dilution but just before the fragmentation tests were begun (i.e., $27\,200 \pm 7450\ \mu m^2$). Although the data are somewhat limited, the EDC is able to correlate the reduction in mean projected area for values greater than those used in the chemostat very well for both impeller types. Thus, this result supports the earlier work of Jüsten et al. (1996) with *P. chrysogenum*, using a greater range of impeller types and geometries (Table 18-4 and Figure 18-18*b*). For EDC values less than $90\ kW/m^3 \cdot s$ as used in the chemostat and marked in Figure 18-18*a*, fragmentation did not occur. This finding is consistent with the idea that the mycelia would be adapted to the agitation conditions in the chemostat. Figure 18-18*b* shows the data of Jüsten et al. (1996) with an indication of the EDC value ($22\ kW/m^3 \cdot s$) found in the chemostat. As before, the normalized data for all the impellers is correlated well by the EDC function for EDC values $> (EDC)_{chemostat}$. So, too, are the data for $(EDC) < (EDC)_{chemostat}$. However, even though the number of data at these low EDC values is much fewer than for $EDC > (EDC)_{chemostat}$, it is clear that there is a distinct change of

slope, suggesting much less breakdown and is consistent with data for *A. oryzae*. Overall, the conclusion that can be drawn from these two examples is that off-line fragmentation, depending on the state of the mycelia, is either very low or zero if the EDC function is less than that used in the chemostat. If the slopes representing the reduction in clump size with increasing values of the EDC above that in the chemostat are compared, a difference is observed. For the *A. oryzae* (Figure 18-18*a*), the slope is $-0.5$, while for the *P. chrysogenum* (Figure 18-18*b*), it is $-0.10$.

The precise reasons for differences in fragmentation behavior for the two strains are unclear, but it would not be unreasonable to invoke differences in cell wall strength, clump size, and structure as possible causes. The implication of clumps in the fragmentation analysis is especially relevant since morphological distributional data showed that fragmentation seemed to be mainly of the clumps, with loss of small fragments gradually reducing clump size (Jüsten et al., 1998b). Clump rupture and fragmentation of freely dispersed hyphae did not appear to be of primary importance. Although the EDC function is successful in correlating hyphal fragmentation using different impeller types and geometries



**Figure 18-18** (*a*) Variation in mean projected area at 30 min agitation time in an off-line vessel (nongrowing conditions) with the energy dissipation/circulation function using *Aspergillus oryzae*. Initial mean projected area (control) $= 27\,200 \pm 7450\ \mu m^2$. The chemostat value of $(P/kD^3)(1/t_c)$ is shown by the arrow (Amanullah et al., 2000). (*Continued*)
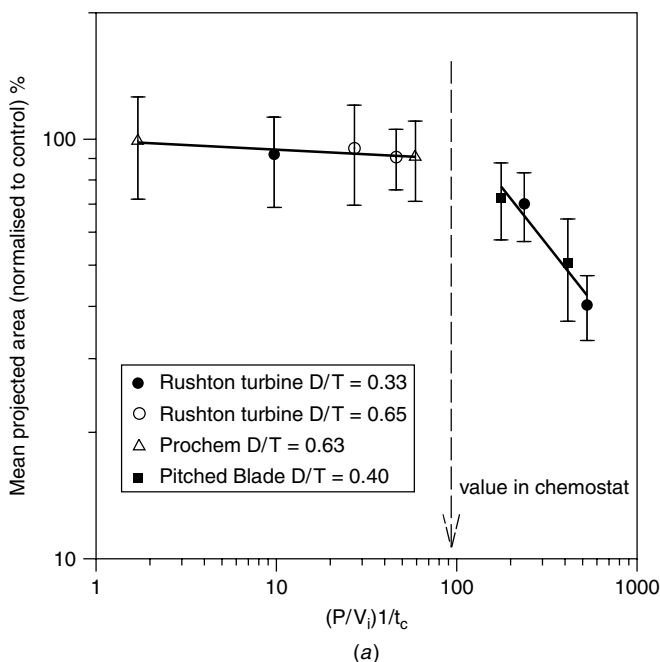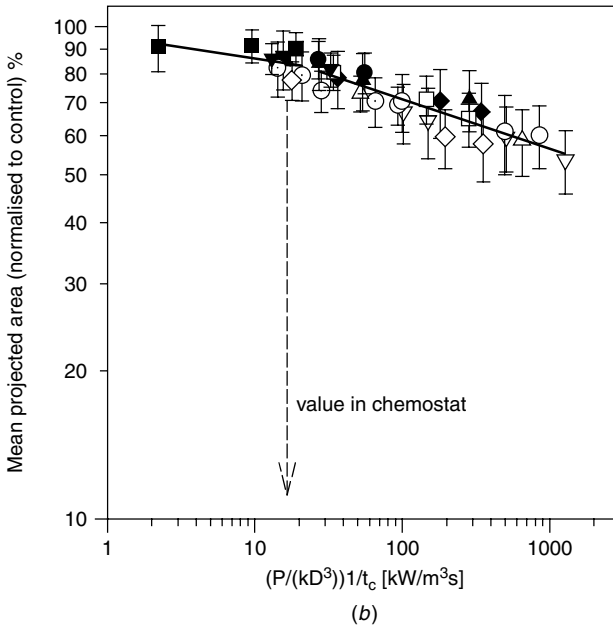
**Figure 18-18** (*b*) Variation of mean projected area at 30 min agitation time in an off-line vessel (nongrowing conditions) with the energy dissipation circulation function using *Penicillium chrysogenum* (Jüsten et al., 1996). Initial mean projected area (control) = $5620 \pm 500 \ \mu m^2$. Refer to Table 18-4 for symbols. The chemostat value of $(P/kD^3)(1/t_c)$ is indicated by the arrow (Amanullah et al., 2000).

as well as scale, it is not based on any fundamental understanding of the breakage process. It is also interesting to consider whether scale-dependent turbulent intermittency (short-term high-energy events), which can manifest itself in long-term turbulent mixing processes, has a role in the breakage process (Baldyga et al., 2001; also refer to Section 18.6.1). Perhaps the fragmentation experiments at different scales was not long enough (1 h) for intermittency to affect hyphal fragmentation.

## 18-4.2  Dynamics of Mycelial Aggregation

Although aggregation has been invoked as one possible way in which mycelia can increase their size, there is little evidence in the literature as to whether or not mycelia aggregate following a reduction in the agitation intensity (due to a reduction in agitator speed in a fermentation in response to a reduction in oxygen demand during a batch fermentation, for example, or when mycelia exit the high-energy dissipation impeller region in a large scale bioreactor). Given the importance of mycelial morphology, it is important to understand the factors, including aggregation, that influence it. Amanullah et al. (2001a) measured the dynamics of changes in mycelial morphology in response to a rapid and

much reduced level of agitation intensity. Analysis of the transients of mycelial morphology in chemostat and batch cultures of *A. oryzae* under conditions of controlled, nonlimiting, dissolved oxygen tension, following a significant decrease in agitation speed, showed that a large and rapid increase in the mean projected area of the clumps plus freely dispersed mycelia occurred at a rate that cannot be explained by growth alone. Clearly, a physical mechanism must have been responsible for the rapid increase in mean projected area and for the changes in the freely dispersed morphology. It was suggested that a physical mycelial aggregation process with a time constant of minutes caused the initial changes. However, it appears that such aggregation only occurs in cultures with the availability of dissolved oxygen, as there was no significant change in the morphology in off-line experiments where the broth was sparged with nitrogen.

Vecht-Lifshitz et al. (1990) proposed that the aggregation of the filamentous bacterium *Streptomyces tendae* was caused by hydrophobicity, which itself was biologically regulated by the supply of oxygen, and it is possible that similar phenomena occur in fungi. These findings are important since it is possible that in a large scale fermentation, with long mean circulation times, mycelia aggregate rapidly outside the impeller swept volume after undergoing fragmentation within it. For instance, in a large scale aerated bioreactor operated with a viscous mycelial fermentation, a mean circulation time between 20 and 60 s would be reasonable, and assuming that the circulation time can be described by a lognormal distribution, they could be distributed in the range 0 to 240 s (i.e., a maximum of a few minutes) (see Section 18.2.4.1). This is of the same order of magnitude as the times measured for mycelial aggregation. Thus, mycelia may be repeatedly fragmented and aggregated as they circulate through a large bioreactor. By the same reasoning, mycelial aggregation may not be relevant in small bioreactors with very short circulation times.

## 18-4.3   Effects of Agitation Intensity on Hyphal Morphology and Product Formation

### 18-4.3.1   *Aspergillus oryzae*. 
The effects of agitation on fragmentation of a recombinant strain of *A. oryzae* and its consequential effects on recombinant protein production were investigated by Amanullah et al. (1999). Constant-mass 5.3 L chemostat cultures at a dilution rate of 0.05 $h^{-1}$ and a dissolved oxygen level of 75% of air saturation were conducted at 550, 700, and 1000 rpm. These agitation speeds were chosen to cover a range of specific power inputs (2.2 to 12 $kW/m^3$) from realistic industrial levels to much higher values. The use of a constant-mass chemostat linked to a gas blender allowed variation of agitation speed and hence gas hold-up without affecting the dilution rate (via gas hold-up effects) or the concentration of dissolved oxygen. The morphology of both the freely dispersed mycelia and clumps was characterized using image analysis. Statistical analysis showed that it was possible to obtain steady states with respect to morphology. The mean projected area at each steady state under growing conditions correlated well with the EDC function. Rapid changes in

the hyphal mean projected area resulted in response to a speed change from 1000 rpm to 550 rpm (Figure 18-19). The steady-state mean projected area of the total biomass was found to increase significantly from $6100 \pm 1100$ $\mu m^2$ (mean $\pm$ standard error) at 1000 rpm to $16\,500 \pm 3800$ $\mu m^2$ at 550 rpm. Protein production ($\alpha$-amylase and amyloglucosidase) was found to be independent of agitation speed in the range 550 to 1000 rpm (P/V = 2.2 and 12.6 kW/m$^3$, respectively) (Figure 18-20), although significant changes in mycelial morphology could be measured for similar changes in agitation conditions. This suggests that mycelial morphology in his strain does not directly affect protein production (at a constant dilution rate and therefore, specific growth rate). Although there is very limited use of continuous culture systems in industry, they are extremely useful research tools since they can give precise information on the influence of a single variable. However, it was important to verify the results in fed-batch fermentations at industrially realistic conditions of biomass concentration and specific power input.

To extend the findings of the chemostat study to realistic operating conditions, fed-batch fermentations of *A. oryzae* were conducted at biomass concentrations up to 34 g dry cell weight per liter and three speeds (525, 675, and 825 rpm) to give specific power inputs between 1 and 5 kW/m$^3$ (Amanullah et al., 2002) using two Rushton turbines (D/T = 0.5) in a 6 L bioreactor. Gas blending was used to control the dissolved oxygen level at 50% of air saturation except at the lowest speed, where it fell below 40% after 60 to 65 h. The effects of agitation intensity on growth, mycelial morphology, hyphal tip activity, and
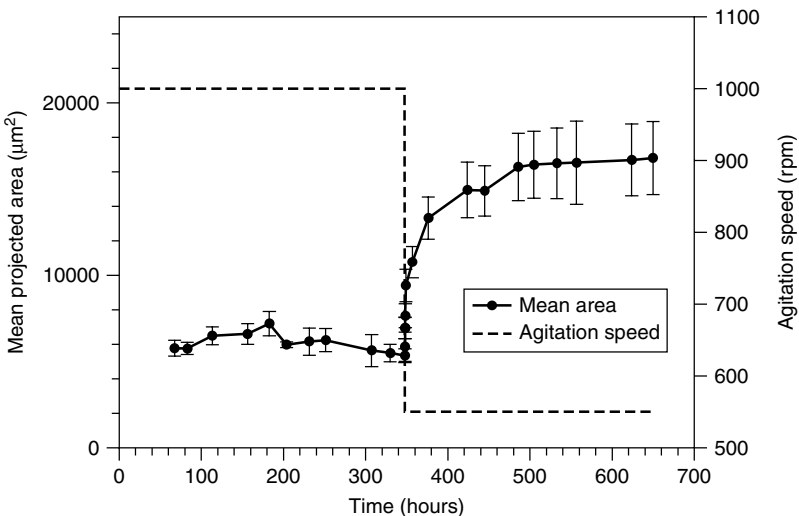


**Figure 18-19** Variation in mean projected area of the biomass with an agitation speed change from 1000 to 550 rpm using two Rushton turbines (D/T = 0.5) in a 5 L constant-mass chemostat at controlled dissolved oxygen of 75% of air saturation. (From Amanullah et al., 1999.)
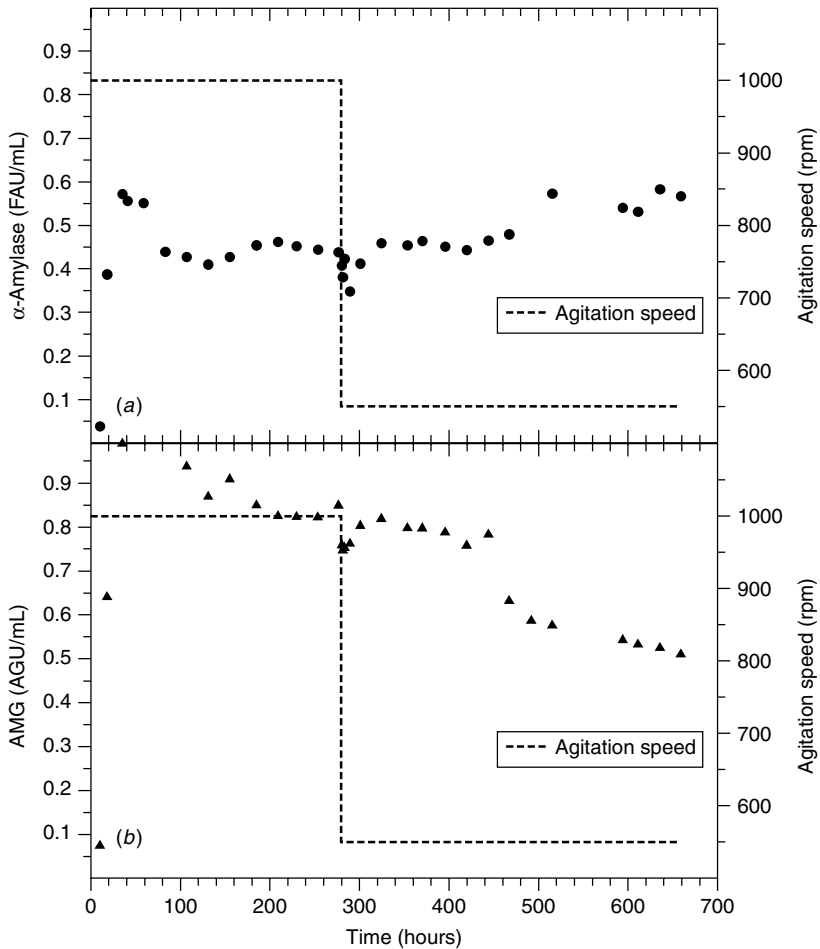
**Figure 18-20** Variation in (*a*) α-amylase and (*b*) AMG activities with an agitation speed change from 1000 to 550 rpm at 279 h in an agitation speed change from 1000 rpm to 550 rpm using two Rushton turbines (D/T = 0.5) in a 5 L constant-mass chemostat at a controlled dissolved oxygen level of 75% of air saturation. The data show that steady-state protein production remained independent of the changes in agitation speed. The decrease in the AMG activity at 450 h is thought to be related to a possible loss in the gene copy number for AMG. (From Amanullah et al., 1999.)

recombinant protein (amyloglucosidase) production in fed-batch cultures were investigated. In the batch phase of the fermentations, biomass concentration, specific growth rates, and AMG secretion increased with increasing agitation intensity. These early differences in specific growth rate were responsible for the dependence of biomass concentration on agitation intensity for the remainder of the fermentation, although the specific growth rate became independent. If in a

fermentation, dissolved oxygen fell below about 40% due to inadequate oxygen transfer associated with enhanced viscosity, AMG production ceased. As with the chemostat cultures, even though mycelial morphology was significantly affected by changes in agitation intensity, enzyme titers (AGU/L) under conditions of substrate-limited growth and controlled dissolved oxygen of more than 50% did not follow these changes.

The practical implication of these results is that the agitation intensity in such fungal fermentations can be manipulated to meet process requirements in terms of dissolved oxygen levels and bulk mixing and possibly to control broth rheology by changing morphology without compromising recombinant protein production. Attempts were also made to repeat this study with higher biomass concentrations of up to 58 g/L when mycelial interactions should be pronounced. These biomass concentrations were achieved, but it became impossible to mix the broth adequately due to its highly shear thinning, viscous nature. This led to a much lower Reynolds number at the small scale and very long mixing times (Nienow, 1998), and possibly even complete stagnation due to yield stresses (Nienow, 1998; Amanullah et al., 1998a,b). A similar biomass and broth rheology on the large scale at equal specific power input would give relatively higher Reynolds numbers and better mixing. The problem of maintaining suitable scale-down conditions with respect to both fluid dynamics and biomass concentration is a particularly difficult one. Further work is still needed to resolve this problem.

**18-4.3.2  *Penicillium chrysogenum*.** The influence of agitation conditions on growth, morphology, vacuolation, and productivity of *P. chrysogenum* in fed-batch 6 L fermentations was reported by Jüsten et al. (1998a). The results were compared using a standard Rushton impeller, a four-blade paddle, and a six-blade pitched blade impeller. Power inputs used ranged from 0.35 to 7.4 W/kg and the DOT was maintained above 40% of air saturation using gas blending. For a given impeller, the specific growth rate and biomass concentration in the batch phase increased with increasing agitation intensity, while the specific penicillin production rate decreased. These changes could be correlated to the EDC function. These results were in broad agreement with those reported by König et al. (1981), Vardar and Lilly (1982), Smith et al. (1990), and Makagiansar et al. (1993). The mean projected area also increased in the batch phase and remained relatively constant (dependent on agitation intensity) in the stationary phase. The proportion of vacillated regions also decreased with increasing agitation intensity possibly due to preferential fragmentation of the weaker vacuolated hyphal regions. This decrease is significant since penicillin synthesis is believed to be located in the vacuolated compartments. Clearly, the results obtained by the variation of agitation intensity in fed-batch cultures of *A. oryzae* (Amanullah et al., 2002) were different to those obtained with *P. chrysogenum*, where agitation intensity was found to strongly influence penicillin production (Jüsten et al., 1996, 1998a). For the latter case, it was suggested that the interrelationship is due to breakage of the relatively weaker vacuolated regions of hyphae, such regions being where penicillin synthesis is located. In contrast, although breakage still probably occurs at

the weaker vacuolated hyphal regions in *A. oryzae*, it does not affect AMG titer under conditions of substrate-limited growth. It is postulated that this lack of a relationship is because protein secretion in such strains appears to occur only at the hyphal tips (Wessels, 1990, 1993). Therefore, the results reported here are not generally applicable to all mycelial fermentations, and each system of interest should be considered individually.

### 18-4.4  Impeller Retrofitting in Large Scale Fungal Fermentations

Standard Rushton turbines of approximately one-third have traditionally been employed in fermentation processes. Bulk blending is also poor in highly shear thinning fungal broths, due to the tendency of Rushton turbines to compartmentalize. Buckland et al. (1988b) retrofitted two standard Rushton turbines (D/T = 0.33) with two low power number (Po = 1.1) Prochem hydrofoil impellers (D/T = 0.45) in 800 L in *Streptomyces avermitilis* fermentations. Two fermenters each equipped with either two Rushton or two Prochems were operated at 300 and 330 rpm with power draws of 4.1 and 2.7 kW, respectively. The values of $k_La$, oxygen uptake rates and Avermectin titers in the two bioreactors were identical. Thus, the Prochem impellers were shown to be capable of providing the same oxygen transfer and product titers, while drawing about 50% less power. They attributed this to the increased well-mixed volumes generated by the Prochem impellers, leading to enhanced oxygen transfer rates. Such results have also been demonstrated in highly viscous xanthan fermentations (see Section 18.3.4). Buckland et al. (1988a) recommended that standard Rushton impellers could be replaced by low-power-number agitators (preferably axial flow) such that the retrofitting would result in similar operating speeds, torque, and power. In this manner, the same shaft, motor, and gearbox could be employed. Similar retrofitting of such impellers in 19 000 L penicillin batch fermentations (Buckland et al., 1988b) demonstrated that the use of Prochem impellers at 1.96 W/kg resulted in higher productivity than Rushton turbines drawing 2.35 W/kg. These results were again explained in terms of enhanced bulk mixing and oxygen mass transfer.

### 18-5  *ESCHERICHIA COLI* FERMENTATIONS

Protein production by recombinant technology has been the subject of much industrial interest. However, production has been limited to a few well-known overexpression systems such as *E. coli*, although knowledge of the process engineering variables on performance is still limited. The cultivation of *E. coli* in fed-batch mode to high cell densities is the preferred industrial method for increasing the volumetric productivity of bacterial-derived products such as nucleic acids (Elsworth et al., 1968), amino acids (Forberg and Haggstrom, 1987), and heterologous recombinant production (Risenberg and Schulz, 1991; Bylund et al., 2000). In such fed-batch *E. coli* cultivations, the carbon source (usually, glucose) is supplied continuously at a growth-limiting rate. This avoids problems associated with excessive oxygen demand, heat generation, and catabolite repression

that occur in batch processes. Glucose is typically supplied at concentrations of up to 500 g/L. When cells grow at half their maximum specific growth rate, the concentration of the substrate is equal to the saturation constant of the Monod model, which for glucose is about 5 mg/L for *E. coli*. This creates a situation where the glucose concentration can vary theoretically in a large scale bioreactor from 500 g/L in the feed addition zone down to 5 mg/L elsewhere, with cells being exposed to very large concentration differences fluctuating in value in time and space. Mixing is critical in such situations to ensure that addition of the concentrated feed is dispersed as quickly as possible. However, the impact of intense mixing on bacterial physiology has not been widely reported.

### 18-5.1   Effects of Agitation Intensity in *E. coli* Fermentations

There are very few reports in the literature on the detrimental impact of fluid mechanical stress on bacteria and yeast in general. This is partly because bacteria are generally regarded as being significantly smaller than the Kolmogorov microscale of turbulence. For a detailed discussion and limitations of the Kolmogorov theory of isotropic turbulence, the reader is referred Section 18-6.1 (see also Chapter 2). The Kolmogorov microscale of turbulence, $\lambda_K$, is related to the local energy dissipation, $\varepsilon_T$, by the equation

$$\lambda_K = \left(\frac{v^3}{\varepsilon_T}\right)^{0.25} \tag{18-72}$$

where $v$ is the kinematic viscosity of the medium. Thus at 1 W/Kg in waterlike fluids, the value of $\lambda_K$ is 30 $\mu$m, while *E. coli* cells are 1 to 2 $\mu$m in length. This concept may also explain why hyphal fragmentation occurs in fungal fermentations since the size of hyphae are generally $>$50 $\mu$m. The only reported study that has investigated the effects of agitation intensity in *E. coli* fermentations was conducted by Hewitt et al. (1998). They cultivated *E. coli* in a chemostat equipped with two six-blade paddle impellers and varied the agitation speed of from 400 to 1200 rpm and back to 400 rpm. Dissolved oxygen was controlled independent of agitation speed using gas blending. This range in agitation speed covered a range in $\varepsilon_T$ from 1 to 30 W/kg, with $\lambda_K$ varying from 30 to 13.5 $\mu$m. Even if the maximum local energy dissipation value as found close to the impeller is used to estimate $\lambda_K$, it would still be about 6 $\mu$m, well above the size of *E. coli* cells. Physiological characteristics (cell viability and membrane potential as indicators of cell metabolism) of the cells were monitored using multiparameter flow cytometry. Neither biomass concentration, respiratory quotient, cell viability, nor membrane potential were affected in the range of agitation speeds tested. The only discernible change that could be detected via transmission electron microscopy was a stripping of the outer polysaccharide layer at the higher agitation speed, the physiological significance of which remains unclear.

Only one study (Toma et al., 1991) has reported growth and metabolic inhibition in *Brevibacterium flavum, S. cerevisiae*, and *Trichoderma reesei* due to

turbulence and remains outside the main paradigm of cell–turbulence interactions and is difficult to explain, even considering local energy dissipation rates. Perhaps turbulent intermittency has a role to play here (see Section 18-6.1).

## 18-6   CELL CULTURE

The commercial use of animal and insect cells at scales greater than 10 000 L for the production of posttranslationally modified proteins in kilogram quantities and viral vaccines using recombinant DNA and cell fusion techniques has made cell culture a cornerstone of modern biotechnology. Cell culture is being used increasingly for the production of highly valuable biologicals such as viral vaccines, hormones, growth factors, enzymes, and monoclonal antibodies. The high cost of media can often result in the cell culture step becoming the most significant cost of the process. Hence, much work has been devoted to optimizing the culture media and feeding strategies for supporting high cell viabilities and productivity and product quality. However, given that animal cells are potentially more sensitive than microbial cells to agitation and aeration in stirred tank bioreactors, the proper design and operation of bioreactors in relation to agitation and aeration is critical to benefit fully from process optimization efforts. The perceived sensitivity of animal cells to hydrodynamic shear stresses has resulted in the use of low agitation intensities and aeration rates, which in turn can lead to inhomogeneities in dissolved oxygen and $CO_2$, but especially in pH at large scales of operation. The discussion in this section focuses on these issues. Although air-lift, hollow-fiber, and fixed bed (for anchorage-dependent cells) bioreactors are also used, the majority of industrial processes use stirred-tank bioreactors, and for that reason, the discussion here has been limited to stirred tank bioreactors. The issues related to agitation and aeration are summarized in this section, although several excellent reviews (Prokop and Bajpai, 1992; Aunins and Henzler, 1993; Wu, 1995; Joshi et al., 1996; Thomas and Zhang, 1998) on this subject have been published and the reader is referred to these for detailed discussions.

### 18-6.1   Shear Damage and Kolmogorov's Theory of Isotropic Turbulence

As Thomas and Zhang (1998) point out, the term *shear* must be one of the most abused words in the biochemical engineering literature and has gained a nearly colloquial usage to imply any hydrodynamic effect on biological materials. Even the term *shear damage* is problematic. It is often used to describe hydrodynamic, fluid mechanical, or interfacial damage. However, just because cell damage increases due to an increase in turbulence intensity, it does necessarily mean that the cell is being "sheared." Its use has not always resulted in an understanding of the underlying mechanisms, and this is symptomatic of many studies conducted to study shear sensitivity of biological materials, including

fungal cultures and enzymes, but particularly cell and plant culture. Technically, *shear* refers to the relative motion of notional layers of liquid past one another due to a velocity gradient (or shear strain, $dv/dy$), and shear stress refers to the force per unit area acting tangentially to the surface of an object. The forces acting on a cell suspended in a fluid are the result of the dissipation of fluid kinetic energy to the external surface of the cell. The magnitude of these forces is a function of the fluid viscosity and velocity gradient immediately surrounding a cell and is given by

$$\tau = \mu\gamma = -\mu\left(\frac{dv}{dy}\right) \tag{18-73}$$

In laminar flow, the shear stress can be calculated relatively easily (Prokop and Bajpai, 1992). However, the situation is more complex in the turbulent flow regime. In this case the instantaneous velocity vector is the sum of the time-averaged velocity and a randomly fluctuating time-dependent velocity vector. The intensity of turbulence is directly related to the magnitude of the fluctuating velocity vector. Therefore, a cell suspended in laminar flow will experience an average shear stress that is independent of time, while in turbulent flow it can experience high shear stresses due to turbulence intermittency (Baldyga and Bourne, 1995; Baldyga et al., 2001). These authors point out that the local rate of energy dissipation displays fluctuations about its mean even under homogeneous flow conditions. These are intermittent (rare) fluctuations due to high energy events that are difficult to measure directly but could have a vital role in understanding cell–fluid interactions. Intermittency is especially important in cases where changes are irreversible and occur over long time frames (as is the case in cell culture systems). Consideration of intermittency also suggests that it is scale dependent, which may serve to undermine the conventional approach of using average energy dissipation rates for estimating cell damage or drop breakage in immiscible liquids. In fact, this was clearly shown in the highly significant paper of Baldyga et al. (2001), where difference in the steady-state Sauter mean drop diameter obtained at two different scales at equal mean energy dissipation rates could be explained by considering turbulence intermittency.

Almost equally abused is the Kolmogorov theory of isotropic turbulence (Kolmogorov, 1941a,b). According to this theory, kinetic energy at sufficiently large Reynolds numbers is imparted to the fluid by the rotating impeller blade and is initially transported by eddies (the largest eddy size is determined by the size of the impeller blade). The kinetic energy in the large eddies is rapidly cascaded to smaller eddies in an isotropic manner (i.e., directional information is lost), until finally most of the energy imparted by the impeller is transferred to the fluid via viscous dissipation of small eddies. These eddies are characterized by a length scale called the *Kolmogorov microscale* (see Section 18-5.1) and are often referred to as the *universal equilibrium range* of wavenumbers (inverse of the eddy size), where the energy carried by the eddies is independent of viscosity. The kinetic energy of turbulence is transferred from eddies to the cell surface to an extent determined by the relative size of eddies and the cells. Thus if the eddy

size is significantly larger than the cell, negligible energy is transferred to the cell surface and the cell can be thought of as a freely rotating object in a relatively quiescent fluid bounded by the dimensions of the eddy. If the eddy size is on the same order as the cell, significant transfer of energy can take place, which can lead to damage.

Although estimates of the Kolmogorov microscale are useful in determining whether damage can occur, care should be taken in estimation of the stresses based on this theory. First, the turbulence intensity in a bioreactor is not homogeneous, with almost 100 fold higher local energy dissipation rates found in the impeller region (Zhou and Kresta, 1996). The maximum time-averaged stresses occur in the trailing vortices behind the impeller blades. Many studies do not consider this heterogeneity and have used an average energy dissipation rate, which may not reflect the local peak values. Second, Kolmogorov's theory does not shed light on the mechanisms of cell damage; it does not describe how the cell and a turbulent eddy may interact. It is possible that the presence of cells may affect the fluid flow field, and estimates of velocity and pressure fluctuations on the scale of the cell may not be accurate (Barresi, 1997), although at the typical 0.01 to 0.001 volume fractions, this is unlikely to occur. Also, Reynolds stresses, which arise from a consideration of momentum transport in turbulence are commonly used to estimate stresses on cells (Prokop and Bajpai, 1992), do not have obvious meaning since they include eddy motions of all sizes, whereas only eddies of sizes comparable to the Kolmogorov microscale may be relevant for cell–eddy interactions. Another problem in the application of Kolmogorov's theory is that related to turbulence intermittency as discussed earlier, and further work is required to determine how intermittency affects cell–fluid interactions.

## 18-6.2   Cell Damage Due to Agitation Intensity in Suspension Cell Cultures

Due to the lack of a cell wall, animal and insect cells have long been perceived to be shear sensitive. This perception has led to intense research over the past two decades to uncover the mechanisms responsible for cell damage in bioreactors, although some of the earliest efforts in this regard can be traced back to the 1960s for the BHK-based foot-and-mouth disease (FMDV) vaccine process (Capstick et al., 1965, 1967; Telling and Elsworth, 1965). The FMDV process developed by the Animal Virus Research Institute and the Wellcome Foundation (England) was groundbreaking in many respects, not least because it utilized stirred tank bioreactors at the 3000 to 8000 L scale for the cultivation of continuous tumorgenic animal cells in suspension. However, these early studies of cell damage were not conducted systematically, and hence the damage mechanisms were not readily identifiable. In fact, it was a similar 8000 L bioreactor that was characterized in the studies reported by Langheinrich et al. (1998) and Nienow et al. (1996) and shown to be unsatisfactory with respect to bulk mixing.

Cell damage can be characterized using a number of techniques, including, but not limited to, trypan blue exclusion test, fluorescein diacetate test,

LDH release, and morphological measurements using specific antibody labeling. Sublethal effects have been measured generally by metabolic parameters such as growth rate, product formation, enzymatic activity, protein synthesis rates, membrane activity, and mitochondrial activity, among others. One of the first systematic studies undertaken was by Oh et al. (1989, 1992) using hybridoma cells. They showed that even at relatively high specific power inputs, $P/\rho V$, compared to industrial practice [up to 0.25 W/kg (400 rpm) using Rushton turbines in baffled 1.4 L bioreactors], provided that surface air entrainment did not occur, hybridomas were insensitive to agitation [i.e., cell damage (defined here as cell membrane disruption and measured via trypan blue staining) did not occur]. They discussed this finding in relation to both the large scale vortices behind impeller blades and to the Kolmogorov eddy scale relative to the cell size (Nienow, 1998). They concluded that interactions between cells and isotropic turbulent eddies were unlikely to cause cell death. Considerable cell damage was measured, on the other hand, when air entrainment occurred or sparging was utilized (the relevance of this finding is discussed later in this section). Further evidence to support these findings was provided by the study of Kunas and Papoutsakis (1990), who grew hybridomas at agitation rates of 700 rpm in a 2 L bioreactor in the absence of an air–liquid interface in the headspace. The authors reported that the specific growth rate of the cells was indistinguishable from the control, which was operated at 60 rpm.

Thomas et al. (1994) showed that even when hybridoma cells were agitated at 1000 ($P/\rho V = 7$ W/kg) and 1500 rpm ($P/\rho V = 24$ W/kg) in a 2 L bioreactor, the viable cell concentration was only reduced by 20% and 40%, respectively, in the first 60 min. Thereafter, little change was measured. Even considering that the maximum energy dissipation rate in the impeller swept volume is typically 100 times greater than the mean energy dissipation rate (Zhou and Kresta, 1996), these translate to values significantly lower than those required ($10^5$ to $10^6$ W/kg) for total disruption of hybridoma cells (Zhang et al., 1993). It should be noted that deleterious effects other than cell disruption are possible, such as reduction in DNA synthesis and cell division (Oh et al., 1992) at high agitation rates (especially under sparged conditions), although cell membrane disruption by mechanical forces is by far the predominant issue.

The results reported by Oh et al. (1992) were also in good in agreement with the data reported by Kioukia et al. (1992), who also subsequently (Kioukia et al., 1996) used the same equipment to culture Sf9 insect cells under both virus-infected and virus-noninfected conditions. No difference in growth, infection kinetics, or recombinant protein expression could be measured in the range 100 to 400 rpm (i.e., up to 0.25 W/kg). However, the sensitivity to aeration was confirmed and was even greater for Sf9 cells than for hybridomas.

In all the studies above, we also need to be aware that the results must be viewed in proper context of cell concentration and culture duration. What may appear negligible in a 4 to 5 day culture at about $1 \times 10^6$ cells/mL may become significant in a modern industrial cell culture process at about $1 \times 10^7$ cells/mL for 14 to 21 days, especially using serum-free media (van der Pol and Tramper,

1998). However, in general the studies have shown that animal cell culture processes in stirred bioreactors can be operated at much higher mean specific energy dissipation rates without cell damage than had previously been thought possible.

Ideally, a mechanistic model is needed to better understand the cell–hydrodynamic interactions. However, bioreactor hydrodynamics are turbulent and complex, especially when sparged and have not yet been fully characterized, and given the difficulty of quantifying the magnitude of the shear stress on cells, it is difficult to compare the results obtained from different mixing systems. Therefore, a number of investigators have made use of relatively simpler laminar flow fields in capillary tubes and viscometers to study cell–hydrodynamic interactions. Many of these studies have drawn inconsistent conclusions, partly because of the range of different cell lines, culture history, mode of growth, and physical environment used, and it is difficult to predict from them whether damage can occur under particular hydrodynamic conditions other than those of the original experiments. Cell disruption was studied by Born et al. (1992) in a laminar flow cone and plate viscometer. Cell deformation was assumed to cause an increase in cell membrane tension, and cells would be disrupted if the intrinsic cell membrane tension was exceeded. A model was developed using micromanipulation measurements of the cell bursting membrane tension. Using these measurements, the model was compared to results from exposing animal cells to laminar shear stresses from 124 to 577 $N/m^2$ for 3 min and found to be able to predict successfully loss of viable cells with a maximum error of less than 30%.

In subsequent studies, Zhang et al. (1993) and Thomas et al. (1994) proposed a model to estimate cell disruption in turbulent capillary flows. The flow field in the capillary was described by a laminar sublayer close to the wall and a homogeneous turbulent region elsewhere consisting of eddies of different sizes. Energy exchange was assumed to occur between cells and eddies for eddies approaching or smaller than the size causing cell deformations, which in turn can cause an increase in the membrane tension. Cells from a holding flask were recirculated through the capillary and it was shown that the cell disruption was a first-order decay process (Zhang et al., 1993). Although the model only underestimated the experimental cell disruption by 15%, it lacked explanation of the independence of the specific lysis rate on the number of passes through the capillary. In a further study (Thomas et al., 1994), this problem was resolved by consideration of the localization of the energy dissipation in turbulent capillary flows to a small volume near the vessel wall. The mean specific energy dissipation rate, $\bar{\varepsilon}_T$, used in the study of Zhang et al. (1993) was on the order of $10^3$ to $10^4$ W/kg, while it was estimated that the $\bar{\varepsilon}_T$ value required to disrupt 95% of cells was $10^5$ to $10^6$ W/kg. Since the local $\varepsilon_T$ close to the capillary wall was estimated to be at least an order of magnitude higher than $\bar{\varepsilon}_T$, and the instantaneous $\varepsilon_T$ (due to the intermittency of turbulence) near the wall might even be another order of magnitude higher, it was suggested that nearly the entire cell population would be damaged close to the wall. The study of Thomas et al. (1994) employed a repeated single-pass exposure of the entire culture in a flask (the total volume of culture was collected in a second flask before repeating cell passage through

the capillary) and demonstrated a deviation from first-order cell disruption kinetics, with a bias toward breakage of weaker cells first. Al-Rubeai et al. (1995) also suggested that the breakage of cells in turbulent capillary flow was cell-cycle dependent and demonstrated a bias toward the destruction of larger (and hence weaker) $G_2$ cells. The shearing studies described above have generally investigated short-term effects of agitation intensity, and it is possible in some cases that secondary deleterious effects can occur due to fatigue phenomena or reduced biosynthetic activity. For instance, Oh et al. (1989) reported that the specific metabolic activity (measured by the MTT assay) of the surviving cells under sparged conditions without Puronic F68 was higher throughout the duration of the culture than under unsparged conditions. Also, the specific MTT value increased with increasing agitation rates. It was suggested that the enhanced MTT levels were a stress response where the cells invoked the synthesis of enzymes involved in damage repair mechanisms. Under sparged conditions and the presence of Pluronic F68, although the MTT levels were higher at the early stages of the cultivation than under unsparged conditions, the differences became negligible with increasing cultivation time.

The general conclusion from the studies conducted in bioreactors and in simpler flow devices on the effects of agitation intensity in cell cultures is that in the absence of bubble entrainment, such cultures can be operated at much higher mean specific energy dissipation rates without cell damage than had previously been thought possible. For example, in the 8 m$^3$ bioreactors installed at the Wellcome Foundation as reported by Langheinrich et al. (1998), the maximum $\bar{\varepsilon}_T$ available was 0.01 W/kg.

## 18-6.3   Bubble-Induced Cell Damage in Sparged Suspension Cultures

The primary aim of aeration is to provide oxygen to cells. The oxygen requirements of animal and insect cells are low compared to bacteria, ranging from 0.1 to $1.6 \times 10^{-8}$ mg/cell per hour for animal cells to 0.64 to $2.4 \times 10^{-8}$ mg/cell per hour for insect cells (Aunins and Henzler, 1993). Furthermore, culture growth in many cell lines (e.g., CHO) is independent of dissolved oxygen across a range of 5 to 100% of air saturation (Oh et al., 1992). For insect cells the optimum value range of dissolved oxygen has been quoted at 40 to 60% of air saturation (Kloppinger et al., 1990). In most cases, it is not a major problem in meeting oxygen requirements. Headspace aeration and silicone tubing aeration is generally sufficient in laboratory, and in some cases, pilot scale equipment. However, as the scale increases, it becomes necessary to sparge air directly into the medium (especially for insect cells under infection conditions). Due to considerations of bubble-induced cell damage, particularly in the absence of surfactants for cell protection as well as $CO_2$ ventilation and pH control, aeration of cell cultures requires care.

After nearly two decades of research, it is now generally accepted that mechanical damage of freely suspended cells is due to bubble hydrodynamics, in particular the bubble-bursting phenomena at the headspace gas–liquid interface (Handa et al., 1987; Tramper et al., 1987; Handa-Corrigan et al., 1989; Oh et al., 1989,

1992; Chalmers and Bavarian, 1991; Kioukia et al., 1992; Meier et al., 1999). Four bubble-liquid-cell regions where cell damage can occur can be identified: (1) bubble formation at the sparger, (2) bubble coalescence and breakup in the impeller discharge, (3) bubble rise through the bioreactor, and (4) bubble bursting at the air–medium interface. Kilburn and Webb (1968) demonstrated the protective effects of Pluronic F68 in moderating cell damage. Tramper et al. (1987) suggested the concept of a killing volume that was associated with bubble frequency and independent of rise height, and therefore, cell damage was primarily as a result of bubble disengagement. Handa et al. (1987) and later Handa-Corrigan et al. (1989) formalized these concepts into an experimental framework and showed that cell damage occurs due to bubble bursting, and that the amount of damage was related to the bubble size and frequency and that cell damage could be reduced by the addition of Pluronic F68. Oh et al. (1992) extended and confirmed these findings and suggested that bubbles with diameters <5 mm were the most lethal and air sparging coupled with aeration led to increased damage compared to aeration alone. Less damage was found when air was sparged above the impeller compared to sparging below it. It was not possible to ascertain unequivocally whether the additional damage was associated with the trailing vortex bubble breakup per se, since this affected both bubble size and frequency, both of which are implicated in bubble bursting cell damage.

Tramper et al. (1987) estimated the shear stress generated by rising bubbles and found that it was considerably lower than that due to bubble bursting and negligible for cell damage. Bubble rupture at the gas–liquid interface involves several dynamic events (Newitt et al., 1954; Garcia-Briones and Chalmers, 1994; Boulton-Stone, 1995; Wu, 1995; Dey et al., 1997) which have been documented using high-speed video photography. For further details the reader is referred to these publications. However, in summary a bursting-bubble rupture starts at the thinnest apex of the film cap, where a hole is formed, followed by a rapid extension of the hole boundary. The receding bubble film is a very fast process, and for instance for a 2 $\mu$m liquid film, the receding velocity is estimated to be 8 m/s. The shear stress in the receding film has been estimated by Cherry and Hulle (1992) at around 95 N/m$^2$ in laminar flow and up to 300 N/m$^2$ in the boundary layer surrounding the bubble cavity (Chalmers and Bavarian, 1991). Following a cascade of events, two liquid jets are produced, one downward into the liquid and one upward over the bubble cavity. The velocity of the rising liquid jet has been estimated at 5 m/s for a 1.7 mm bubble (MacIntyre, 1972). Calculations by Kowalski and Thomas (1994) suggest that power dissipated during the ejection of the jet is in the region of 0.5 kW/mL ($5 \times 10^5$ W/kg), which itself can be a source of cell damage. The liquid jet eventually breaks into smaller liquid droplets, often at speeds up to 10 m/s. Wu and Gossen (1995) suggested that unless cells are concentrated into the bubble film cap before it ruptures, the contribution of this region to cell damage is likely to be small, as it constitutes a small proportion of the total bubble interface. Therefore, according to these results, the bubble crater collapse is the prime cause of cell death, although some caution should be applied in interpreting these results since Wu and Gossen

(1995) employed cell viability rather than viable cell concentration as an indicator of damage. Boulton-Stone (1995) developed a numerical model of the bubble-bursting process and was able to predict the bubble-bursting effects of a wide range of surface properties. The surface dilatational viscosity seemed particularly important. Dey et al. (1997) attempted to validate the model but could do so successfully only by setting the value of the surface dilatational viscosity to at least an order of magnitude higher than the value determined experimentally.

A foam layer can also develop at the gas–liquid interface at the surface in many cultures since most animal cell media contain chemicals that cause foaming. Cell damage measured in such cases have shown there to be a greater percentage of dead cells in the foam layer than in the bulk (Wu, 1995), probably attributable to liquid film drainage processes. It is likely that all the high-energy events associated with bubble bursting described above contribute to cell damage. From a practical viewpoint, an understanding of how the transport of cells to the headspace gas–liquid interface can be minimized can be used to reduce cell death.

The question of how cells are transported to the headspace gas–liquid interface has been addressed by various authors, including Tramper et al. (1987), Handa-Corrigan et al. (1989), Jöbses et al. (1991), Cherry and Hulle (1992), Garcia-Briones and Chalmers (1992), and Meier et al. (1997). Garcia-Briones and Chalmers (1992), who visualized cells attached to rising bubbles and suggested that the major cause of cell bubble attachment appears to be hydrophobic interaction via bubble–cell collision. This was in contrast to the observations made by Cherry and Hulle (1992) with insect cells and by Handa-Corrigan et al. (1989) with hybridoma cells—that few cells were attached to rising bubbles. The major cause of cell–bubble contact appears to be through hydrophobic interaction (Wu, 1995), although very little is known about such mechanisms with respect to animal and insect cultures. Knowledge of the mechanism of cell attachment to bubbles and the conditions under which such attachment occurs may help in minimizing cell damage due to bubble bursting.

## 18-6.4   Use of Surfactants to Reduce Cell Damage Due to Bubble Aeration in Suspension Culture

Surfactants such as the various members of the Pluronic family, especially Pluronic F68 (Kilburn and Webb, 1968), methylcellulose, polyethylene glycol, and serum, have long been known to decrease cell damage due to bubble aeration (Handa et al., 1987; Murhammer and Goochee, 1990). Papoutsakis (1991) reviewed the role of these media additives for protecting freely suspended cells and suggested that the all surfactants mentioned earlier imparted shear protective effects to differing degrees. However, a mechanistic understanding of their role in preventing cell damage was still lacking, and attempts to compare the results of using these additives in various studies was hampered by the diversity in equipment type, scale, operating conditions, and cell line. Michaels et al. (1991) suggested that the protective effects of surfactants can be both biological and physical in nature. A biological mechanism was taken to imply when addition of

the surfactant directly resulted in an increase in the cell membrane strength. A physical mechanism implied that the cell resistance to shear remains unaltered, but the factors such as the medium properties that affect both the level and frequency of high-shear events (e.g., bubble bursting) change in a manner such that cell damage decreases. By far the most commonly used additive is Pluronic F68. Attempts to correlate cell death with media (containing Pluronic F68) properties such as surface tension (both static and dynamic) and viscosity have been unsuccessful (Dey et al., 1997). Dey et al. (1997) showed that bubble burst could be moderated by the addition of various concentrations of Pluronic F68 to basal medium: in particular, a decrease in the time of jet formation, the height and width of jets, and the number of subsequent liquid drops released.

The role of surfactants to reduce cell attachment as a means to reduce cell damage due to bubble bursting has been investigated by various researchers with inconsistent findings. Tramper et al. (1987), using a medium with 0.1% methylcellulose as surfactant, reported that cell death rate was directly proportional to gas flow rate and inversely proportional to culture volume in bubble columns, suggesting that the death rate is independent of the bubble residence time, a conclusion supported by the work of Handa-Corrigan et al. (1989), and Jöbses et al. (1991). On the other hand, others, including Cherry and Hulle (1992) and Garcia-Briones and Chalmers (1992), have clearly shown cell attachment to bubbles. Thus cell attachment to bubbles should result in a death rate that is dependent on bubble residence time, which in turn determines the number of attached cells. Meier et al. (1999) incorporated the foregoing findings into a single framework and concluded that cell death due to bubble bursting depends on cell attachment to bubbles. The discrepancy in the literature data was attributed to the differences in experimental setup (presence of surfactant in media, reactor geometry, and bubble size) and cell line.

Meier et al. (1999) concluded that insignificant cell attachment occurred in the presence of surfactants such as Pluronic F68 and that large scale bioreactors should be designed with a high aspect ratio, since bubble residence time is not important for cell damage mediated by bubble bursting. However, it is also important to remember that good homogenization is also required (see Section 18-6.6) and is much slower in vessels of high aspect ratio (Langheinrich et al., 1998), so this conclusion of Meier et al. (1999) may be inappropriate. On the other hand, in the absence of surfactants where bubble residence time is important, Meier et al. (1999) recommended a lower-aspect-ratio bioreactor, since this should lead to lower rates of cell attachment to bubbles and hence reduced cell damage.

Another mechanism by which surfactants such as Pluronic F68 can render a protective effect is biological in nature. Murhammer and Goochee (1990) and Goldblum et al. (1990) found that Pluronic F68 could be rapidly incorporated onto the membranes of insect cells and thus offer protection. Ramirez and Mutharasan (1990) used a fluorescence polarization method to demonstrate that Pluronic F68 decreased the membrane fluidity (and hence membrane strength) throughout a batch culture. Furthermore, Zhang et al. (1992) used a micromanipulation method

to measure the strength of a hybridoma cell line from a continuous culture with and without added Pluronic F68. A significant increase in both the bursting membrane tension and mean elastic compressibility modulus (both indicators of strengthened cell membranes) was found in the presence of 0.5 g/L of Pluronic F68. It is likely that no single parameter is solely responsible for the protective effects offered by surfactants such as Pluronic F68, but rather, a combination of moderation of the bubble burst, reduced cell attachment to bubbles, and adsorption/incorporation into the cell membrane.

### 18-6.5   Cell Damage Due to Agitation Intensity in Microcarrier Cultures

Many animal cell lines such as VERO cannot be adapted to suspension culture, and such adherent cells are often grown on both conventional and macroporous microcarriers. For information on the effects of shear stress on anchorage-dependent cells, the reader is referred to the reviews by Prokop and Bajpai (1992) and Aunins and Henzler (1993). Microcarriers offer advantages of supporting high cell densities via large surface areas for growth, relatively easy cell-media separation, and scalability. Macroporous microcarriers provide some protection to adherent cells from agitation and aeration. However, to maximize this advantage, the internal space must be readily accessible to cells. Although agitation sufficient for microcarrier suspension may allow for adequate oxygen mass transfer, higher levels of agitation may be required if oxygenation is via surface aeration (especially at large scales of operation) or if high cell density cultures are desired. The main goal of successful microcarrier cultivation is to maximize cell density without detrimental effects of agitation, while providing adequate oxygen transfer and a homogeneous bioreactor environment. A major problem is that adherent cells can be removed from the microcarrier surfaces at steady laminar stresses in the range 0.5 to 10 N/m$^2$ accompanied by loss of viable cells and productivity (Aunins and Henzler, 1993). Unlike in suspension cultures at realistic power inputs (Oh et al., 1989, 1992), Croughan and Wang (1987) showed that cell damage in microcarrier cultures could be related to the Kolmogorov scale of turbulent eddy dissipation. In microcarrier suspension cultures, turbulent eddies in the viscous dissipation region are often intermediate in size between the cells and microcarriers. In this case, the high rate of specific energy dissipation as eddies interact with the surface of the microcarriers causes local transient shear rates to be sufficiently high to remove the cells from the microcarrier surface.

Croughan et al. (1989) analyzed selected published data on microcarrier cultivation of FS-4 cells in spinner flasks and showed that cell death occurred when the eddy size ($\approx$100 μm) calculated using the global energy input to the reactor was smaller than the average microcarrier diameter (185 μm) and proposed a model for cell death:

$$\frac{dx}{dt} = \begin{cases} \mu x & \text{for } \lambda_{\text{global}} > d_{\text{microcarrier}} & (18\text{-}74) \\ (\mu - k_d)x & \text{for } \lambda_{\text{global}} < d_{\text{microcarrier}} & (18\text{-}75) \end{cases}$$

where

$$k_d = K \left( \frac{\bar{\varepsilon}_T}{\nu^3} \right)^{0.75} \tag{18-76}$$

and x is the cell concentration, $\mu$ the specific growth rate of the cells, $k_d$ the specific death rate constant, K a cell and bioreactor-dependent constant (Croughan et al., 1987), $\bar{\varepsilon}_T$ the mean specific energy dissipation rate in the bioreactor (= P/$\rho$V), and $\nu$ the medium kinematic viscosity. A note of caution may be appropriate when comparing the predictions of the models with experimental data given the inaccuracy of estimating the power input using a stirrer bar in the spinner flasks from literature correlations and the fact that the assumption of isotropic turbulence in a spinner of such scales at the Reynolds numbers employed was probably not valid. However, analysis of literature data showed that the dependency of $k_d$ on the average energy dissipation rate (slope = 0.75) was close to that suggested by eq. (18-76). From a scale-up viewpoint, provided that the turbulent eddy-cell model is valid, scale-up at equal energy dissipation rates should not lead to detrimental hydrodynamic effects. It should also be noted that data on the effects of aeration with respect to cell damage in microcarrier cultures are scarce (Aunins et al., 1986).

Croughan et al. (1988) also addressed the effects of cell–cell collisions and cell–impeller collisions with respect to cell damage. In a typical microcarrier bioreactor, the beads can collide with one another as well as with the impeller and other vessel internals if the collision forces are greater than the force required to remove the liquid film between them (Prokop and Bajpai, 1992). In this case, cell damage will be a function of collision frequency and the amount of energy transmitted during the collision event. They found that the rate of cell damage due to bead–bead collision, dc/dt $(\bar{\varepsilon}_T)^{3/4}C_b$, where $C_b$ is the microcarrier bead concentration. Design implications for bead–impeller collisions were also discussed by Croughan et al. (1988). The effects of cell–cell and cell–impeller collisions in suspension cultures is not significant compared to the hydrodynamic forces due to agitation and aeration and also because of dissipation of the collision energy due to cell-surface deformation.

A number of cell lines like BHK also exhibit aggregation behavior, and in such cases, Moreira et al. (1995) demonstrated that the aggregate size can be correlated to the Kolmogorov eddy scale using both $\bar{\varepsilon}_T$ and the local specific energy dissipation rates, although the latter was shown to be marginally superior in correlating the aggregate breakage. However, in contrast to microcarriers, breakage of cell aggregates at high agitation speeds led to smaller and more compact aggregates without resulting in cell damage. This advantage can be used to grow cells in aggregates as a natural immobilization system at higher energy dissipation rates where microcarriers cannot be used.

## 18-6.6 Physical and Chemical Environment

One of the consequences of the perceived shear sensitivity of animal cells to agitation intensity and operation at low agitation speeds is the inability to provide

adequate liquid homogenization in large scale bioreactors. Typical values of energy dissipation rates are two orders below that used in bacterial fermentations. One of the very few mixing and aeration studies in large scale bioreactors under animal cell conditions, other than the one reported by Kiss et al. (1994), was reported by Nienow et al. (1996) and Langheinrich et al. (1998). These authors conducted comprehensive studies of homogenization in a commercial scale 8 m$^3$ bioreactor and in a geometrically similar scaled-down 0.61 m mixing tank. The 8 m$^3$ bioreactor was operated in industrial applications for cell culture growth at a maximum speed of 60 rpm with a single Rushton turbine with an unusually low D/T and clearance ratios (C/T) of 0.22 and an aeration rate via a pipe sparger of 0.005 vvm. Under such conditions the energy dissipation rates due to agitation and aeration were $11.5 \times 10^{-3}$ and $2 \times 10^{-3}$ W/kg, respectively. First, they showed that under such operating conditions the mixing time was >200 s for H/T = 1.3 and that the mixing time correlations derived in the literature for 1 < H/T ratio < 3 (Cooke et al., 1988) were capable of predicting the experimentally derived mixing times in the 8 m$^3$ bioreactor, even though the energy dissipation and aeration rates were two orders of magnitude lower than those used to derive the correlations. Second, they demonstrated that mixing at the top of the bioreactor was poor, due to the inability of the upper recirculation loop to reach the top of the bioreactor, and also that the aerated mixing time was significantly shorter than under unaerated conditions at the top of the bioreactor, due to the energy dissipated by bubble disengagement and convective flow. Suggested strategies for significant improvement in liquid blending arising from experimentation in the scaled-down tank included retrofitting the small diameter high power number Rushton with a large diameter low power number axial flow impeller such as an up-pumping Chemineer HE3 or a Prochem Maxflo T, the use of increased energy dissipation rates, and an increased impeller clearance ratio C/T of 0.5.

For caustic pH control, alkali is generally added at the liquid surface at the later stages of cell culture processes, and it is here that pH excursions are known to occur, especially if liquid blending is poor. Langheinrich and Nienow (1999) also used the geometrically scaled down 0.61 m tank to investigate possible pH excursions in the 8 m$^3$ bioreactor. At the operating conditions described earlier, they found significant pH excursions of up to 0.8 pH unit at the point of alkali addition in a buffered system using both pH probe measurements and flow visualization studies. Such excursions can be detrimental for cell viability and product formation (Brown and Birch, 1996; Osman et al., 2001, 2002). The pH variations were absent when alkali was added to the impeller region. They also found that an increase in the overall energy dissipation rate did not have a significant impact on the pH excursions given the substantial differences in the local energy dissipation rates at the liquid surface and the impeller region. The authors recommended that the pH excursions could, realistically, be avoided only with alkali added to the impeller region via a pipe. Traditionally, this option has not been implemented in industrial scale bioreactors due to "clean in place" (CIP) considerations.

One consequence of using low aeration rates to prevent bubble-associated cell damage is the possible accumulation of dissolved $CO_2$ with increasing hydrostatic pressure (or scale) to inhibitory or metabolism-altering concentrations, due to insufficient ventilation as a result of low air sparging rates or using oxygen-enriched air. This can be a major problem in large scale bioreactors, especially when operated at high cell densities. $CO_2$ production rates between 0.17 to $1.3 \times 10^{-8}$ mg/cell per hour have been reported for a range of cell lines (Aunins and Henzler, 1993). Kimura and Miller (1996) reported that CHO cells cultivated in laboratory scale bioreactors were moderately tolerant to dissolved $CO_2$ (up to 18% $CO_2$), while Gray et al. (1996) reported an inhibitory effect at 14% dissolved $CO_2$ in large scale cultures. $CO_2$ ventilation rate is affected by control strategy used to control dissolved oxygen (surface aeration, air sparging, partial pressure of oxygen in the inlet gas, and type of sparger) and therefore, a balance between oxygenation, $CO_2$ ventilation, and pH control needs to be made. One solution to this problem is to employ two spargers serving different functions; a sintered sparger to provide small bubbles to enhance oxygen mass transfer and a pipe sparger producing relatively larger bubbles for $CO_2$ ventilation while ensuring minimal cell damage. The inhibitory effects of $CO_2$ are evident at lower concentrations if the culture osmolality is >300 mOs, as may be the case in fed-batch cultures. Increased osmolality up to 400 mOs has also been shown to increase the specific antibody production rate, although this enhancement is cell-line dependent. Cyclic exposure of cells to increasing hydrostatic pressure with scale can also occur, although results reported by Tagaki et al. (1995) at constant pH, $pCO_2$, and $pO_2$ using hybridoma cultures suggested that this is unlikely to affect culture metabolism per se.

Despite advances in our understanding of cell damage due to bubble aeration and under realistic conditions of agitation, we still lack sufficient knowledge for an optimal a priori design. This is due to incomplete understanding of the complex two-phase hydrodynamics in bioreactors (e.g., bubble size distribution in large scale cell culture media), bubble–cell attachment mechanisms, effects of surfactants on media physical properties and due to the diversity of cell line, type of culture media, and operating conditions. However, a general guideline for design and operation of large scale bioreactors for freely suspended animal cells should probably consider the following (Nienow, 1997):

- Multiple impellers in high aspect ratio bioreactors with a large diameter radial flow Rushton turbine or Scaba (or up-pumping axial flow) impeller with clearance ratios between 0.33 and 0.5, good for gas dispersion, and an up-pumping or down-pumping large diameter axial flow impeller for liquid blending above it. Increased agitation intensity to ensure good liquid blending is also recommended.

- Design and operating conditions should be chosen to avoid pH excursions. "Clean in place" issues related to addition pipes for subsurface addition of concentrated reagents should be addressed.

- Oxygenation requirements should be balanced against $CO_2$ ventilation rates, perhaps employing different sparger types for each purpose if needed. Mean bubble sizes should generally be maintained above 5 mm, although this is not easy in practice.
- Pluronic at concentrations greater than 0.5 g/L should be used to minimize cell damage due to bubble aeration.

## 18-7    PLANT CELL CULTURES

Plants are recognized as an important source of natural compounds for use in the pharmaceutical and food industries. For example, the commercially important anticancer drug Taxol (Bristol-Myers Squibb) was originally isolated from the Pacific yew tree, *Taxus brevifolia*, requiring the bark of 1000 trees to produce 1 kg of Taxol (Kieran et al., 1997). It is currently produced via a semisynthetic route using taxane precursors extracted from trees. Plant cell cultures provide an alternative technology to produce such chemicals if the source plant is scarce, difficult to cultivate, or where chemical synthesis is challenging or not possible. The commercialization of plant cell culture has been limited due mainly to process economics, which in turn is governed by biological and engineering considerations. The success of industrial scale plant cell cultures depends on a number of factors, but is principally on the development of high-yielding cell lines and the ability to grow the plant cell suspension at large scales. The stirred tank bioreactor is still considered the most economically feasible bioreactor design for the cultivation of plant cells. In this section we summarize the key engineering factors that need to be considered from a mixing viewpoint. For detailed aspects of the impact of mixing in plant cell cultures, the reader is referred to selected publications and reviews by Leckie et al. (1991), Prokop and Bajpai (1992), Scragg (1992), Meijer et al. (1993, 1994), Shuler (1993), Namdev and Dunlop (1995), Joshi et al. (1996), Kieran et al. (1997), Doran (1999), and Rodríguez and Galindo (1999).

Although much of the know-how to design mixing systems for plant cell cultures can be borrowed from the fermentation and cell culture fields, a number of characteristics of plant cells make them unique. Plant cells are typically 10 to 100 $\mu$m in diameter and often grow in aggregates up to 500 to 2000 $\mu$m in size, due to the presence of hydrophobic glycan in the cell wall and incomplete cell separation after cell division. Due to their size and their rigid cellulosic cell wall, plant cells and their aggregates, similar to animal cells, are commonly considered to be sensitive to hydrodynamic shear stress. However, commercial production requires high cell densities, and coupled with the excretion of polysaccharides (unlike animal cells), often as a response to hydrodynamic stress (Rodríguez and Galindo, 1999), can result in rheological complexity, with the broth often exhibiting non-Newtonian behavior. Although the oxygen requirements of plant cells is low, with reported values in the range 1.5 to $6.3 \times 10^{-3}$ g $O_2$/kg · s (Doran, 1999), the ability to provide sufficient oxygen transfer is limited by considerations of shear sensitivity and rheology. Another requirement in plant cell cultures

is cell suspension. Foaming is also a particular problem and in some cases can be severe (Zhong et al., 1992). In many cases the product of interest is intracellular, and cell disruption is required for downstream processing.

From a mixing viewpoint, only the effects of hydrodynamic shear stress and agitator design have been reported in the literature and to a much lesser extent and rigor compared to microbial, fungal, and animal cells. Hydrodynamic shear stress has been investigated both in bioreactors under growth conditions (using energy dissipation and tip speed as correlating factors) and under well-defined flow conditions in viscometric devices. Critical shear stress (using regrowth of cells as an indicator) in the range 50 to 200 $N/m^2$ have been reported (Kieran et al., 1997). Translation of such values to stirred tank conditions is difficult. Cell damage can be manifested as a lethal or sublethal effect. Lethal effects have been characterized by cell lysis, release of intracellular compounds, changes in aggregate size, and biomass yield. Prokop and Bajpai (1992) discussed the limitations of some of these measurements. For instance, since plant cells form large aggregates, cell number per unit volume is not an easily accessible parameter. Data on aggregate size distribution are scarce and often without statistical analysis. In addition, reports on biomass yields vary greatly among investigators, even using the same cell line and growth conditions. Namdev and Dunlop (1995) also cited the limitations of shear-related studies in plant cell culture and proposed a more systematic approach focusing on sublethal responses such as transmembrane activity, stress protein expression, osmoregulation, and aggregation.

Despite the difficulties in studying the effects of hydrodynamic shear stress in bioreactors, some useful conclusions have emerged. Doran (1999) reported a theoretical engineering analysis (cultivation of the culture was not performed) of impeller type and geometry for the application of plant cell culture in a 10 $m^3$ fermenter under continuous flow conditions. Mixing, mass transfer, impeller gas handling, and cell suspension characteristics of both Rushton turbines and axial flow impellers (both up- and down-pumping) demonstrated that upward-pumping axial flow impellers offered advantages compared to Rushton turbines for gas handling and cell suspension when the power input was restricted by cell damage considerations (Figure 18-21). Initial concerns of universal hydrodynamic damage to plant cells encouraged the widespread adoption of airlift bioreactors. As Meijer et al. (1993) point out, shear sensitivity of plant cells became established as a near axiom after quotation by many investigators. Meijer et al. (1993) conducted a through review of the effects of hydrodynamic stress on plant cells and concluded that although significant differences in shear tolerance existed between cell lines, plant cells were not as susceptible to hydrodynamic damage as had originally been thought. For instance, Leckie et al. (1991) demonstrated that using Rushton turbines and pitched blade impellers in 12 L fermenters, agitation speeds up to 300 rpm did not affect the growth of *Catharanthus roseus* and alkaloid production. In fact, culture growth was possible even up to 1000 rpm, although alkaloid production decreased. Similar conclusions were also reported by Scragg et al. (1988) and Meijer et al. (1994). Meijer et al. (1994) reported no difference in growth or product formation capabilities of *Catharanthus roseus*
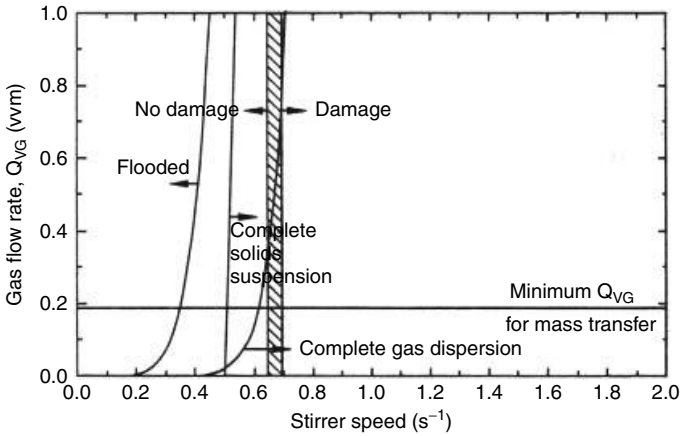
**Figure 18-21**   Flow regime map for upward-pumping six-blade 45° pitched blade turbine with a D/T ratio of 0.40 using plant cell cultures in a 10 m³ bioreactor. The flow regime map shows that complete cell suspension occurs below the agitation speed required to damage cells independent of gas flow rate. Taking into account the minimum gas flow rate required for oxygen requirements, there is a small window of operating conditions where the impeller functions of complete gas dispersion, cell suspension, and oxygen mass transfer are met while avoiding cell damage. (From Doran, 1999.)

and *Nicotiana tabacum* up to agitation speeds of 1000 rpm using a Rushton turbine in a 12 L bioreactor, although cultures of *Cinchona robusta* and *Tabernaemontana divaricata* did exhibit detrimental effects at these agitation speeds. In general, plant cell damage mechanisms have been difficult to identify, due to the diversity of cell lines, aggregate morphologies, culture age, and cultivation history. Further systematic studies of oxygen mass transfer, nutrient availability, cell suspension, aggregation behavior, and cell damage in response to the intensity of mixing are required to provide a better understanding for successful scale-up. Furthermore, very little has been reported on the metabolism of plant cells, the effects of aeration as a cell-damaging parameter, and the influence of morphology on growth and product formation.

Interestingly, Meijer et al. (1993) and Kieran et al. (1997) also suggested that more effort should be devoted to establishing robust and reproducible cell lines than developing low shear bioreactors for fragile cell lines, which may not ultimately be robust and grow well. In some instances, plant cells can be adapted to withstand higher shear stresses by changing subculturing conditions and allowing the cells to proliferate for a longer time at low shear stresses in vitro (Drapeau et al., 1987).

## NOMENCLATURE

C           impeller clearance (m)
C           tracer concentration at time t (−)

| | |
|---|---|
| $C_L{}^*$ | dissolved oxygen concentration at air saturation (% air saturation) |
| $C_L$ | dissolved oxygen concentration in the liquid phase (% air saturation) |
| CTD | circulation time distribution $(-)$ |
| $C_b$ | microcarrier bead concentration |
| $C_v$ | cavern volume $(m^3)$ |
| D | impeller diameter (m) |
| $D_c$ | cavern diameter (m) |
| DOT | dissolved oxygen tension (% air saturation) |
| Da | Damkoehler number—system residence time/characteristic reaction time (dimensionless) |
| $d_{microcarrier}$ | diameter of microcarrier beads $(\mu m)$ |
| EDC | energy dissipation/circulation function $P/(kD^3\ t_c)$ $(kWm^{-3}s^{-1})$ |
| F | total force imparted by the impeller, radial and axial (eq. 18-64) $(Nm^{-2})$ |
| F | $Q_R/V_{STR}$ $(s^{-1})$ |
| $F_a$ | axial force (eq. 18-65) $(Nm^{-2})$ |
| Fl | flow number $Q/ND^3$ (dimensionless) |
| $Fl_G$ | gassed flow number $(Q_G/ND^3)$ (dimensionless) |
| Fr | Froude number $(N^2D/g)$ (dimensionless) |
| F(t) | circulation time distribution $(-)$ |
| g | gravitational constant $(ms^{-2})$ |
| H | liquid height (m) |
| $H_c$ | cavern height (m) |
| $H_{cw}$ | height of cavern when cavern diameter = vessel diameter (eq. 18-67) (m) |
| K | fluid consistency index $(Nm^{-2})$ |
| k | geometric constant for a given impeller (eq. 18-69) |
| $k_d$ | specific death rate constant of cells $(h^{-1})$ |
| $k_La$ | mass transfer coefficient $(s^{-1})$ |
| m | number of circulations (eq. 18-54) $(-)$ |
| N | impeller rotational speed (rps) |
| N | number of tanks $(-)$ |
| $N_F$ | minimum impeller speed to prevent flooding |
| $N_f$ | axial force number (eq. 18-65) (dimensionless) |
| $N_R$ | speed at which onset of gas recirculation occurs (rps) |
| $N_w$ | impeller speed at which cavern touches vessel wall (eq. 18-68) (rps) |
| n | flow behavior index $(-)$ |
| OUR | oxygen uptake rate $(mmol\ L^{-1}\ h^{-1})$ |
| OTR | oxygen transfer rate $(mmol\ L^{-1}\ h^{-1})$ |
| P | fluid mixing power (W) |
| $P_g$ | gassed power (W) |
| Po | power number (dimensionless) |
| PFR | plug flow reactor |

| | |
|---|---|
| p | impeller dependent exponent defining cavern expansion (eq. 18-66) $(-)$ |
| Q | impeller pumping capacity $(m^3\,s^{-1})$ |
| $Q_{O2max}$ | maximum specific oxygen uptake rate (mmol/g biomass/s) |
| $Q_G$ | gas flow rate $(m^3\,s^{-1})$ |
| $Q_R$ | gas recirculation rate |
| Re | Reynolds Number $(ND^2/\mu)$ (dimensionless) |
| $r_c$ | radius of a torus shaped cavern (eq. 18-63) (m) |
| STR | stirred tank reactor |
| t | time (s) |
| T | vessel diameter (m) |
| $t_c$ | circulation time (s) |
| $\bar{t}_c$ | mean circulation time (s) |
| $t_{oc}$ | oxygen consumption time (s) |
| $t_m$ | mixing time (s) |
| $t_R$ | residence time in the PFR (s) |
| $U_T$ | impeller tip speed $(ms^{-1})$ |
| V | total volume of fluid in the vessel $(m^3)$ |
| $V_a$ | volume of the active zone $(m^3)$ |
| $V_i$ | impeller swept volume $(m^3)$ |
| $V_o$ | fluid velocity at cavern boundary $(ms^{-1})$ |
| $V_q$ | volume of the quiescent zone $(m^3)$ |
| $V_{PFR}$ | volume of PFR $(m^3)$ |
| $V_{STR}$ | volume of STR $(m^3)$ |
| $v_s$ | superficial gas velocity $(ms^{-1})$ |
| vvm | volumetric flow of gas per liquid volume per minute $(min^{-1})$ |
| w | impeller blade width (m) |
| x | cell concentration $(g\,L^{-1})$ |
| x | biomass concentration |
| $\dot{\gamma}$ | fluid shear rate (eq. 18-60) $(s^{-1})$ |
| $\varepsilon$ | gas holdup (%) |
| $\varepsilon_T, \bar{\varepsilon}_T$ | rate of dissipation of turbulent kinetic energy $(W\,kg^{-1})$ |
| $\lambda_k$ | Kolmogorov scale $(\mu m)$ |
| $\mu$ | fluid viscosity $(Nm^{-2}s)$ |
| $\eta$ | efficiency index (eq. 18-28) $(-)$ |
| $\mu$ | specific growth rate $(h^{-1})$ |
| $\mu_l$ | mean of lognormal distribution (s) |
| $\nu$ | kinematic viscosity $(m^2s^{-1})$ |
| $\rho$ | density $(kg\,m^{-3})$ |
| $\sigma$ | surface tension $(Jm^{-2})$ |
| $\sigma, \sigma_\theta$ | standard and normalized deviations of mean circulation time (S, $-$) |
| $\tau$ | fluid shear stress (eq. 18-60) $(Nm^{-2})$ |
| $\tau_y$ | fluid yield stress $(Nm^{-2})$ |

*Subscripts*

c     Casson
CD   Complete dispersion
F     flooding
HB   Herschel–Bulkley
t     turbulent flow regime

## REFERENCES

Al-Rubeai, M., R. P. Singh, A. N. Emery, and Z. Zhang (1995). Cell cycle and cell size dependence of susceptibility to hydrodynamic forces, *Biotechnol. Bioeng.*, **46**(1), 88–92.

Amanullah, A. (1994). Scale down models of mixing performance in large scale bioreactors, Ph.D. dissertation, University of Birmingham, England.

Amanullah, A., A. Baba, C. M. McFarlane, A. N. Emery, and A. W. Nienow (1993a). Biological Models of Mixing Performance in Bioreactors, *Proc. 3rd International Conference on Bioreactor and Bioprocess Fluid Dynamics*, Cambridge University, Sept. 14–16, pp. 381–400.

Amanullah, A., A. W. Nienow, A. N. Emery, and C. M. McFarlane (1993b). The use of *Bacillus subtilis* as an oxygen sensitive culture to simulate dissolved oxygen cycling in large scale fermenters, *Trans. Inst. Chem. Eng., Part C*, **71**, Sept., pp. 206–208.

Amanullah, A., S. A. Hjorth, and A. W. Nienow (1998a). A new mathematical model to predict cavern diameter in highly shear thinning power law liquids using axial flow impellers, *Chem. Eng. Sci.*, **53**(3), 455–469.

Amanullah, A., L. Carreon-Serrano, B. Castro, E. Galindo, and A. W. Nienow (1998b). The influence of impeller type in pilot scale xanthan fermentations, *Biotechnol. Bioeng.*, **57**(1), 95–108.

Amanullah, A., B. Tuttiett, and A. W. Nienow (1998c). Agitator speed and dissolved oxygen effects in xanthan fermentations, *Biotechnol. Bioeng.*, **57**(2), 198–210.

Amanullah, A., R. Blair, C. R. Thomas, and A. W. Nienow (1999). Effects of agitation speed on mycelial morphology and protein production in chemostat cultures of recombinant Aspergillus oryzae, *Biotechnol. Bioeng.*, **62**(4), 434–446.

Amanullah, A., P. Jüsten, A. Davies, A. W. Nienow, and C. R. Thomas (2000). Agitation speed induced mycelial fragmentation in *Penicillium chrysogenum* and *Aspergillus oryzae* cultures, *Biochem. Eng. J.*, **5**, 109–114.

Amanullah, A., E. Leonildi, A. W. Nienow, and C. R. Thomas (2001a). Dynamics of mycelial aggregation in cultures of *Aspergillus oryzae*, *Bioprocess. Biosys. Eng.*, **24**, 101–107.

Amanullah, A., C. M. McFarlane, A. N. Emery, and A. W. Nienow (2001b). Experimental simulations of pH gradients in large scale bioreactors using scale down models, *Biotechnol. Bioeng.*, **73**(5), 390–399.

Amanullah, A., L. H. Christensen, K. Hansen, A. W. Nienow, and C. R. Thomas (2002). Dependence of morphology on agitation intensity in fed-batch cultures of *Aspergillus oryzae* and its implications for recombinant protein production, *Biotechnol. Bioeng.*, **77**(7), 815–826.

Aunins, J. G., and H. J. Henzler (1993). Aeration in cell cultures, in *Biotechnology*, 2nd ed., H. J. Rehm and G. Reed, eds., Vol. 3, *Bioprocessing*, G. Stephanopoulos, vol. ed., VCH, Weinheim, Germany.

Aunins, J. G., J. M. Goldstein, M. S. Croughan, and D. I. C. Wang (1986). Engineering developments in the homogenous culture of animal cells: oxygenation of reactors and scale-up, *Biotechnol. Bioeng. Symp.*, **17**, 699.

Ayazi Shamlou, P., H. Y. Makagiansar, A. P. Ison, and M. D. Lilly (1994). Turbulent breakage of filamentous micro-organisms in submerged culture in mechanically stirred bioreactors, *Chem. Eng. Sci.*, **49**(16), 2621–2631.

Bailey, J. E., and D. F. Ollis (1986). *Biochemical Engineering Fundamentals*, 2nd ed., McGraw-Hill, New York.

Bajpai, R. K., and M. Reuss (1982). Coupling of mixing and microbial kinetics for evaluating the performance of bioreactors, *Can. J. Chem. Eng.*, **60**, 384–392.

Baldyga, J., and J. R. Bourne (1995). Interpretation of turbulent mixing using fractals and multifractals, *Chem. Eng. Sci.*, **50**, 381–400.

Baldyga, J., J. R. Bourne, A. W. Pacek, A. Amanullah, and A. W. Nienow (2001). Effects of agitation and scale-up on drop size in turbulent dispersions: allowance for intermittency, *Chem. Eng. Sci.*, **56**, 3377–3385.

Barnes, H. A., and K. Walters (1985). The yield stress myth, *Rheol. Acta*, **24**(4), 323–326.

Barresi, A. A. (1997). Experimental investigation of interaction between turbulent liquid flow and solid particles and its effects on fast reactions, *Chem. Eng. Sci.*, **52**, 807–814.

Bartholomew, W. H. (1960). Scale-up of submersed fermentations, *Adv. App. Microbiol.*, **2**, 289–300.

Born, C., Z. Zhang, M. Al-Rubeai, and C. R. Thomas (1992). Estimation of disruption of animal cells by laminar shear stress, *Biotechnol. Bioeng.*, **40**, 1004–1010.

Boulton-Stone, J. M. (1995). The effect of surfactant on bursting gas bubbles, *J. Fluid Mech.*, **302**, 231–257.

Braun, S., and S. E. Vecht-Lifshitz (1991). Mycelial morphology and metabolite production, *Trends Biotechnol.*, **9**, 63–68.

Brown, M. E., and J. R. Birch (1996). The effect of pH on growth and productivity of cell lines producing monoclonal antibodies at large scale, *Cytotechnol.*, **17**, Suppl. 1, Abstr. 1.

Bryant, J. (1977). Characterisation of mixing in fermenters, *Adv. Biochem. Eng.*, **5**, 101–123.

Bryant, J., and S. Sadeghzadeh (1979). Circulation rates in stirred and aerated tanks, *Proc. 3rd European Conference on Mixing*, York, Yorkshire, England, Apr. 4–6, pp. 325–336.

Buckland, B. C., T. Brix, H. Fastert, K. Gbewonyo, G. Hunt, and D. Jain (1985). Fermentation exhaust gas analysis using mass spectrometry, *Bio/Technology*, **3**, 984–988.

Buckland, B. C., K. Gbewonyo, D. DiMasi, G. Hunt, G. Westerfield, and A. W. Nienow (1988a). Improved performance in viscous mycelial fermentations by agitator retrofitting, *Biotechnol. Bioeng.*, **31**, 737–742.

Buckland, B. C., K. Gbewonyo, D. Jain, K. Glazomitsky, G. Hunt, and S. W. Drew (1988b). Oxygen transfer efficiency of hydrofoil impellers in both 800L and 19000L fermenters, *Proc. 2nd International Conference on Bioreactor Fluid Dynamics*, R. King, ed., BHRA/Elsevier, London, pp. 1–15.

Bylund, F., E. Collet, S. O. Enfors, and G. Larsson (1998). Substrate gradient formation in the large-scale bioreactor lowers cell yield and increases by-product formation, *Bioprocess. Eng.*, **18**(3), 171–180.

Bylund, F., F. Guillard, S. O. Enfors, C. Tragardh, and G. Larsson (1999). Scale down of recombinant protein production: a comparative study of scaling performance, *Bioprocess. Eng.*, **20**(5), 377–389.

Bylund, F., A. Castan, R. Mikkola, A. Viede, and G. Larsson (2000). Influence of scale up on the quality of recombinant human growth hormone, *Biotechnol. Bioeng.*, **69**(2), 119–128.

Calderbank, P. H. (1958). Physical rate processes in industrial fermentation: 1. The interfacial area in gas–liquid contacting with mechanical agitation, *Trans. Inst. Chem. Eng.*, **36**, 443–463.

Capstick, P. B., A. J. Garland, W. G. Chapman, and R. C. Masters (1965). Production of foot-and-mouth disease virus antigen from BHK 21 clone 13 cells grown and infected in deep suspension cultures, *Nature*, **205**, 1135.

Capstick, P. B., A. J. Garland, W. G. Chapman, and R. C. Masters (1967). Factors affecting the production of foot-and-mouth disease virus in deep suspension cultures of BHK21 C13 cells, *J. Hyg. Camb.*, **645**, 273.

Carilli, A., E. B. Chain, G. Gualandi, and G. Morisi (1961). Continuous measurement of dissolved oxygen during fermentation in large fermenters, *Sci. Rep. Inst. Super Sanita*, **1**, 177–189.

Chalmers, J. J., and F. Bavarian (1991). Microscopic visualisation of insect cell–bubble interactions: II. The bubble film and bubble rupture, *Biotechnol. Prog.*, **7**, 151–158.

Charles, M. (1978). Technical aspects of the rheological properties of microbial cultures, *Adv. Biochem. Eng.*, **8**, 1–61.

Charles, M. (1985). Fermenter design and scale-up, in *Comprehensive Biotechnology*, Vol. 2, M. Moo-Young, ed., Pergamon Press, New York, pp. 57–75.

Cherry, R. S., and C. T. Hulle (1992). Cell death in the thin films of bursting bubbles, *Biotechnol. Prog.*, **8**, 11–18.

Cooke, M., J. C. Middleton, and J. Bush (1988). Mixing and mass transfer in filamentous fermentations, *Proc. 2nd International Conference on Bioreactor Fluid Dynamics*, R. King, ed., Elsevier, Amsterdam, pp. 37–64.

Croughan, M. S., and D. I. C. Wang (1987). Hydrodynamic effects on animal cells grown in microcarrier cultures, *Biotechnol. Bioeng.*, **29**, 130–141.

Croughan, M. S., J. F. Hamel, and D. I. C. Wang (1988). Effects of microcarrier concentration in animal cell cultures, *Biotechnol. Bioeng.*, **32**, 975–982.

Croughan, M. S., J. F. Hamel, and D. I. C. Wang (1989). Growth and death in microcarrier cultures, *Biotechnol. Bioeng.*, **33**, 731–744.

Cutter, L. A. (1966). Flow and turbulence in a stirred tank, *AIChE J.*, **12**, 35–45.

Dey, D., J. M. Boulton-Stone, A. N. Emery, and J. R. Blake (1997). Experimental comparisons with a numerical model of surfactant effects on the burst of a single bubble, *Chem. Eng. Sci.*, **52**(16), 2769–2783.

Dion, W. M., A. Carilli, G. Sermonti, and E. B. Chain (1954). The effect of mechanical agitation on the morphology of *Penicillium chrysogenum* Thom in stirred fermenters, *Rend. 1st Super. Sanita*, **17**, 187–205.

Doran, P. (1999). Design of mixing systems for plant cell suspension in stirred reactors, *Biotechnol. Prog.*, **15**, 319–335.

Drapeau, D., H. W. Blanch, C. R. Wilke (1987). Economic assessment of plant cell culture for the production of ajmalicine, *Biotechnol. Bioeng.* **30**, 946–953.

Dreveton, E., F. Monot, J. Lecourtier, D. Ballerini, and L. Choplin (1996). Influence of fermentation hydrodynamics on Gellan gum physico-chemical characteristics, *J. Ferment. Bioeng.*, **82**(3), 272–276.

Einsele, A. (1978). Scaling up bioreactors, *Proc. Biochem.*, **13**(7), 13–14.

Einsele, A., and R. K. Finn (1980). Influence of gas flow rates and gas holdup on blending efficiency in stirred tanks, *Ind. Eng. Chem. Process. Des. Dev.*, **19**, 600–603.

Elson, T. P. (1988). Mixing of fluids possessing a yield stress, *Proc. 6th European Conference on Mixing*, R. King, ed., BHRA, Cranfield, Bedfordshire, England, pp. 485–492.

Elson, T. P. (1990). The growth of caverns formed around rotating impellers during the mixing of a yield stress fluid, *Chem. Eng. Commun.*, **96**, 303–319.

Elson, T. P., D. J. Cheesman, and A. W. Nienow (1986). X-ray studies of cavern sizes and mixing performance with fluids possessing a yield stress, *Chem. Eng. Sci.*, **41**(10), 2555–2562.

Elsworth, R., G. Miller, A. Whitaker, D. Kitching, and P. Sayer (1968). Production of *E. coli* as a source of nucleic acids, *J. Appl. Chem.*, **17**, 157–166.

Enfors, S. O., M. Jahic, A. Rozkov, B. Xu, M. Hecker, B. Jürgen, E. Krüger, T. Schweder, G. Hamer, D. O'Beirne, N. Noisommit-Rizzi, M. Reuss, L. Boone, C. Hewitt, C. McFarlane, A. W. Nienow, T. Kovacs, C. Trägårdh, L. Uchs, J. Revteldt, P. C. Friberg, B. Hjertager, G. Blomsten, H. Skogman, S. Hjort, F. Hoeks, H. -Y. Lin, P. Neubauer, R. van der Lans, K. Luyben, P. Vrabel, and A. Manelius (2001). Physiological responses to mixing in large scale bioreactors, *J. Biotechnol.*, **85**, 175–185.

Etchells, A. W., W. N. Ford, and D. G. R. Short (1987). Mixing of Bingham plastics on an industrial scale, *Fluid Mixing 3, Inst. Chem. Eng. Symp. Ser.*, **108**, 1–10.

Flores, F., L. G. Torres, and E. Galindo (1994). Effect of the dissolved oxygen tension during the cultivation of *X. campestris* on the production and quality of xanthan gum, *J. Biotechnol.*, **34**, 165–173.

Forberg, C., and L. Haggstrom (1987). Effects of culture conditions on the production of phenylalanine from a plasmid-harboring *Escherichia coli* strain, *Appl. Microbiol. Biotechnol.*, **26**, 136–140.

Fowler, J. D., and E. H. Dunlop (1989). Effects of reactant heterogeneity and mixing on catabolite repression in cultures of *Saccharomyces cerevisiae*, *Biotechnol. Bioeng.*, **33**(8), 1039–1046.

Funahashi, H., H. Harada, H. Taguchi, and T. Yoshida (1987a). Circulation time distribution and volume of mixing regions in highly viscous xanthan gum solution in a stirred vessel, *J. Ferment. Technol.*, **20**, 277–282.

Funahashi, H., M. Machara, H. Taguchi, and T. Yoshida (1987b). Effect of glucose concentration on xanthan gum production by *Xanthomonas campestris*, *J. Chem. Eng. Jpn.*, **65**(6), 603–606.

Funahashi, H., M. Machara, H. Taguchi, and T. Yoshida (1987c). Effects of agitation by flat bladed turbine impeller on microbial production of xanthan gum, *J. Chem. Eng. Jpn.*, **20**(1), 16–22.

Funahashi, H., K. I. Hirai, T. Yoshida, and H. Taguchi (1988a). Mixing state of xanthan gum solution in aerated and agitated fermenter: effects of impeller size on volumes of mixed regions and circulation time distribution, *J. Ferment. Technol.*, **66**, 103–109.

Funahashi, H., K. I. Hirai, T. Yoshida, and H. Taguchi (1988b). Mechanistic analysis of xanthan gum production in a stirred tank, *J. Ferment. Technol.*, **3**, 355–364.

Furukawa, K., E. Heinzle, and I. J. Dunn (1983). Influence of oxygen on the growth of *Saccharomyces cerevisiae* in continuous culture, *Biotechnol. Bioeng.*, **25**(10), 2293–2317.

Galindo, E. (1994). Aspects of the Process for Xanthan Production, *Trans. Inst. Chem. Eng., Part C*, **72**, 227–237.

Galindo, E., and A. W. Nienow (1992). Mixing of highly viscous simulated xanthan fermentation broths with the Lightnin A315 impeller, *Biotechnol. Prog.*, **8**, 233–239.

Galindo, E., and A. W. Nienow (1993). Performance of the Scaba 6SRGT agitator in mixing of simulated xanthan gum broths, *Chem. Eng. Technol.*, **16**, 102–108.

Garcia-Briones, M., and J. J. Chalmers (1992). Cell–bubble interactions: mechanisms of suspended cell damage, *Ann. N.Y. Acad. Sci.*, **665**, 219–229.

Garcia-Briones, M., and J. J. Chalmers (1994). Flow parameters associated with hydrodynamic cell injury, *Biotechnol. Bioeng.*, **44**, 1089–1098.

Gbewonyo, K., D. DiMasi, and B. C. Buckland (1987). Characterization of oxygen transfer and power absorption of hydrofoil impellers in viscous mycelial fermentations, in *Biotechnology Processes, Mixing and Scale up*, C. S. Ho and J. J. Ulbrecht, eds., AIChE, New York, pp. 128–134.

Gbewonyo, K., G. Hunt, and B. C. Buckland (1992). Interactions of cell morphology and transport processes in the lovastatin fermentation, *Bioprocess. Eng.*, **8**, 1–7.

George, S., G. Larsson, and S. O. Enfors (1993). A scale-down 2-compartment reactor with controlled substrate oscillations: metabolic response of *Saccharomyces cerevisiae*, *Bioprocess. Eng.*, **9**(6), 249–257.

George, S., G. Larsson, and S. O. Enfors (1998). Comparison of Baker's yeast process performance in laboratory and production scale, *Bioprocess. Eng.*, **18**(2), 135–142.

Gibbs, P. A., and R. J. Seviour (1996). Does the agitation rate and/or oxygen saturation influence exopolysaccharide production by *Aureobasidium pullulans* in batch culture? *Appl. Microbiol. Biotechnol.*, **46**, 503–510.

Goldblum, S., Y. K. Bea, and J. Chalmers (1990). Protective effect of methylcellulose and other polymers on insect cells subjected to laminar stress, *Biotechnol. Prog.*, **6**, 383–390.

Gray, D. R., S. Shen, W. Howarth, D. Inlow, and B. L. Maiorella (1996). $CO_2$ in large-scale and high density CHO cell perfusion culture, *Cytotechnol.* **22**, 65–78.

Greaves, M., and K. A. H. Kobaccy (1981). Fluid Mixing 1, *Inst. Chem. Eng. Symp. Ser.*, **64**.

Griot, M., J. Moes, E. Heinzle, I. J. Dunn, and J. R. Bourne (1986). A microbial culture for the measurement of macro and micro mixing phenomena in biological reactors, *Proc. International Conference on Bioreactor Fluid Dynamics*, Cambridge, pp. 203–216.

Griot, M., E. Heinzle, I. J. Dunn, and J. R. Bourne (1987). Optimization of a MS-membrane probe for the measurement of acetoin and butanediol, in *Mass Spectrometry in Biotechnological Process Analysis and Control*, E. Heinzle and M. Reuss, eds., Plenum Press, New York, pp. 75–90.

Handa, A., A. N. Emery, and R. E. Spier (1987). On the evaluation of gas-liquid inter-facial effects on hybridoma viability in bubble column bioreactors, *Develop. Biol. Standard.* **66**, 241–253.

Handa-Corrigan, A., A. N. Emery, and R. E. Spier (1989). Effects of gas-liquid interfaces on the growth of suspended mammalian cells: mechanisms of cell damage by bubbles, *Enz. Microb. Technol.* **11**, 230–235.

Harnby, N., M. F. Edwards, and A. W. Nienow, eds. (1997). *Mixing in the Process Industries*. 2nd Edition, Butterworths Heinemann, London.

Hempel, D. C., and H. Dziallas (1999). Scale-up, stirred tank reactors, in *Encyclopaedia of Bioprocess Technology: Fermentation, Biocatalysis and Bioseparation*, Vol. 3, M. C. Flickinger and S. W. Drew, eds., Wiley, New York, pp. 2314–2332.

Herbst, H., A. Schumpe, and W. Deckwer (1992). Xanthan production in stirred tank fermenters: oxygen transfer and scale up, *Chem. Eng. Technol.*, **15**, 425–434.

Hewitt, C. J., L. A. Boon, C. M. McFarlane, and A. W. Nienow (1998). The use of flow cytometry to study the impact of fluid mechanical stress on *Escherichia coli* W3110 during continuous cultivation in an agitated bioreactor, *Biotechnol. Bioeng.*, **59**(5), 612–620.

Hewitt C. J., G. Nebe-von-Caron, A. W. Nienow, and C. M. McFarlane (1999). The use of multi-parameter flow cytometry to compare the physiological response of *Escherichia coli* W3110 to glucose limitation during batch, fed-batch and continuous culture cultivation, *J. Biotechnol.*, **75**, 251–254.

Hickman, A. D., and A. W. Nienow (1986). *Proc. International Conference on Bioreactor Fluid Dynamics*, Cambridge, pp. 301–306.

Hughmark, G. A. (1980). Power requirements and interfacial area in gas–liquid turbine agitated systems, *Ind. Eng. Chem. Process. Des. Dev.*, **19**, 638–641.

Humphrey, A. E. (1977). Biochemical Engineering, in *Encyclopedia of Chemical Processing and Design*, Vol. 4, J. J. McKetta and W. A. Cunningham, eds., Marcel Dekker, New York, pp. 359–394.

Jeanes, A., P. Rogovin, M. C. Cadmus, R. W. Silman, and C. A. Knutson (1976). Procedures for culture maintenance and polysaccharide production, purification and analysis, *ARS-NC-51*, Agricultural Research Service, U.S. Department of Agriculture, North Central Region.

Jeenes, D. J., D. A. Mackenzie, I. N. Roberts, and D. B. Archer (1991). Heterologous protein production by filamentous fungi, *Biotechnol. Genet. Eng. Rev.*, **9**, 327–367.

Jöbses, I., D. Martens, and J. Tramper (1991). Lethal events during gas sparging in animal cell culture, *Biotechnol. Bioeng.*, **37**, 484–490.

Johnston, R. E., and M. W. Thring (1957). *Pilot Plants, Models and Scale-up Methods in Chemical Engineering*, McGraw-Hill, New York.

Joshi, J. B., C. B. Elias, and M. S. Patole (1996). Role of hydrodynamic shear in the cultivation of animal, plant and microbial cells, *Chem. Eng. J.*, **62**, 121–141.

Jüsten, P., G. C. Paul, A. W. Nienow, and C. R. Thomas (1996). Dependence of mycelial morphology on impeller type and agitation intensity, *Biotechnol. Bioeng.*, **52**, 634–648.

Jüsten, P., G. C. Paul, A. W. Nienow, and C. R. Thomas (1998a). Dependence of *Penicillium chrysogenum* growth, morphology, vacuolation and productivity in fed-batch fermentations on impeller type and agitation intensity, *Biotechnol. Bioeng.*, **59**, 762–775.

Jüsten, P., G. C. Paul, A. W. Nienow, and C. R. Thomas (1998b). A mathematical model for agitation induced fragmentation of *P. chrysogenum*, *Bioprocess. Eng.*, **18**, 7–16.

Kieran, P., P. MacLoughlin, and D. Malone (1997). Plant cell suspension cultures: some engineering considerations, *J. Biotechnol.*, **59**, 39–52.

Kilburn, D., and F. C. Webb (1968). The cultivation of animal cells at controlled dissolved oxygen partial pressure, *Biotechnol. Bioeng.*, **10**, 801–814.

Kimura, R., and W. M. Miller (1996). Glycosylation of CHO-derived recombinant tPA produced under elevated $pCO_2$, *Biotechnol. Prog.*, **13**, 311–317.

Kioukia, N., A. W. Nienow, A. N. Emery, and M. Al-Rubeai (1992). The impact of fluid dynamics on the biological performance of free suspension animal cell culture: further studies, *Food Bioprod. Process.*, **70**, 143–148.

Kioukia, N., A. W. Nienow, M. Al-Rubeai, and A. N. Emery (1996). Influence of agitation and sparging on the growth rate and infection of insect cells in bioreactors and a comparison of hybridoma culture, *Biotechnol. Prog.*, **12**, 779–785.

Kiss, R., M. Croughan, J. Trask, G. Polastri, M. Groenhout, A. Banka, S. Shurin, J. Paul, and H. Koning-Bastiaan (1994). Mixing time characterisation in large scale mammalian cell bioreactors, *AIChE Annual Meeting*, November 1994, San Francisco, CA.

Kloppinger, M., G. Fertig, E. Fraune, and H. G. Miltenburger (1990). Multi-stage production of *Autographa californica* nuclear polyhydrosis virus in insect cell bioreactors, *Cytotechnol.* **4**, 271–278.

Kolmogorov, A. (1941a). The local structure of turbulence in incompressible viscous fluid for very large Reynolds numbers, *Compt. Rend. (Dokl.) Acad. Sci. URSS*, **30**, 301–305.

Kolmogorov, A. (1941b). Dissipation of Energy in the Locally Isotropic Turbulence, *Compt. Rend. (Dokl.) Acad. Sci. URSS*, **32**, 16–18.

König, B., Ch. Seewald, and K. Schügerl (1981). Process engineering investigations of penicillin production, *Eur. J. Appl. Microbiol. Biotechnol.*, **12**, 205–211.

Kossen, N. W. F., and N. M. G. Oosterhuis (1985). Modelling and scaling up of bioreactors, in *Biotechnology*, Vol. 2, H. J. Rehm, and G. Reed, eds., VCH, Weinheim, Germany, pp. 572–605.

Kowalski, A. J., and N. H. Thomas (1994). Bursting of bubbles stabilised by surfactants for control of cell damage, in *Bubble Dynamics and Interface Phenomena*, J. R. Blake, J. M. Boulton-Stone, and N. H. Thomas, eds., Kluwer, Dordrecht, The Netherlands.

Kunas, K. T., and E. T. Papoutsakis (1990). Damage mechanisms of suspended animal cells in agitated bioreactors with and without bubble entrainment, *Biotechnol. Bioeng.*, **30**, 368–373.

Langheinrich, C., and A. W. Nienow (1999). Control of pH in large scale, free suspension animal cell bioreactors: alkali addition and pH excursions, *Biotechnol. Bioeng.*, **66**(3), 171–179.

Langheinrich, C., A. W. Nienow, N. C. Stevenson, A. N. Emery, T. M. Clayton, and N. K. H. Slater (1998). Liquid homogenisation studies in animal cell bioreactors of up to 8 m$^3$ in volume, *Trans. Inst. Chem. Eng., Part C*, **76**, 107–116.

Larsson, G., and S. O. Enfors (1985). Influence of oxygen starvation on the respiratory capacity of *Penicillium chrysogenum*, *Appl. Microbiol. Biotechnol.*, **21**, 228–233.

Larsson, G., and S. O. Enfors (1988). Studies of insufficient mixing in bioreactors: effects of limiting oxygen concentrations and short term oxygen starvation on *Penicillium chrysogenum*, *Bioprocess. Eng.*, **3**(3), 123–127.

Larsson, G., M. Tornkvist, E. S. Wernersson, C. Tragardh, H. Noorman, and S. O. Enfors (1996). Substrate gradients in bioreactors: origin and consequences, *Bioprocess. Eng.*, **14**(6), 281–289.

Lawford, H. G., and J. D. Rousseau (1991). Bioreactor design considerations in the production of high-quality microbial exopolysaccharide, *Appl. Biochem. Biotechnol.*, **28/29**, 667–684.

Leckie, F., H. Scragg, and K. Cliffe (1991). Effect of impeller design and speed on the large- scale cultivation of suspension cultures of *Catharanthus roseous*, *Enzyme Microb. Technol.*, **13**, 801–810.

Lee, I. Y., M. K. Kim, J. H. Lee, W. T. Seo, J. K. Jung, H. W. Lee, and Y. H. Park (1999). Influence of agitation speed on production of curdlan by *Agrobacterium species*, *Bioprocess. Eng.*, **20**, 283–287.

Levenspiel, O. (1972). *Chemical Reaction Engineering*, 2nd ed., Wiley, New York.

Luong, H. T., and B. Volesky (1979). Mechanical power requirements of gas–liquid agitated systems, *AIChE J.*, **25**, 893–895.

MacIntyre, F. (1972). Flow patterns in breaking bubbles, *J. Geo-Phys. Res.*, **77**, 5211–5228.

Mackenzie, D. A., D. J. Jeenes, N. J. Belshaw, and D. B. Archer (1993). Regulation of secreted protein production by filamentous fungi: recent development and perspectives, *J. Genet. Microbiol.*, **139**, 2295–2307.

Makagiansar, H. Y., P. A. Shamlou, C. R. Thomas, and M. D. Lilly (1993). The influence of mechanical forces on the morphology and penicillin production of *Penicillium chrysogenum*, *Bioprocess. Eng.*, **9**, 83–90.

Manfredini, R., V. Cavallera, L. Marini, and G. Donati (1983). Mixing and oxygen transfer in conventional stirred fermenters, *Biotechnol. Bioeng.*, **25**, 3115–3131.

Mann, R., P. P. Mavros, and J. C. Middleton (1981). A structured stochastic flow model for interpreting flow: follower data from a stirred vessel, *Trans. Inst. Chem. Eng.*, **59**, 271–278.

Manning, F. S., D. Wolf, and D. L. Keairns (1965). Model simulation of stirred tank reactors, *AIChE J.*, **11**(4), 723–727.

Märkl, H., R. Bronnenmeier, and B. Wittek (1991). The resistance of micro-organisms to hydrodynamic stress, *Int. Chem. Eng.*, **31**(2), 185.

Martin, T., C. M. McFarlane, and A. W. Nienow (1994). The influence of liquid properties and impeller type on bubble coalescence behaviour and mass transfer in sparged agitated bioreactors, *Proc. 8th European Conf. on Mixing*. Cambridge, Sept. 1994. I. ChemE., Rugby, pp. 57–64.

Meier, S. J., T. A. Hatton, and D. I. C. Wang (1999). Cell death from bursting bubbles: role of cell attachment to rising bubbles in sparged reactors, *Biotechnol. Bioeng.*, **62**(4), 468–478.

Meijer, J., H. ten Hoopen, K. Luyben, and R. Libbenga (1993). Effects of hydrodynamic stress on cultured plant cells: a literature survey, *Enzyme Microb. Technol.*, **15**, 234–238.

Meijer, J. J., H. J. G. ten Hoopen, Y. M. van Gameren, Ch. A. M. Luyben, and K. R. Libbenga (1994). Effects of hydrodynamic stress on the growth of plant cells in batch and continuous culture, *Enzyme Microb. Technol.*, **16**, 467–477.

Merchuk, J. C. (1991). Shear effects on suspended cells, *Adv. Biochem. Eng. Biotechnol.*, **44**, 66–95.

Metz, B. (1976). From pulp to pellet. Ph.D. dissertation, Delft Technical University, The Netherlands.

Metz, B., E. W. de Bruijn, and J. C. van Suijdam (1981). Method for quantitative representation of the morphology of molds, *Biotechnol. Bioeng.*, **23**, 149–163.

Metz, B., and N. W. F. Kossen (1977). Biotechnology review: the growth of molds in the form of pellets—a literature review, *Biotechnol. Bioeng.* **19**, 781–799.

Metzner, A. B., and R. E. Otto (1957). Agitation of non-Newtonian fluids, *AIChE J.*, **3**, 3–10.

Michaels, J. D., J. F. Peterson, L. V. McIntire, and E. T. Papoutsakis (1991). Protection mechanism of freely suspended animal cells (Crl 8018) from fluid mechanical injury: viscometric and bioreactor studies using serum, pluronic F68 and polyethylene glycol, *Biotechnol. Bioeng.* **38**, 169–180.

Middleton, J. C. (1979). Measurement of circulation in large mixing vessels, *Proc. 3rd European Conference on Mixing*, York, Yorkshire England, pp. 15–36.

Moes, J., M. Griot, J. Keller, E. Heinzle, I. J. Dunn, and J. R. Bourne (1985). A microbial culture with oxygen sensitive product distribution as a potential tool for characterising bioreactor oxygen transport, *Biotechnol. Bioeng.*, **27**, 482–489.

Moo-Young, M., and H. W. Blanch (1981). Design of biochemical reactors. Mass transfer criteria for simple and complex systems, *Adv. Biochem. Eng.*, **19**, 2–69.

Moraine, R. A., and P. Rogovin (1973). Kinetics of xanthan fermentation, *Biotechnol. Bioeng.*, **15**, 225–237.

Moreira, J. L., P. M. Alves, J. G. Aunins, and M. J. T. Carrondo (1995). Hydrodynamic effects on *Bhk* cells grown as suspended natural aggregates, *Biotechnol. Bioeng.*, **46**(4), 351–360.

Murhammer, D. W., and C. F. Goochee (1990). Structural features of non-ionic polyglycol polymer molecules responsible for the protective effect in sparged animal cell bioreactors, *Biotechnol. Prog.*, **6**, 142–148.

Muskett, M. J., and A. W. Nienow (1987). Capital and running costs: the economics of mixer selection, in Fluid Mixing III, *Inst. Chem. Eng. Symp. Ser.*, **108**, 33–48.

Nagata, S. (1975). *Mixing: Principles and Applications*, Halstead Press, New York.

Namdev, P. K., and E. H. Dunlop (1995). Shear sensitivity of plant cells in suspension, *Appl. Biochem. Biotechnol.*, **54**, 109–131.

Namdev, P. K., P. K. Yegneswaran, B. G. Thompson, and M. R. Gray (1991). Experimental simulation of large scale bioreactor environments using a Monte Carlo method, *Can. J. Chem. Eng.*, **69**, 513–519.

Namdev, P. K., B. G. Thompson, and M. R. Gray (1992). Effect of feed zone in fed-batch fermentations of *Saccharomyces cerevisiae*, *Biotechnol. Bioeng.*, **40**, 235–246.

Newitt, D. M., N. Dombrowski, and F. H. Knelman (1954). Liquid entrainment: 1. The mechanism of drop formation from gas or vapour bubbles, *Trans. Inst. Chem. Eng.*, **32**, 244–261.

Nielsen, J. (1992). Modelling the growth of filamentous fungi, *Adv. Biochem. Eng.*, **46**, 187–223.

Nielsen, J., C. L. Johansen, M. Jacobsen, P. Krabben, and J. Villadsen (1995). Pellet formation and fragmentation in submerged cultures of *Penicillium chrysogenum* and its relation to penicillin production, *Biotechnol. Prog.*, **11**, 93–98.

Nienow, A. W. (1984). Mixing studies on high viscosity fermentation processes: xanthan gums, in *World Biotech Report*, Vol. 1, Europe Online Publication, pp. 293–304.

Nienow, A. W. (1990). Agitators for mycelial fermentations, *Trends Biotechnol.*, **8**, 224–233.

Nienow, A. W. (1997). Large scale free suspension animal cell culture; cell fragility versus homogeneity, *Genet. Eng. Biotechnol.*, **17**, 111–113.

Nienow, A. W. (1998). Hydrodynamics of stirred bioreactors, *Appl. Mech. Rev.*, **51**, 3–32.

Nienow, A. W., and T. P. Elson (1988). Aspects of mixing in rheologically complex fluids, *Chem. Eng. Res. Des.*, **66**, 5–15.

Nienow, A. W., and J. J. Ulbrecht (1985). Gas–liquid mixing in high viscosity systems, in *Mixing of Liquids by Mechanical Agitation*, J. J. Ulbrecht and G. K. Patterson, eds., Gordon and Breach, New York, pp. 203–235.

Nienow, A. W., C. M. Chapman, and J. C. Middleton (1979). Gas recirculation rate through impeller cavities and surface aeration in sparged, agitated vessels, *Chem. Eng. J.*, **17**, 111–118.

Nienow, A. W., D. J. Wisdom, J. Solomon, V. Machon, and J. Vlcek (1983). The effect of rheological complexities on power consumption in an aerated, agitated vessel, *Chem. Eng. Commun.*, **19**, 273–293.

Nienow, A. W., M. M. C. G. Warmoeskerken, J. M. Smith, and M. Konno (1985). *Proc. 5th European Conference on Mixing*, Wurzburg, Germany, pp. 143–154.

Nienow, A. W., G. Hunt, and B. C. Buckland (1995). A fluid dynamic study using a simulated viscous shear thinning broth of the retrofitting of large agitated bioreactors, *Biotechnol. Bioeng.*, **49**, 15–19.

Nienow, A. W., C. Langheinrich, N. C. Stevenson, A. N. Emery, T. M. Clayton, and N. K. H. Slater (1996). Homogenisation and oxygen transfer in large agitated and sparged animal cell bioreactors: some implications for growth and production, *Cytotechnology*, **22**, 87–94.

Norton, C. J., D. O. Falk, and W. E. Luetzelschwab (1981). Xanthan biopolymer semi-pilot fermentation, *Soc. Petrol. Eng. J.*, **5**, Apr., pp. 205–217.

Oh, S. K. W., A. W. Nienow, M. Al-Rubeai, and A. N. Emery (1989). The effects of agitation intensity with and without continuous sparging on the growth and antibody production of hybridoma cells, *J. Biotechnol.*, **12**, 45–62.

Oh, S. K. W., A. W. Nienow, M. Al-Rubeai, and A. N. Emery (1992). Further studies on the culture of mouse hybridomas in an agitated bioreactor with and without continuous sparging, *J. Biotechnol.*, **22**, 245–270.

Oldshue, J. Y. (1966). Fermentation mixing scale-up techniques, *Biotechnol. Bioeng.*, **8**, 3–24.

Oldshue, J. Y. (1983). *Fluid Mixing Technology*, McGraw-Hill, New York, pp. 89–92, 192–215.

Oosterhuis, N. M. G. (1984). *Scale up of bioreactors: a scale down approach*, Ph.D. dissertation, Delft University of Technology, The Netherlands.

Oosterhuis, N. M. G., and N. W. F. Kossen (1983). Oxygen transfer in a production scale bioreactor, *Chem. Eng. Res. Des.*, **61**, 308–312.

Oosterhuis, N. M. G., and N. W. F. Kossen (1984). Dissolved oxygen concentration profiles in a production scale bioreactor, *Biotechnol. Bioeng.*, **26**, 546–550.

Oosterhuis, N. M. G., N. M. Groesbeek, A. P. C. Olivier, and N. W. F. Kossen (1983). Scale down aspects of the gluconic acid fermentation, *Biotechnol. Lett.*, **5**(3), 141–146.

Oosterhuis, N. M. G., N. W. F. Kossen, A. P. C. Olivier, and E. S. Schenk (1985). Scale down and optimisation studies of the gluconic acid fermentation by *Gluconobacter oxydans*, *Biotechnol. Bioeng.*, **27**, 711–720.

Osman, J. J., J. Birch, and J. Varley (2001). The response of GS-NSO myeloma cells to pH shifts and pH perturbations, *Biotechnol. Bioeng.*, **75**, 63–73.

Osman, J. J., J. Birch, and J. Varley (2002). The response of GS-NSO myeloma cells to single and multiple pH perturbations, *Biotechnol. Bioeng.*, **79**(4), 398–407.

Paca, J., P. Ettler, and V. Grègr (1976). Hydrodynamic behaviour and oxygen transfer rate in a pilot plant fermenter: 1. Influence of viscosity, *J. Appl. Chem. Biotechnol.*, **26**(6), 309–317.

Pace, G. W., and R. C. Righelato (1980). Production of extracellular microbial polysaccharides, *Adv. Biochem. Eng.*, **15**, 1–70.

Packer, H. L., and C. R. Thomas (1990). Morphological measurements on filamentous micro-organisms by fully automatic image analysis, *Biotechnol. Bioeng.*, **35**, 870–881.

Papoutsakis, E. T. (1991). Media additives for protecting freely suspended animal cells against agitation and aeration damage, *Tibtech*, **9**, 316–324.

Paul, G. C., and C. R. Thomas (1998). Characterisation of mycelial morphology using image analysis, *Adv. Biochem. Eng.*, **60**, 1–59.

Paul, G. C., C. A. Kent, and C. R. Thomas (1994). Hyphal vacuolation and fragmentation in *Penicillium chrysogenum*, *Biotechnol. Bioeng.*, **44**, 655–660.

Peña, C., M. A. Trujillo-Roldán, and E. Galindo (2000). Influence of dissolved oxygen tension and agitation speed on alginate production and its molecular weight in cultures of *Azotobacter vinelandii*, *Enzyme Microb. Technol.*, **27**, 390–398.

Peters, H. U., H. Herbst, P. G. M. Heselink, H. Lunsdorf, A. Schumpe, and W. D. Deckwer (1989a). The influence of agitation rate on xanthan production by *Xanthomonas campestris*. *Biotechnol. Bioeng.*, **34**, 1393–1397.

Peters, H. U., H. Herbst, I. H. Suh, A. Shumpe, and W. D. Deckwer (1989b). The influence of fermenter hydrodynamics on xanthan production by *Xanthomonas Campestris*, in *Biomedical and Biotechnological Advances in Industrial Polysaccharides*, V. Crescenzi et al., eds., Gordon & Breach, New York, pp. 275–281.

Peters, H. U., I. S. Suh, A. Schumpe, and W. D. Deckwer (1992). Modelling of batchwise xanthan production, *Can. J. Chem. Eng.*, **70**, 742–750.

Prokop, A., and R. Bajpai (1992). The sensitivity of biocatalysts to hydrodynamic shear stress, *Adv. Appl. Microbiol.*, **37**, 165–232.

Purgstaller, A., and A. Moser (1987). Mixing-modelling of a two compartment bioreactor for scale down approaches, *Chem. Biochem. Eng.*, **1**(4), 157–161.

Ramirez, O. T., and R. Mutharasan (1990). The role of the plasma membrane fluidity on the shear sensitivity of hybridomas grown under hydrodynamic stress, *Biotechnol. Bioeng.*, **36**, 911–920.

Reuss, M. (1988). Influence of mechanical stress on the growth of *Rhizopus nigricans* in stirred bioreactors, *Chem. Eng. Technol.*, **11**, 178–187.

Reuss, M., R. K. Bajpai, and K. Lenze (1980). Scale-up strategies based on the interactions of transport and reaction, *Paper F-7.2.1*, presented at the 6th International Fermentation Symposium, London, Ontario, Canada.

Revill, B. K. (1982). Pumping capacity of disc turbine agitators—a literature review, *Paper B1, Proc. 4th European Conference on Mixing*, Noordwijkerhout, The Netherlands.

Riley, G. L., K. G. Tucker, G. C. Paul, and C. R. Thomas (2000). Effect of biomass concentration and mycelial morphology on fermentation Broth Rheology, *Biotechnol. Bioeng.*, **68**(2), 160–172.

Risenberg, D., and V. Schulz (1991). High cell density cultivation of *E. coli* at controlled specific growth rates, *J. Biotechnol.*, **20**, 17–28.

Rodríguez-Monroy, M., and E. Galindo (1999). Broth rheology, growth and metabolite production of *Beta vulgaris* suspension culture: a comparative study between cultures grown in shake flasks and in a stirred tank, *Enzyme Microb. Technol.*, **24**, 687–693.

Roels, J. A. (1982). Mathematical models and the design of biochemical reactors, *J. Chem. Technol. Biotechnol.*, 59–72.

Rogovin, S. P., R. F. Anderson, and M. C. Cadmus (1961). Production of polysaccharide with *Xanthomonas campestris*, *J. Biochem. Microbiol. Technol. Eng.* **3**: 51–63.

Scragg, A. H., E. J. Allan, and F. Leckie (1988). Effect of shear on the viability of plant cell suspensions, *Enzym. Microb. Technol*. **10**, 361–367.

Scragg, A. H. (1992). Large scale plant cell culture: methods, applications and products, *Curr. Opin. Biotechnol.*, **3**, 105–109.

Shuler, M. L. (1993). Strategies for improving productivity in plant cell, tissue and organ culture in bioreactors in *Bioproducts and Bioprocesses*, Vol. 2, T. Yoshida and R. D. Tanner, eds., Springer-Verlag, Berlin.

Singh, V., W. Hensler, R. Fuchs, and A. Constantinides (1986). On-line determination of mixing parameters in fermentors using pH transients, *Proc. International Conference on Bioreactor Fluid Dynamics*, BHRA, Cambridge, pp. 231–256.

Smith, J. J., M. D. Lilly, and R. L. Fox (1990). Morphology and penicillin production of *Penicillium chrysogenum*, *Biotechnol. Bioeng.*, **35**, 1011–1023.

Smith, J. M., K. Van't Riet, J. C. Middleton (1978). Scale-up of agitated gas–liquid reactors for mass transfer, *Proc. 2nd European Conf. on Mixing*, Cambridge, 1977. BHRA Fluid Engineering, Cranfield, pp. F4-51 to F4-66.

Sokolov, D. P., S. A. Livova, and E. A. Sokolova (1983). Effect of cyclical changes in culturing conditions on the growth kinetices and physiological characteristics of yeasts, *Microbiologiya*, **52**, 909–916.

Solomon, J., T. P. Elson, A. W. Nienow, and G. W. Pace (1981a). Cavern sizes in agitated fluids with a yield stress, *Chem. Eng. Commun.*, **11**, 143–164.

Solomon, J., A. W. Nienow, and G. W. Pace (1981b). Flow patterns in aerated plastic and pseudoplastic viscoelastic fluids, in Fluid Mixing I, *Inst. Chem. Eng. Symp. Ser.*, **64**, A1–A13.

Steel, R., and W. D. Maxon (1966). Dissolved oxygen measurements in pilot and production scale novobiocin fermentations, *Biotechnol. Bioeng.*, **8**, 97–108.

Sweere, A. P. J., J. R. Mesters, K. Ch. A. M. Luyben, and N. W. F. Kossen (1986). Regime analysis of the Baker's yeast production, *Proc. International Conference on Bioreactor Fluid Dynamics*, BHRA, Cambridge, pp. 217–230.

Sweere, A. P. J., K. Ch. A. M. Luyben, and N. W. F. Kossen (1987). Regime analysis and scale down: tools to investigate the performance of bioreactors, *Enzyme Microb. Technol.*, **9**, 386–398.

Sweere, A. P. J., J. R. Mesters, L. Janse, K. Ch. A. M. Luyben, and N. W. F. Kossen (1988a). Experimental simulation of oxygen profiles and their influence of Baker's yeast production: I. One-fermenter system, *Biotechnol. Bioeng.*, **31**, 567–578.

Sweere, A. P. J., L. Janse, K. Ch. A. M. Luyben, and N. W. F. Kossen (1988b). Experimental simulation of oxygen profiles and their influence of Baker's yeast production: II. Two-fermenter system, *Biotechnol. Bioeng.*, **31**, 579–586.

Sweere, A. P. J., Y. A. Matla, J. Zandvliet, K. Ch. A. M. Luyben, and N. W. F. Kossen (1988c). Experimental simulation of glucose fluctuation, *Appl. Microbiol. Biotechnol.*, **28**, 109–115.

Tagaki, M., K. Ohara, and T. Yoshida (1995). Effect of hydrostatic pressure on hybridoma cell metabolism, *J. Ferment. Bioeng.*, **80**, 619–621.

Telling, R. C., and R. Elsworth (1965). Submerged culture of hamster kidney cells in a stainless steel vessel, *Biotechnol. Bioeng.*, **7**, 417.

Thomas, C. R., and Z. Zhang (1998). The effects of hydrodynamics on biological materials, in *Advances in Bioprocess Engineering*, Vol. II, E. Galindo and O. T. Ramírez, eds., Kluwer Academic, Norwell, MA, pp. 137–170.

Thomas, C. R., M. Al-Rubeai, and Z. Zhang (1994). Prediction of mechanical damage to animal cells in turbulence, *Cytotechnology*, **15**, 329–335.

Toma, M. K., M. P. Rukliska, J. J. Vanags, M. O. Zeltina, M. P. Leite, N. I. Galinina, U. E. Viesturs, and R. P. Tengerdy (1991). Inhibition of microbial growth and metabolism by excess turbulence, *Biotechnol. Bioeng.*, **38**, 552–556.

Tramper, J. J., D. Joustra, and J. M. Vlak (1987). Bioreactor design for growth of shear-sensitive insect cells, in *Plant and Animal Cell Cultures: Process Possibilities*, C. Webb and F. Mavituna, eds., Ellis Horwood, Chichester, West Sussex, England, pp. 125–136.

Trujillo-Roldán, M. A., C. Peña, O. T. Ramírez, and E. Galindo (2001). The effect of oscillating dissolved oxygen tension on the production of alginate by *Azotobacter vinelandi*, *Biotechnol. Prog.*, **17**, 1042–1048.

Tucker, K. G., T. Kelly, P. Delgrazia, and C. R. Thomas (1992). Fully automatic measurement of mycelial morphology by image analysis, *Biotechnol. Prog.*, **8**, 353–359.

Ujcova, E., Z. Fencl, M. Musilkova, and L. Seichert (1980). Dependence of release of nucleotides from fungi on fermenter turbine speed, *Biotechnol. Bioeng.*, **22**, 237–241.

Underwood, S. (1994). Mixing performance of the Prochem Maxflo T impeller in highly viscous model fluids, M.Sc. thesis, University of Birmingham, England.

Van Barneveld, J., W. Smit, N. M. G. Oosterhuis, and H. J. Pragt (1987). Measuring the liquid circulation time in a large gas–liquid contactor by means of a radio pill: 2. Circulation time distribution, *Ind. Eng. Chem. Process. Des. Dev.*, **26**, 2192–2195.

Van Brunt, J. (1986). Fungi: the perfect hosts? *Bio/Technology*, **4**, 1057–1062.

Van Suijdam, J. C., and B. Metz (1981). Influence of engineering variables upon the morphology of filamentous molds, *Biotechnol. Bioeng.*, **23**, 111–148.

Van der Pol, L., and J. Tramper (1998). Shear sensitivity of animal cells from a culture medium perspective, *Trends. Biotechnol.* **16**:8, 323–328.

Van't Riet, K. (1975). Turbine agitator hydrodynamics and dispersion performance, Ph.D. dissertation, University of Delft, The Netherlands.

Van't Riet, K. (1979). Review of measuring methods and results in nonviscous gas–liquid mass transfer in stirred vessels, *Ind. Eng. Chem. Process. Des. Dev.*, **18**(3), 357–363.

Vardar, F., and M. D. Lilly (1982). Effect of cycling dissolved oxygen concentrations on product formation in penicillin fermentations, *Eur. J. Appl. Microbiol. Biotechnol.*, **14**(4), 203–211.

Vecht-Lifshitz, S. E., S. Magdassi, and S. Braun (1990). Pellet formation and cellular aggregation in *Streptomyces tendae*, *Biotechnol. Bioeng.*, **35**, 890–896.

Wang, D. I. C., C. L. Cooney, A. L. Demain, P. Dunnill, A. E. Humphrey, and M. D. Lilly (1979). Aeration and agitation, Chapter 9 in *Fermentation and Enzyme Technology*, Wiley, New York, pp. 157–193.

Warmoeskerken, M. M. C. G. (1986). Gas-liquid dispersing characteristics of turbine agitators, Ph.D. dissertation, University of Delft, The Netherlands.

Warmoeskerken, M. M. C. G., and J. M. Smith (1985). *Proc. 5th European Conference on Mixing*, BHRA, Cranfield, Bedfordshire, England, pp. 127–142.

Wecker, A., and U. Onken (1991). Influence of dissolved oxygen concentration and shear rate on the production of pullulan by *Aureobasidium pullulans*, *Biotechnol. Lett.*, **13**(3), 155–160.

Wessels, J. G. H. (1990). Role of cell wall architecture in fungal tip growth generation, in *Tip Growth in Plant and Fungal Walls*, I. B. Heath, ed., Academic Press, San Diego, CA, pp. 1–29.

Wessels, J. G. H. (1993). Wall growth, protein excretion morphogenesis in fungi, *New Phytol.*, **123**, 397–413.

Wichterle, K., and O. Wein (1975). Agitation of concentrated suspensions, *Paper B4.6*, presented at CHISA '75, Prague, Czechoslovakia.

Wu, J. (1995). Mechanisms of animal cell damage associated with gas bubbles and cell protection by medium additives, *J. Biotechnol.*, **43**, 81–94.

Wu, J., and M. F. A. Gossen (1995). Evaluation of the killing volume of gas bubbles in sparged animal cell culture reactors, *Enzyme Microb. Technol.*, **14**, 980–983.

Yegneswaran, P. K., M. R. Gray, and B. G. Thompson (1991). Experimental simulation of dissolved oxygen fluctuations in large fermenters: effect on *Streptomyces clavuligerus*, *Biotechnol. Bioeng.*, **38**, 1203–1209.

Zhao, X., A. W. Nienow, S. Chatwin, C. A. Kent, and E. Galindo (1991). Improving xanthan fermentation performance by changing agitators, in *Proc. 7th European Conference on Mixing*, M. Bruxelmane and G. Froment, eds., Brugge, Belgium, pp. 277–283.

Zhao, X., H. Zongding, A. W. Nienow, C. A. Kent, and S. Chatwin (1994). Rheological characteristics, power consumption, mass and heat transfer during xanthan gum fermentation, *Chin. J. Chem. Eng.*, **2**(4), 198–209.

Zhang, Z., M. Al-Rubeai, and C. R. Thomas (1992). Effect of Pluronic F68 on the mechanical properties of mammalian cells, *Enzyme Microb. Technol.*, **14**, 980–983.

Zhang, Z., M. Al-Rubeai, and C. R. Thomas (1993). Estimation of disruption of animal cells by turbulent capillary flow, *Biotechnol. Bioeng.*, **42**(8), 987–993.

Zhong, J. J., T. Seki, S. Kinoshita, and T. Yoshida (1992). Effects of surfactants on cell growth and pigment production in suspension cultures of *Perilla frutescens*, *World J. Microbiol. Biotechnol.*, **8**, 106–109.

Zhou, G., and S. M. Kresta (1996). Impact of tank geometry on the maximum turbulence energy dissipation rate for impellers, *AIChE J.*, **42**, 2476–2490.